



**Utrecht University**

# Investigating the Connection Between Chitosan Structure and Stability by Glyco- sylation of D-Glucosamine Derivatives and their Possible Application as a Film

## Master Thesis

*Zhou Zhou Lan 5988977*

*Supervisor: Kordula Schnabl*

*1<sup>st</sup> examiner: Dr. Ina Vollmer*

*2<sup>nd</sup> examiner: Prof. dr. Pieter Bruijninx*

*Inorganic Chemistry and Catalysis*

*Faculty of Science*

*Debye Institute for Nanomaterials Science*

*December 2021*

---

## Abstract

Chitosan is the deacetylated derivative of the second most abundant polysaccharide chitin. The copolymer consists out of two sugar monomers, D-glucosamine (GlcN) and *N*-acetyl-D-glucosamine (GlcNAc). Chitin is insoluble in common organic and aqueous solvents. In contrary to chitin, chitosan is soluble in aqueous acidic organic solvents and because of this, chitosan finds many applications in various fields (food, agriculture, medical, cosmetic, and many more). Chitosan-based packaging has drawn increasing attention from the scientific community due to its ability to make excellent biodegradable films and coating. However, large-scale application of chitosan can lead to health hazards and environmental pollution due to the use of organic acidic solvents. This work had two goals. The first aim was to investigate the limit of the solubility of the chitosan structure. This was done by making short chitosan chains from a bottom-up approach (glycosylation). An attempt was made to make a glycosyl acceptor and two thioglycosyl donors to achieve this glycosylation reaction. Here, a fully protected GlcNAc  $\alpha$ -anomer was synthesized and two thioglycosyl donors were made from GlcN and GlcNAc. The synthesis of the acceptor and donors were confirmed by analysis with ATR-IR,  $^1\text{H-NMR}$ , and  $^{13}\text{C-NMR}$  spectroscopy.

Since the treatment of chitosan leads to unwanted pollution, the second goal was to make films out of the GlcN and GlcNAc monomers since they are readily soluble in water, where their film properties would have been tested. The monomers were dissolved in different solvents such as water, acetic acid, and citric acid. Here, several crosslinking agents with bifunctional groups were employed to help the linking between the monomers and small chains. However, no films were formed, and only brittle powder was left. Although, crosslinking between the free amine of GlcN and the crosslinkers were observed with ATR-IR spectroscopy. It is implied that no films were formed due to the weak 3D-structure of the crosslinked monomers.

## Layman Abstract

Chitosan is a large substance composed of many repeating units. These units consist out of two different sugar molecules, D-glucosamine (GlcN) and *N*-acetyl-D-glucosamine (GlcNAc). Chitosan can be applied in many industries, for example the food industry as biodegradable food packaging. One of the drawbacks of chitosan is that it is only soluble in organic acidic solvents. However, the individual GlcN and GlcNAc sugar units are already soluble in just water, which led to the goals of this work. The first goal was to find the relationship between the chitosan structure and its solubility. This can be done by making small chitosan chains out of GlcN and GlcNAc units. Then, the limit of its solubility could be investigated. To make these small chains, both sugar units must go through multiple chemical modifications before they can be ready to attach. After these modifications, these sugar units are called acceptors and donors. In this project, an attempt was made to make this acceptor. However, it was one step away from being finished, as the yields of the intermediate products were too low. Also, two kinds of donors were made. Unfortunately, the goal to make this small chain was not achieved.

Traditional food packaging is not biodegradable and can lead to environmental pollution and hazards. As mentioned above, the disadvantage of chitosan is that it is only soluble in organic acidic solvents. So, when chitosan is used on a large scale, large amounts of organic solvents are used, which can be dangerous for human health and the environment. So, the second goal of this study was to make films out of the sugar units GlcN and GlcNAc, since it is known that these sugar molecules are soluble in just water. During these experiments, materials were added called crosslinking agents. Crosslinking agents are molecules that can act as a bridge between the sugar molecules, so they can bind together and help make the films. During the experiments, however, no films were formed even though a bridge was formed. This means that the linked sugar molecules were not strong enough to make films.

## Table of Contents

Abstract.....	1
Layman Abstract .....	1
1. Introduction .....	4
1.1. Chitosan Production and Properties .....	6
2. Aim of Research .....	7
3. Plan Experimental .....	8
3.1. Glycosylation.....	8
3.1.1. Introducing Acceptor Protecting Groups .....	8
3.1.2. Introducing Donor Protecting Groups .....	8
3.2. Crosslinking .....	12
4. Experimental .....	13
4.1. Materials .....	13
4.2. Chemical Structure Analysis.....	14
4.3. Synthesis of Glycosyl Acceptor .....	14
4.4. Synthesis of Glycosyl Donors .....	15
4.5. Experimental Crosslinking.....	16
5. Results and Discussion .....	17
5.1. Glycosyl Acceptor Synthesis.....	17
5.1.1. D-glucosamine Acceptor .....	17
5.1.2. N-acetyl-D-glucosamine Acceptor .....	18
5.2. Glycosyl Donor Synthesis .....	20
5.2.1. N-acetyl-D-glucosamine Donor Synthesis.....	20
5.2.2. D-glucosamine Donor .....	25
5.3. Crosslinking Experiments .....	30
5.3.1. Chitosan Characterization .....	30
5.3.2. Chitosan Crosslinking .....	30
5.3.3. Crosslinking of Monomers .....	35
5.3.4. Comparison Chitosan and Monomers Crosslinking .....	42
6. Conclusion.....	43
7. Outlook .....	44
8. Acknowledgments.....	44
9. References .....	45
Support Information .....	51
Unsuccessful Experiments .....	51
SI1. Anomeric Allylation of GlcN .....	51

SI2.	Anomeric Methylation of GlcN .....	51
SI3.	Benzylidenation of methyl GlcNAc.....	52
SI4.	Selective Benzylidene Acetal Ring Opening .....	53
Successful Experiments: Data of Glycosyl Acceptor .....		54
SI5.	Anomeric Methylation of GlcNAc .....	54
SI6.	4,6-O-Benzylidenation .....	56
SI7.	Benzylation.....	58
Successful Experiments: Data of Glycosyl Donors .....		60
SI8.	Acetylation of <i>N</i> -acetyl-D-glucosamine .....	60
SI9.	Thio- <i>N</i> -acetyl-D-glucosamine Donor.....	60
SI10.	Troc Protection and Acetylation of D-glucosamine .....	60
SI11.	N-Troc-Protected Thio-D-glucosamine Donor .....	61

## 1. Introduction

Chitin, poly- $\beta$ -(1 $\rightarrow$ 4)-*N*-acetyl-D-glucosamine, is the most abundant polysaccharide after cellulose.<sup>1</sup> This linear heteropolymer consists of two randomly distributed saccharides, D-glucosamine (GlcN) and *N*-acetyl-D-glucosamine (GlcNAc). Chitin occurs widespread in nature, but the main source is found in the marine ecosystem from the shells of crustaceans, like shrimps and crabs.<sup>2,3</sup> In industry, chitin is extracted from crustaceans by acid treatment to dissolve calcium carbonate. After, the polymer is treated with alkaline solutions to disrupt the chemical bonds between proteins and chitin. Then, an additional decolorization step is required to remove pigments to obtain a colorless product (**Figure 1**).<sup>1,4</sup>

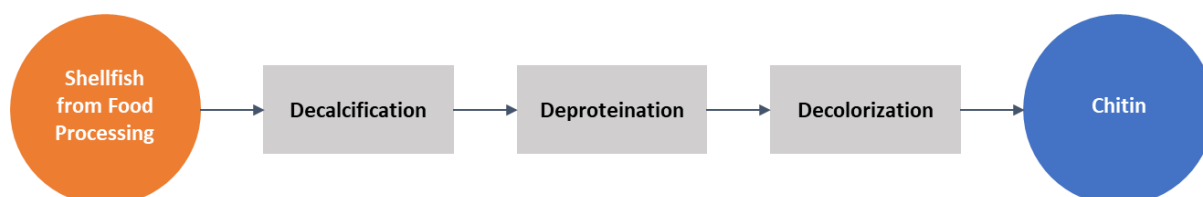


**Figure 1** - Chitin extraction from seafood waste. Adapted from Yadav et al.<sup>1</sup>

Chitin exhibits remarkable intrinsic biological properties: it is biocompatible, biodegradable, has anti-tumor and antioxidant activities, and is non-toxic with antimicrobial activity and low immunogenicity.<sup>1,5</sup> Due to these interesting properties, a lot of attention is spent on the applicability of this specific biopolymer. However, its commercial applicability is limited due to the poor solubility of chitin in common organic and aqueous solvents. Chitin is highly hydrophobic due to the expanded hydrogen-bonded semicrystalline structure, making it very stable to physical and chemical agents.<sup>6,7</sup>

Therefore, the deacetylated derivative of chitin, chitosan, is seen as a much more promising material. Chitosan is a linear polysaccharide consisting out of GlcN and GlcNAc units, where the non-acetylated monomer (GlcN) percentage is higher than the acetylated monomer (GlcNAc). In other words, the degree of acetylation (DA) is lower than 50%, see **Figure 2**. The chemical and biological properties of chitosan highly depend on the DA and the chain length of the polymer, and are shown in **Table 1**.<sup>4</sup> In contrary to chitin, chitosan is soluble in dilute acidic solutions below pH 6.0. The solubility originates from the fact that there are more primary amine groups present in the polymer. The amine groups have a pKa value of 6.3, where the solubilization takes place by protonation of the amine functional group. Here, chitosan is made into a cationic polyelectrolyte which allows it to be soluble in an acidic medium (**Figure 3**).<sup>7</sup> Being soluble in aqueous solutions, it finds many applications in numerous fields (food, agriculture, medical, cosmetic industries, etc.).<sup>2,4,8</sup>

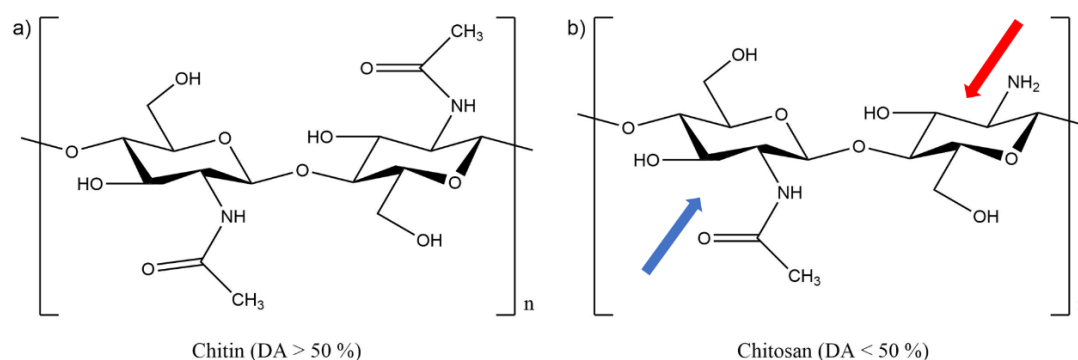


**Figure 2** – Chemical structure of (a) Chitin with a degree of acetylation (DA) of more than 50% and (b) chitosan with a degree of acetylation of less than 50%. Blue arrow indicates the *N*-acetyl-D-glucosamine unit. The red arrow indicates the *D*-glucosamine unit. Adapted from Ferreira et al.<sup>9</sup>

**Table 1** – Chemical and biological properties of chitosan.<sup>4</sup>

Chemical Properties	Biological Properties
Linear amino polysaccharide with much nitrogen content	Bioadhesivity
Rigid D-glucosamine structure; high hydrophilicity; crystallinity	Bioactivity
Weak base; deprotonated amino groups acts as a powerful nucleophile (pKa 6.3)	Nontoxic
Ability to form intermolecular hydrogen bonds; high viscosity	Biodegradable
Consists of great reactive groups for crosslinking and chemical activation	Adsorbable
Insoluble in water and organic solvents; soluble in aqueous acidic solutions	Antimicrobial activity
Able to form salts with organic and inorganic acids	Antiacid, antiulcer and antitumoral properties
Chelating and complexing properties	Blood anticoagulants
Ionic conductivity	Hypolipidemic activity
Polyelectrolytes at acidic pH	
Cationic biopolymer with high charge density	
Interacts with negatively charged molecules	
Entrapment and adsorption properties	
Film-forming ability	

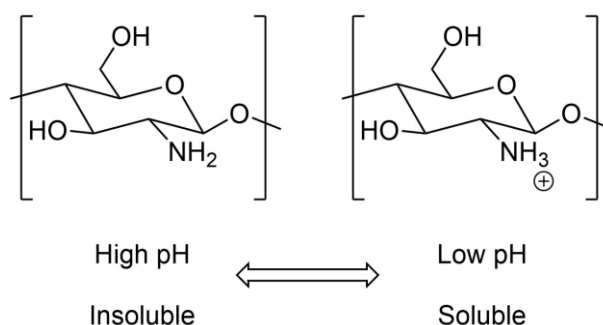


**Figure 3** - Illustration of chitosan's adaptability in solution. At low pH (< 6.0), the amine groups on chitosan are protonated, making chitosan a water-soluble cationic polyelectrolyte. At higher pH, the amine groups are deprotonated, making chitosan insoluble. Adapted from Dash et al.<sup>8</sup>

Recently, a lot of attention is aimed at developing alternative packaging products based on bio-based polymers, co-products, agricultural and food waste products due to the concerns about the limited natural fossil resources, and the negative impact on the environment caused by the use of non-biodegradable plastic-based packaging materials.<sup>10</sup> As mentioned in **Table 1**, chitosan offers the possibility for the formation of excellent edible films and coating due to its ability to make transparent films.<sup>10</sup> Moreover, chitosan also has bioactive properties and it can act as oxygen and grease barriers.<sup>4,11,12</sup> Hence, chitosan-based packaging has drawn increasing attention from the scientific community. One of the main obstacles of biopolymer films is their high sensitivity towards water, making them break down when in contact with water or having their mechanical and barrier properties hindered because of water absorption and swelling.<sup>13</sup> So, many reported works focused on using crosslinkers to enhance the film properties, such as the water resistance as well as mechanical and barrier properties.<sup>14</sup> Moreover, crosslinking leads to an increase in resistance against heat and light, improvement of the dimensional stability, and an increase in chemical and solvent resistancy.<sup>11,14</sup>

## 1.1. Chitosan Production and Properties

Chitin can be deacetylated into chitosan by enzymatic or chemical processes, however, chemical preparations are preferably used because of their low production cost and appropriateness to mass production at commercial applications.<sup>1,5,6,15</sup>

The deacetylation of chitin can be performed under acidic or alkali conditions. However, the glycosidic bonds throughout the chitin chain are vulnerable to acid and therefore, deacetylation under alkali conditions is more commonly used.<sup>16</sup> The deacetylation of chitin can be performed either heterogeneously or homogeneously. In the heterogeneous method, an insoluble chitosan with a DA of ~ 1%-15% is yielded after treatment with hot concentrated NaOH solution, where the GlcN and GlcNAc repeating units are randomly distributed along the polymeric chain.<sup>1,5,17</sup> While during a homogenous process, soluble chitosan can be obtained with a DA of 48% - 55%. After a long treatment, this process can lead to a DA of 90% with homogeneously dispersed acetyl groups along the chains.<sup>1,5</sup>

During the deacetylation step, depolymerization of the chitin polymer occurs, resulting in changes in the molecular weight of chitosan.<sup>1,4</sup> Therefore, various types of commercial chitosan are available. For example, commercial chitosan can be available in three grades of low, medium and high molecular weight (Sigma-Aldrich).<sup>18</sup> Low molecular weight chitosan grade is indicated between 50 kDa and 190 kDa with a DA of 15 – 25%. The medium molecular weight is characterized between 190 kDa and 310 kDa with a DA of 15 – 25%. The high molecular weight chitosan is defined between 310 kDa and 375 kDa with a DA of < 25%. Thus, the deacetylation step can lead to chitosan structures with different DA and molecular weights. Since the pKa value is highly dependent on the DA, the solubility of chitosan depends on these factors as well, in which lower DA increases the solubility.<sup>4,5,19</sup> The solubility of chitosan chains in aqueous solutions have been extensively studied as a function of the DA.<sup>20</sup> Schatz et al. proposed general laws of the behavior of chitosan in aqueous solutions:

- At DA < 20%: chitosan displays the highest structural charge density, where it shows polyelectrolyte behavior. This behavior is connected to the long distance intra- and intermolecular electrostatic interactions, which are among other things responsible for high solubility.
- At DA between 20 – 50%: the solubility remains constant, which is connected to the fact that hydrophilic and hydrophobic interactions are counterbalanced.
- At DA > 50%: the electrostatic interactions have become short-distance interactions, because these hydrophobic interactions become predominant due to the increase of acetyl groups.

Shorter chitosan chains (chitosan oligomers) can be made by chemical hydrolysis involving both deacetylation and depolymerization.<sup>1,21</sup> Chitosan oligomers possess more GlcN units than GlcNAc, which is similar to the chitosan polymer. The more exposed amino groups are the main reason for the difference between their structures. In relation to chitosan polymer, chitosan oligomers have a much better solubility, which is attributed to their shorter chain lengths and lower DA leading to more free amino groups.<sup>22</sup> In this case, the shorter chains reduce the hydrogen bond formations between the macromolecules and also reduce the amount of amino groups, which consequently decreases the formation of intermolecular hydrogen bonds.<sup>23</sup>

Other physicochemical properties (e.g. crystallinity, biodegradability, viscosity and biocompatibility) are influenced by the structure properties too, see **Table 2**.<sup>5,7,8,15</sup> Thus, depending on the deacetylation step, chitosan products can be obtained with different properties.

**Table 2** – The influence of degree of acetylation (DA), molecular weight, and chain length on the physicochemical properties of chitosan.<sup>12</sup>

Physicochemical property	Structural characteristics <sup>a</sup>	References
Solubility	↓ DA, ↓ Chain length, ↓ Molecular weight	[7,12,20,22]
Crystallinity	↑ DA	[15,24]
Biodegradability	↑ DA, ↓ Molecular weight	[25–27]
Viscosity	↓ DA, ↑ Chain length	[4,22,28]
Biocompatibility	↓ DA	[29]

<sup>a</sup> ↑ - Directly proportional to property. ↓ - Inversely proportional to property.

## 2. Aim of Research

Since chitosan is only soluble in aqueous organic solvents, the application of chitosan usually requires large amounts of organic solvents which can have a negative impact on the human health and the environment. Also, the preparation of chitin and chitosan involves rough conditions, where highly acidic or basic solutions are used. Current production methods result in the formation of undesired by-products and large amounts of aqueous organic waste, leading to high production costs and environmental risks.<sup>1,5,30</sup> Considering these factors, this makes the application of chitosan not suitable for a more sustainable world. This leads to the aim of this research, which is to find an alternative approach to produce chitosan chains and find the limit in which the chains are still water soluble. This will be done by making dimers out of the water-soluble GlcN and GlcNAc monomeric units. Since the monomers and small oligomers are readily soluble in water, this would reduce unwanted pollution during the application of these structures. Additionally, water soluble chitosan chains would be a great solution for the application in environments where acidic solvents are unsuitable. In this project, the glycosylation reaction using a glycosyl acceptor and donor will be described. Also, the relation between the glucosamine chain structure and its solubility will be investigated.

Since chitosan can form films, the monomers and dimers will be applied to making films as well. Here, the strength of the films will be investigated. The formation of films out of monomer and/or dimer can offer an alternative way to form sustainable and simple films, since the monomers are readily available and less extreme reaction conditions are needed for their modification compared to chitosan. For the film formation, crosslinking agents will be used to help the crosslinking between the repeating units and therefore assist with the formation of the films.



### 3. Plan Experimental

#### 3.1. Glycosylation

The desired glucosamine acceptor and donor (**Figure 4**) were designed to allow selective  $\beta$ -(1 $\rightarrow$ 4)-glycoside bond formation. To obtain these compounds, multiple reaction steps are required, however, due to the best of my knowledge, no studies have been done on synthesizing these compounds with these structural properties. So, multiple steps from various papers were considered and combined to obtain the acceptors and donors.<sup>31–36</sup>

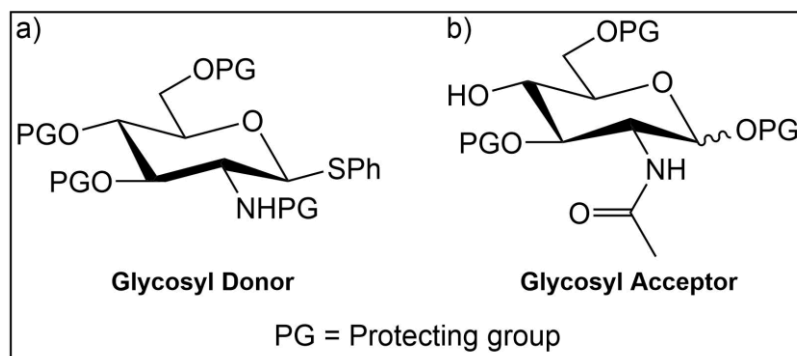


*Figure 4 - Proposed a) glycosyl donor and b) acceptor employed in this study.*

##### 3.1.1. Introducing Acceptor Protecting Groups

###### Anomeric Protection

Two anomeric protecting groups were proposed. Usually, for the protection of the anomeric position, allyl ethers are employed as the protecting group (**Scheme 1**, reaction 1).<sup>37–41</sup> The alternative anomeric protecting group is a methyl group (**Scheme 1**, reaction 2). Both protecting groups can be introduced by Fischer glycosylation reactions and are stable under reaction conditions when introducing the other protecting groups.<sup>42</sup> The methyl group, however, is preferred as an anomeric protecting group to avoid the use of a strong base like potassium tert-butoxide ( $\text{KO}^t\text{Bu}$ ) and the use of expensive metal catalysts that are commonly employed during the deallylation procedures.<sup>37–41</sup> Both strategies will be employed to test the feasibility of both experimental approaches.

###### OH Protection

To protect the remaining hydroxyl groups, a benzylidene and benzylation reaction on the 4,6-OH and 3-OH groups is employed respectively. The benzylidene reaction can be carried out by treatment of benzaldehyde and zinc chloride ( $\text{ZnCl}$ ). However, this approach requires the use of excess benzaldehyde.<sup>43</sup> Alternatively, benzaldehyde dimethyl acetal and para-toluenesulfonic acid ( $p\text{-TsOH}$ ) will be utilized as well for this step.<sup>33</sup>

The 3-OH will be protected by introducing benzyl ethers through a benzylation reaction as they are extensively utilized as hydroxyl protecting groups.<sup>44</sup> The benzyl ethers are easily introduced by typical benzylating conditions, using sodium hydride ( $\text{NaH}$ ) and benzyl bromide ( $\text{BnBr}$ ) in dimethylformamide ( $\text{DMF}$ ).<sup>43,45</sup>

##### 3.1.2. Introducing Donor Protecting Groups

###### Amine protection

Since the amine group on GlcNAc is already protected by an acetyl group ( $N\text{-Ac}$ ), it was decided to use GlcNAc as the starting compound. GlcNAc could be modified readily, without additional protection of the amine group, to reduce the amount of protecting and deprotecting steps. This allows for easier control of the degree of acetylation when making the dimers and oligomers.

GlcN was used as a starting compound as well. It has been shown before that the reactivity of 2-amino sugar donors can be adjusted by the choice of the protecting group at the nitrogen.<sup>46</sup> For example, *N*-trichloroethoxycarbonyl (*N*-Troc) protected glucosamines are more reactive than the corresponding *N*-Ac and *N*-phthalimide (*N*-Phth) protected glucosamines (**Figure 5**).<sup>47</sup> Moreover, the Troc group gives higher  $\beta$ -selectivities than other *N*-protecting groups and it can be removed under mild conditions.<sup>47,48</sup> Therefore, the Troc group was selected as an amine protecting group for GlcN, by treating GlcN with trichloroethoxycarbonyl chloride (TrocCl) and NaHCO<sub>3</sub> in water.<sup>36</sup>

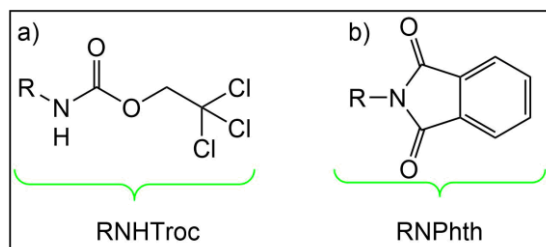


**Figure 5** – Amino protecting groups. A) 2,2,2-Trichloroethoxycarbonyl (Troc) protecting group and b) phthalimide (Phth) protecting group.

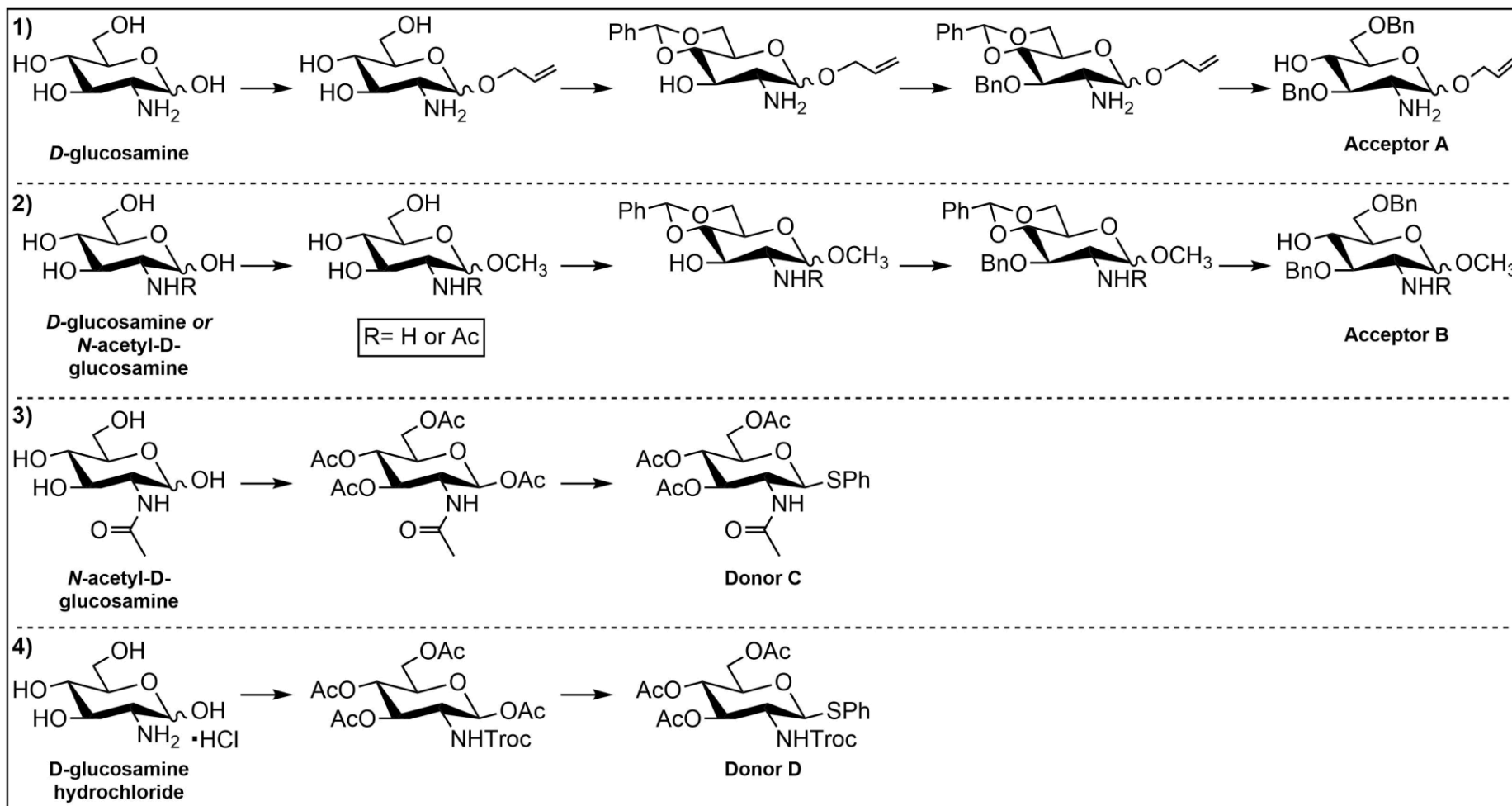
### OH protection

The OH groups on both GlcNAc and GlcN are protected by acetyl protecting groups, which were selected in terms of their ease of attachment and removal and stability under the reaction conditions throughout the reaction. The acetyl protecting groups are introduced by treating the monomers with acetic anhydride in pyridine.

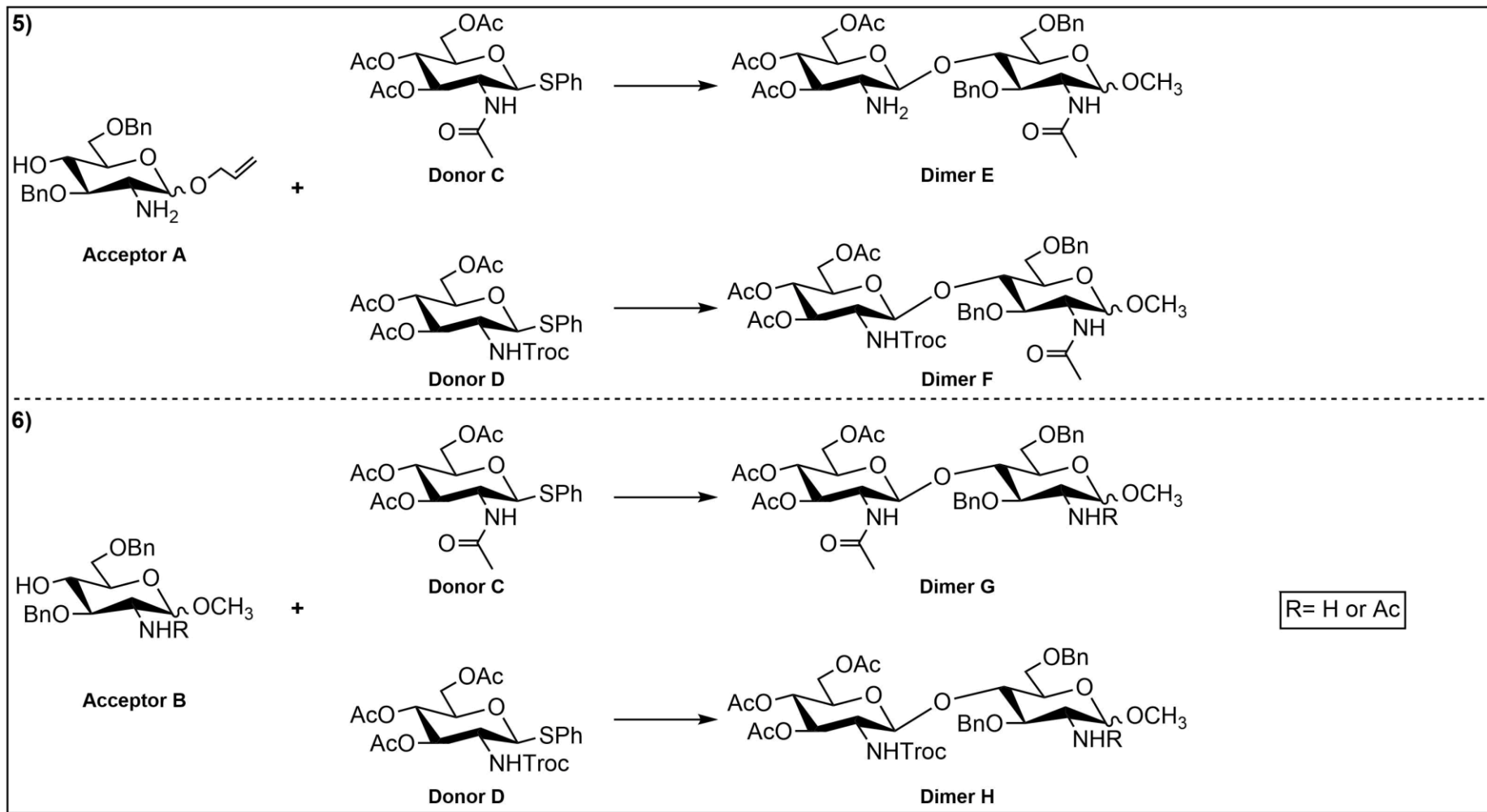
### Donor preparation

Finally, a thioglycoside has been selected as a glycosyl donor due to its stability under most reaction conditions frequently used for the introduction of protecting and functional groups.<sup>49</sup> Also, during glycosylations, the thio group can be activated using a variety of electrophiles under mild conditions to provide a glycosylating species.<sup>49</sup> The thio group is introduced on the anomeric position by treating the monomer with thiophenol and boron trifluoride etherate in cooled dichloromethane (CH<sub>2</sub>Cl<sub>2</sub>).<sup>33</sup>

The reaction schemes were proposed for the preparation of the acceptors and donors in **Scheme 1**. The proposed reactions for the glycosylation between the designed acceptors and donors to form dimers are shown in **Scheme 2**, where trimethylsilyl trifluoromethanesulfonate (TMSOTf) and *N*-iodosuccinimide (NIS) will be employed.<sup>31,50</sup> The experimental approaches are shown in **section 4**.



*Scheme 1 - Proposed reaction scheme for the preparation of the 1) free 4-OH acceptor A, 2) free 4-OH acceptors B, 3) thioglycoside donor C and 4) thioglycoside donor D.*



*Scheme 2 – Proposed glycosylation reaction between the 4-OH acceptors A and B and the thioglycoside donors C and D to form the desired  $\beta$ -(1→4)-dimers E, F, G and H.*

### 3.2. Crosslinking

The modification of chitosan occurs mainly on the amino groups.<sup>11,14,51</sup> Since the production and application of chitosan comes with disadvantages as mentioned in **Section 2**, an attempt will be made to crosslink the monomers, GlcN and GlcNAc, to make films as well. If possible, this can lead to a more sustainable way of making films based on the sugar molecules instead of the chitosan polymer.

However, to the best of my knowledge, no studies have been done on making films out of D-glucosamine monomers and their derivatives. Therefore, we were interested in studying the use of several organic bifunctional compounds for developing GlcN and/or GlcNAc monomer films. Two types of bifunctional compounds will be used: a linear dialdehyde and dicarboxylic acids with different chain lengths. For the former, glutaraldehyde will be used, while oxalic acid, malonic acid, succinic acid and suberic acid will be used for the latter (see **Figure 6**). Maleic anhydride will be employed as well, since it is a common crosslinker used for crosslinking chitosan.<sup>52,53</sup> Moreover, chitosan (75% deacetylated) will be crosslinked as a reference. To mimic the chitosan structure, a mixture of GlcN and GlcNAc in a ratio of 3:1 (w/w) will be crosslinked. Furthermore, a system of only GlcN will be crosslinked as well to see the influence of the degree of acetylation between the monomers.

Acetic acid and citric acid solutions are some of the most frequently used solvents to dissolve chitosan during film preparation.<sup>10,11,54</sup> Therefore, in addition to water, the crosslinking of chitosan and the monomers will be done by dissolving in acetic acid and citric acid as well. Crosslinking the monomers in water can lead to a decrease in unwanted organic solution waste.

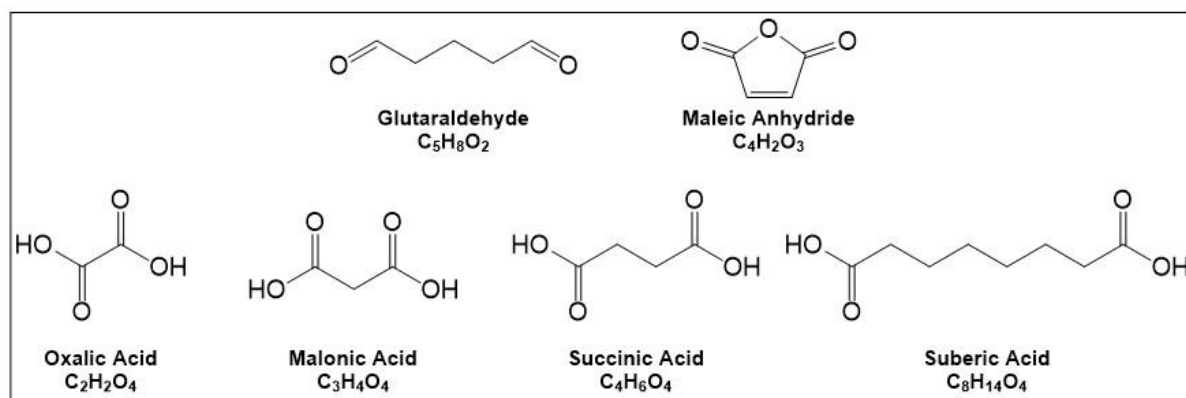


**Figure 6** – Structures of glutaraldehyde, maleic anhydride and dicarboxylic acid crosslinkers used for the crosslinking experiments.

## 4. Experimental

### 4.1. Materials

	Sigma-Aldrich (United States)		Merck (Germany)	Fluka (United States)	Alfa Aesar (United States)
Glycoside Experiments	Allyl alcohol (≥99%)	Zinc chloride	Thiophenol	Maleic anhydride (≥99%)	Potassium hydroxide (85%)
	Chlorotrimethylsilane (≥98.0%)	Benzyl bromide (98%)	Acetic acid (glacial, 100%)		
	Methanol (≥99.9%)	Anhydrous N,N-dimethylformamide (99.8%)			
	Acetyl chloride (≥99.0%)	Acetic anhydride (99.5%)			
	Silver acetate (99%)	Anhydrous pyridine (99.8%)			
	Benzaldehyde dimethyl acetal (99%)	Dichloromethane (over molecular sieves, 99.8%)			
	Acetonitrile (99.8%)	Boron trifluoride diethyl etherate			
	p-Toluenesulfonic acid monohydrate (99%)	Sodium bicarbonate (≥99.7%)			
	Benzaldehyde (>99%)	2,2,2-trichloroethyl chloroformate (98%)			
Crosslinking Experiments	Chitosan (degree of acetylation of ≥75%)				
	N-Acetyl-D-glucosamine (≥95%)				
	D-(+)-Glucosamine hydrochloride (≥99%)				
	Citric acid (99%)				
	Glutaraldehyde solution (25% in H <sub>2</sub> O)				
	Anhydrous oxalic acid				
	Malonic acid (99%)				
	Succinic acid (≥99%)				
Suberic acid (98%)					

## 4.2. Chemical Structure Analysis

The chemical structures of the products were analyzed by infrared spectroscopy (IR) and proton and carbon nuclear magnetic resonance ( $^1\text{H-NMR}$  and  $^{13}\text{C-NMR}$ ).

FT-IR/ATR analysis was performed using Perkin Elmer IR spectrometer (LiTaO<sub>3</sub> detector). The range was between 400 and 4000  $\text{cm}^{-1}$  with 32 scans and 2  $\text{cm}^{-1}$  resolution.

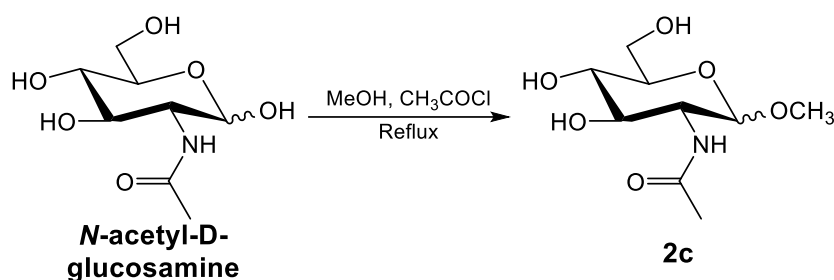
$^1\text{H}$ - and  $^{13}\text{C}$ -NMR spectra were recorded at 400 and 100 MHz, respectively on a MRF400.

The melting points were measured by heating the products on a heating plate until they melted.

## 4.3. Synthesis of Glycosyl Acceptor

### Anomeric Methylation

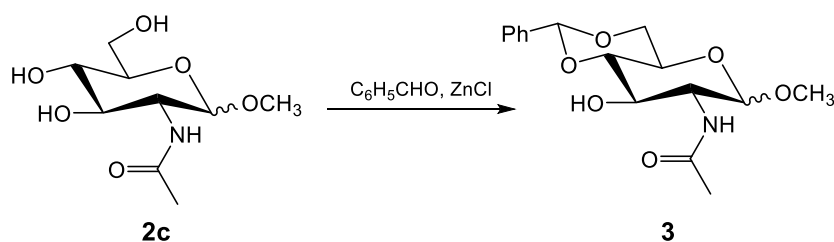
#### Methyl 2-acetamido-2-deoxy- $\alpha,\beta$ -D-glucopyranoside (**2c**)<sup>35</sup>



In a 50-mL three-neck flask, *N*-acetyl-D-glucosamine (2.5 g, 11.3 mmol) was suspended in a cooled down MeOH (25 mL). Acetyl chloride (0.5 mL) was added dropwise. Then, the mixture was refluxed under argon flow. After 48 h, the solution was cooled down to RT. Finely powdered silver acetate (1.98 g, 11.86 mmol) was added and stirred overnight. The mixture was filtered, and the silver salts were washed with methanol. The solvent was removed in vacuo to obtain a solid. The solid was recrystallized in ethanol to give brown crystals **2c** as a mixture of the  $\alpha$  and  $\beta$  anomer.

### 4,6-*O*-Benzylideneation

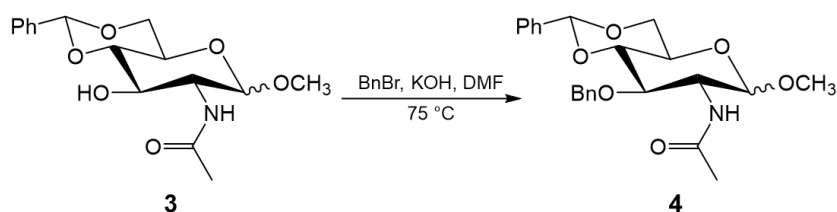
#### Methyl 2-acetamido-4,6-*O*-benzylidene-2-deoxy- $\alpha/\beta$ -D-glucopyranoside (**3**)<sup>35</sup>



To a suspension of dried **2c** (401.0 mg, 1.71 mmol) in benzaldehyde (1.25 mL, 12.25 mmol), anhydrous zinc chloride (311.7 mg, 2.29 mmol) was added. The mixture was stirred at RT under argon flow. After, 1 day, a mixture of hexane (10 mL) and water (10 mL) was added to the mixture and stirred for 30 mins. The resulting off-white precipitation was filtered and washed with a mixture of hexane and water (1:1, v/v). The solid was dried on an exicator overnight. The white powder was recrystallized with a mixture of methanol and water to get needles **3**.

### Benzylation

#### Methyl 2-acetamido-3-*O*-benzyl-4,6-*O*-benzylidene-2-deoxy- $\alpha/\beta$ -D-glucopyranoside (**4**)<sup>43</sup>

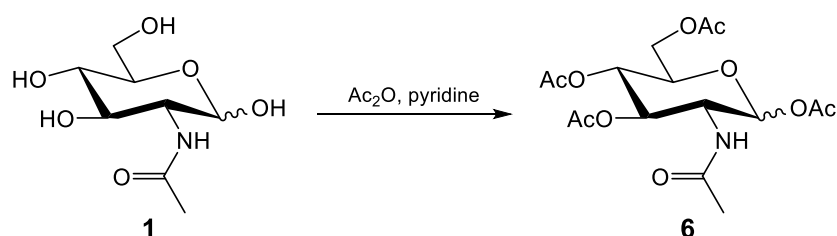


To a mixture of dried **3** (93.13 mg, 0.29 mmol), *N,N*-dimethylformamide (2.5 mL), and powdered potassium hydroxide (94.01 mg, 1.68 mmol), benzyl bromide (2 mL, 16.84 mmol) was added dropwise. The mixture was stirred vigorously for 15 min at 75° C under argon flow. The reaction was continued for 2 h while stirring. The solution was cooled down to RT and poured into cold water (25 mL) while stirring to get an off-white precipitation. The solid was collected by filtration, washed several times with cold water, and recrystallized from chloroform-hexane (3:1, v/v). The solid was dried in an exicator overnight to give a yellow solid **4**.

#### 4.4. Synthesis of Glycosyl Donors

##### *Acetylation of N-acetyl-D-glucosamine*

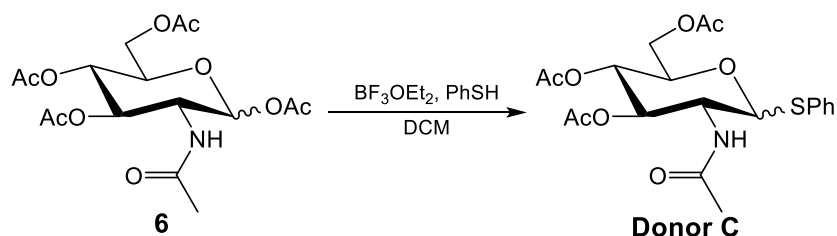
##### **1,3,4,6-Tetra-O-acetyl-2-acetamido-2-deoxy- $\alpha,\beta$ -D-glucopyranoside (6)**<sup>33</sup>



Acetic anhydride (4.7 mL, 49.72 mmol) was added to a solution of *N*-acetyl-D-glucosamine **1** (2.0 g, 9.05 mmol) in anhydrous pyridine (10 ml) under argon flow. The solution was stirred overnight at RT. After, the solution was diluted with CH<sub>2</sub>Cl<sub>2</sub> (20 ml) and washed with 1M aq. HCl (3 x 20 mL). The combined aqueous layers were extracted with CH<sub>2</sub>Cl<sub>2</sub> (3 x 20 ml). Then, the combined organic layers were washed with saturated aqueous NaHCO<sub>3</sub> solution (40 mL) and brine (40 ml), dried with Na<sub>2</sub>SO<sub>4</sub> and concentrated in vacuo to get a colorless gel. The gel was recrystallized in ether to yield a white solid **6** as a mixture of the  $\alpha$  and  $\beta$  anomer.

##### *Thio-N-acetyl-D-glucosamine donor*

##### **Phenyl 3,4,6-Tri-O-acetyl-2-acetamido-2-deoxy-1-thio- $\alpha,\beta$ -D-glucopyranoside donor (7)**<sup>33</sup>

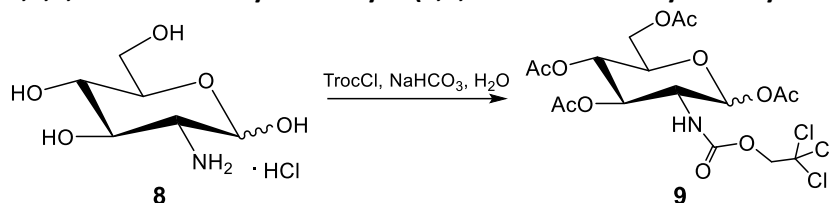


In a Schlenk flask, dried CH<sub>2</sub>Cl<sub>2</sub> (6.4 mL) was added to a dried compound **6** (299.5 mg, 0.77 mmol) while stirring under argon flow. Then, thiophenol (0.16 mL, 1.57 mmol) was added. The solution was cooled down in an ice/water bath. After, boron trifluoride etherate (0.4 mL, 3.24 mmol) was added. The reaction mixture was stirred at RT under argon flow. After 7 days, the pink solution was diluted with CH<sub>2</sub>Cl<sub>2</sub> (15 mL), washed with brine (15 mL) and dried with Na<sub>2</sub>SO<sub>4</sub>. The solution was dried in vacuo while heating at 43 °C to afford a yellow solid, **donor C**, as a mixture of the  $\alpha$  and  $\beta$  anomer.



### Troc Protection and Acetylation of D-glucosamine

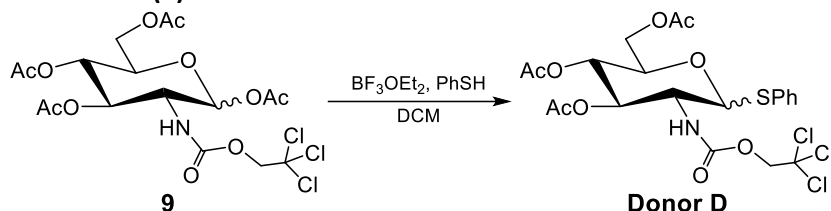
#### 1,3,4,6-Tetra-O-acetyl-2-deoxy-2-(2,2,2-trichloroethoxycarbonylamino)- $\alpha,\beta$ -D-glucopyranose (**9**)<sup>36</sup>



To a solution of dried D-glucosamine hydrochloride (2.16 g, 12.06 mmol) and NaHCO<sub>3</sub> (2.52 g, 30 mmol) in water (20 mL), trichloroethoxycarbonyl chloride (1.62 mL, 11.77 mmol) was added dropwise at RT, while vigorously stirring under argon flow. The mixture was stirred for 1 h, then neutralized with 1 M HCl (25 mL), concentrated, and dried in vacuo to yield a white powder. Anhydrous pyridine (10 mL) was added to the white powder and acetic anhydride (5 mL, 52.89 mmol) was added. The solution was stirred overnight under argon. The solution was diluted with 10 mL CH<sub>2</sub>Cl<sub>2</sub> and washed with 1M HCl (3 x 10 mL). The combined aqueous layers were extracted with CH<sub>2</sub>Cl<sub>2</sub> (3 x 10 mL). Then, the combined organic layers were washed with saturated aqueous NaHCO<sub>3</sub> solution (10 mL) and brine (10 mL), dried with Na<sub>2</sub>SO<sub>4</sub> and concentrated in vacuo to get a colorless oil **9** as a mixture of the  $\alpha$  and  $\beta$  anomer.

### N-Troc-Protected Thio-D-glucosamine Donor

#### Phenyl-3,4,6-Tri-O-acetyl-2-(2,2,2-trichloroethoxycarbonylamino)-2-deoxy-1-thio- $\alpha,\beta$ -D-glucopyranose donor (**9**)<sup>33</sup>



In a Schlenk flask, dried CH<sub>2</sub>Cl<sub>2</sub> (10 mL) was added to a dried compound **9** (469.52 mg, 0.90 mmol) while stirring under argon flow. Then, thiophenol (0.26 mL, 2.55 mmol) was added. The solution was cooled down in an ice/water bath. After, boron trifluoride etherate (0.7 mL, 5.67 mmol) was added. The reaction mixture was stirred at RT under argon flow. After 7 days, the orange solution was diluted with CH<sub>2</sub>Cl<sub>2</sub> (15 mL), washed with brine (15 mL) and dried with Na<sub>2</sub>SO<sub>4</sub>. The solution was dried in vacuo while heating at 50 °C to afford a brown solid, **donor D**, as a mixture of the  $\alpha$  and  $\beta$  anomer.

### 4.5. Experimental Crosslinking

1% (w/w) Chitosan, 1% (w/w) D-glucosamine hydrochloride or 1% (w/w) D-glucosamine hydrochloride : N-acetyl-D-glucosamine (3:1, w/w) was dissolved in 5% (w/w) acetic acid (20 mL) or 5% (w/w) citric acid (20 mL) at room temperature. The solutions were stirred overnight. After, 1% (w/w) crosslinking agent (glutaraldehyde, maleic anhydride, oxalic acid, malonic acid, succinic acid or suberic acid) was added to the solutions and stirred for 1 hour. Then, approximately 2.2 mL of each solution was cast on a glass plate and let dry in air. The solutions were warmed up to 80 °C and stirred for 2 hours. Again, approximately 2.2 mL of each solution was cast on a glass plate again and let dry in air.

The same experiments were also done by dissolving 1% (w/w) D-glucosamine hydrochloride or 1% (w/w) D-glucosamine hydrochloride: N-acetyl-D-glucosamine (3:1, w/w) in water (20 mL).

## 5. Results and Discussion

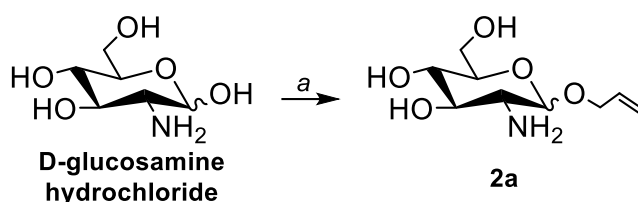
### 5.1. Glycosyl Acceptor Synthesis

#### 5.1.1. D-glucosamine Acceptor

##### *Anomeric Alkylation*

The experimental for the anomeric alkylation is mentioned in **SI1**. The synthesis of the acceptor started with the alkylation of GlcN (**Scheme 3**). After treatment with allyl alcohol and chlorotrimethylsilane (TMSCl), the reaction afforded compound **2a** as a white powder. However, the spectroscopic data of **2a** were not in agreement with those reported in the literature.<sup>31,55</sup> The <sup>1</sup>H-NMR spectrum (**SI1, Figure 33B**) was similar to the unmodified GlcN monomer and did not show peaks corresponding to the protons attached to the allyl group. In the literature, the protons on the allyl group are characterized by multiple multiplets between 5 and 6 ppm, but these were absent in the spectrum.<sup>31,55</sup>

So, this step was redone with a few modifications. The GlcN powder was dried under vacuum to remove potential presence of moisture, moreover, the allyl alcohol was bubbled with argon to remove additional air and moisture. Also, the experiment was carried out under argon flow to remove air from the system, since it was thought that moisture and air were interfering with the reaction. Again, a white powder was obtained, and the corresponding <sup>1</sup>H-NMR spectrum is shown in **Figure 33C (SI1)**. Furthermore, the peaks belonging to the protons of the allyl group were not detected. Thus, the anomeric alkylation of GlcN monomer was not achieved. In the source used for this step, glucose was used instead of GlcN.<sup>31</sup> So, the basic amine group on GlcN could have been interfering with the alkylation, causing TMSCl to not work efficiently as an acid catalyst. Contrary to the literature, where it was reported that TMSCl is able to effectively promote Fischer glycosylation reactions.<sup>31,55</sup> Moreover, during the experiments, the system was probably not sufficiently moisture free, which may have caused TMSCl to trap water and therefore blocking the reaction. So, it was decided to halt this reaction and continue with the synthesis of the methyl acceptor **B** in the following section.



**Scheme 3** - Anomeric alkylation of *N*-acetyl-*D*-glucosamine. Reaction conditions a) Allyl alcohol, TMSCl, RT, 12h.

##### *Anomeric Methylation*

The experimental anomeric methylation of GlcN is described in **SI2**.<sup>32</sup> The acceptor synthesis started with the anomeric methylation of GlcN (**Figure 7**). After a standard reaction of 2 hours at RT, a slightly yellow compound was obtained, which was characterized with <sup>1</sup>H-NMR (**SI2, Figure 34B**). The spectroscopic data were not in agreement with those in literature.<sup>32</sup> The spectrum did not show any new proton peaks corresponding to the methyl group. Also, the measured spectrum was almost identical to the spectrum of the unmodified GlcN monomer (except for some impurities caused by triethylamine and methanol).

So, the reaction was carried out twice again but under different conditions: for 67 hours at room temperature and 67 hours while refluxing. Both experiments yielded slightly yellow powder and the corresponding <sup>1</sup>H-NMR spectra are shown in **Figure 34C** and **Figure 34D (SI2)** respectively. Again, the data were not in accordance with the literature, as no peaks were present corresponding to the methyl group.<sup>32</sup> Again, the source was based on the methylation of glucose instead of GlcN. Just like the

previous allylation experiments, the basic amine group could be hindering the reaction as it is more basic than the -OH groups.<sup>56</sup>

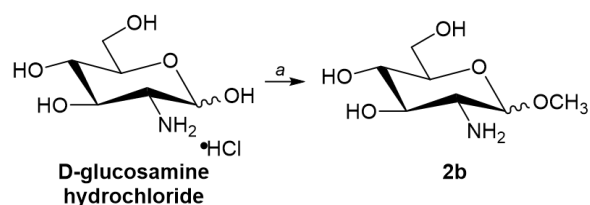
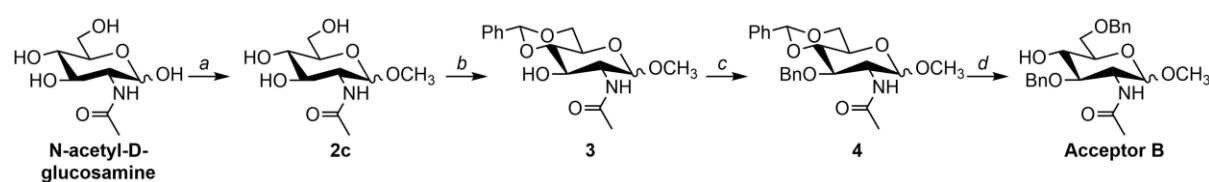


**Figure 7** - Anomeric methylation of D-glucosamine hydrochloride. Reaction conditions a) MeOH, CH<sub>3</sub>COCl, RT.

### 5.1.2. N-acetyl-D-glucosamine Acceptor

Since the anomeric protection on GlcN was not accomplished, the synthesis of the free 4-OH acceptor was performed on the GlcNAc monomer (**Scheme 4**).



**Scheme 4** - Proposed reaction scheme for the preparation of the free 4-OH acceptor. Reaction conditions: a) MeOH, CH<sub>3</sub>COCl, 0 °C to RT, 2 days; b) Method 1: benzaldehyde dimethyl acetal, p-TsOH, RT, 2h or method 2: Benzaldehyde, ZnCl<sub>2</sub>, RT, 1 day; c) BnBr, KOH, DMF, 75 °C, 2 h; d) NaBH<sub>3</sub>CN, THF, sat. HCl in ether, 0 °C, 3 h.

#### Anomeric Methylation

The methylation of N-Acetyl-D-glucosamine afforded brown crystals with 69% yield. The crystals were analyzed with IR spectroscopy (**Figure 36**) and <sup>1</sup>H-NMR (**Figure 37B**) in **SI5**. The IR spectra show an increase in the peak intensity at 2840 cm<sup>-1</sup>, corresponding to the vibration of C-H stretching bond. This suggests that the methyl group is attached to the anomeric position.

The <sup>1</sup>H-NMR spectrum shows a shift in all peaks compared to the <sup>1</sup>H-NMR spectrum of the unmodified GlcNAc monomer. Furthermore, two new singlet peaks appeared at 3.37 ppm and 3.25 ppm, which confirms the presence of the methyl group on compound **2c**. Then, the compound was measured with <sup>13</sup>C-NMR, which is shown in **Figure 38 (SI5)**. The spectrum demonstrates that there is a double peak for every carbon atom present in the molecule, meaning that the brown crystals consist out of an anomeric mixture of **2c**. The characterization analysis of this methylation step is consistent with the literature.<sup>35</sup>

In contrary to the allylation and methylation of GlcN in the previous sections, the methylation was achieved on the GlcNAc monomer. The difference between the two experiments originates from the used monomer. The difference between the two methylation experiments, is probably due to the presence of the N-Acetyl group, which reduces the accessibility of the amine group and therefore preventing the basic amine group from hindering the methylation reaction.

#### 4,6-O-Benzylidenation

The next step involved the protection of the 4,6-OH groups through the formation of a benzylidene acetal to afford intermediate **3**. Benzaldehyde dimethyl acetal and p-toluenesulfonic acid (p-TsOH) were employed.<sup>33</sup> The corresponding experimental is shown in **SI3**. Brown crystals were obtained, which were then analyzed with ATR-IR and <sup>1</sup>H-NMR spectroscopy. The afforded IR spectrum **Figure 35 (SI3)** did not show absorption peaks belonging to the vibration of the CH bonds on the benzylidene protecting group. Also, the broad OH peak around 3294 cm<sup>-1</sup> was still present, meaning that no 4,6-O-benzylidenation reaction has taken place on compound **2c**. This did not correspond with literature,

which was carried out under same conditions.<sup>33</sup> During the reaction, the solute was not able to dissolve, which could have obstructed the reaction.

Thus, the benzylideneation step was carried out by modifying **2c** through the traditional way with benzaldehyde in the presence of powdered zinc chloride.<sup>35</sup> These conditions afforded the production of **3** in 34% yield. The off-white powder was measured with ATR-IR spectroscopy, which is shown in **Figure 39 (SI6)**. New absorption peaks between  $650\text{ cm}^{-1}$  and  $750\text{ cm}^{-1}$  appeared, belonging to the vibration of a benzene ring. Furthermore, the original broad peak between  $3000\text{ cm}^{-1}$  and  $3600\text{ cm}^{-1}$  from **Figure 36** narrowed into a sharp peak corresponding to an NH- and OH-group at  $3290\text{ cm}^{-1}$  and  $3297\text{ cm}^{-1}$  respectively. The narrow, sharp peaks and the benzene peaks suggest that multiple OH groups were protected by the benzylidene protecting group.

The  $^1\text{H}$ - and  $^{13}\text{C}$ -NMR spectra are shown in **Figure 40** and **Figure 41 (SI6)** respectively. The former spectrum shows new peaks (multiplet) at 7.42 – 7.30 ppm and 5.58 ppm belonging to the five protons on the benzene ring and the -CHPh proton accordingly, which were in accordance with literature.<sup>35</sup>

The  $^{13}\text{C}$ -NMR does not show double peaks, meaning that product **3** does not consist out of an anomeric mixture anymore. This is due to the unsuccessful separation of the anomers during the recrystallization process, as no product was found in the recrystallization solvent. It can be speculated that the product is the  $\alpha$ -anomer since the J-coupling constant of H-1 is 3.6 Hz. According to the Karplus equation, the rotational angle between the coupled protons is small.<sup>57</sup> As a result, the anomeric proton (H-1) is in the equatorial position, leading to the formation of an  $\alpha$ -anomer. The preference for the formation of the  $\alpha$ -anomer has been reported multiple times before.<sup>35,43,58</sup> Despite the goal to make a linear  $\beta(1,4)$ -linked chain, it was decided to continue the synthesis with the  $\alpha$ -anomer.

#### Benzylation

The last protecting step was the benzylation of the free 3-OH position of compound **3** to afford a yellow solid **4** in 61% yield. The benzylation was achieved by using benzyl bromide and powdered potassium hydroxide in N,N-dimethylformamide (DMF). The IR spectrum (**SI7, Figure 42**) displays that the prominent OH peak around  $3297\text{ cm}^{-1}$  disappeared completely, leaving only a small amine peak at  $3284\text{ cm}^{-1}$ , suggesting that the reaction had taken place on the free 3-OH group.

The  $^1\text{H}$ -NMR (**SI7, Figure 43**) exhibits more conspicuous peaks (multiplet) between 7.01 – 7.40 ppm, belonging to the 10 protons on the two aromatic rings. Also, a distinct multiplet between 4.51 - 4.64 ppm belongs to the two protons on the -CH<sub>2</sub>Ph protecting group.

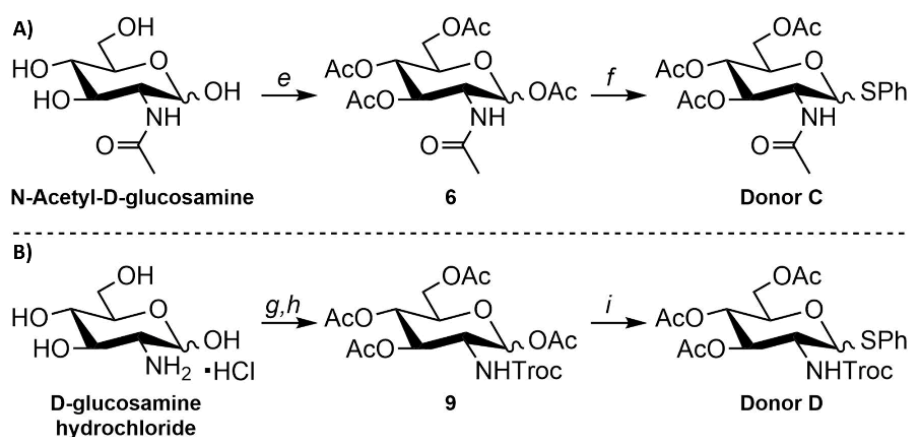
The  $^{13}\text{C}$ -NMR spectrum is shown in **Figure 44 (SI7)**. The appearance of multiple new peaks between 126 – 140 ppm and at 100.71 ppm correspond to the carbon atoms on the benzene ring and CH-Ar bond of the benzyl ether protecting group respectively.

So, all the results mentioned above suggest that all hydroxyl groups on GlcNAc were protected, agreeing with the literature sources.<sup>34,35</sup>

The last step of the acceptor synthesis (**SI4**), involving the selective benzylidene acetal ring opening towards the free 4-OH acceptor **B** was not achieved. Moreover, the separation of the two different anomers throughout the sequence intermediates was unsuccessful, due to the use of differing eluents during the thin layer chromatography (TLC) and the column chromatography. Thus, the synthesis towards acceptor **5** was not accomplished and the provided procedure was challenged by difficult control of the intermediates and low yield.

## 5.2. Glycosyl Donor Synthesis

The preparations of the donor moieties were performed using a simple sequence starting from *N*-Acetyl-D-glucosamine and D-glucosamine hydrochloride (**Scheme 5**). Martín-Lomas et al. showed that this synthesis was possible by using GlcN as the starting monomer, however, in this research both GlcN and GlcNAc will be modified under similar conditions.<sup>33</sup> Two differences are noted: 1) the amine group on GlcNAc was not modified as it is already protected by the acetyl group, and 2) the free amine group on GlcN was not protected with an azide group, due to explosive hazards. Instead, it was protected with a Troc protecting group.<sup>59</sup>



**Scheme 5** – Reaction scheme for the preparation of the thioglycoside donors from A) *N*-acetyl-D-glucosamine and B) D-glucosamine hydrochloride. Reaction conditions: e)  $\text{Ac}_2\text{O}$ , pyridine, RT, overnight; f)  $\text{BF}_3\text{OEt}_2$ , PhSH, DCM, 0 °C to RT, 7 days; g) TrocCl,  $\text{H}_2\text{O}$ ,  $\text{NaHCO}_3$ , 0 °C to RT, 1 h; h)  $\text{Ac}_2\text{O}$ , pyridine, RT, overnight; i)  $\text{BF}_3\text{OEt}_2$ , PhSH, DCM, 0 °C to RT, 7 days.

### 5.2.1. *N*-acetyl-D-glucosamine Donor Synthesis

#### Acetylation

The acetylation of all the OH groups on GlcNAc was obtained by treatment with acetic anhydride in pyridine. Thus, 1,3,4,6-Tetra-*O*-acetyl-GlcNAc (**6**) was obtained in 71% yield. The IR spectrum shown in **Figure 8** shows that the distinct OH absorption peak around  $3500\text{ cm}^{-1}$  is missing. Also, a prominent ester peak at  $1740\text{ cm}^{-1}$  suggests that all OH groups transformed into acetyl groups.

The presence of the 5 peaks around 2 ppm in the corresponding  $^1\text{H}$ -NMR spectrum (**Figure 9**) confirms that the acetylation of all OH groups was achieved where all four OH groups were acetylated.

This was further confirmed by the  $^{13}\text{C}$ -NMR spectrum in **Figure 10**, where the five peaks between 169 – 170 ppm originate from the  $-\text{COO}$  acetyl bonds. Furthermore, the five peaks between 20 - 23 ppm arise from the  $-\text{CH}_3\text{CO}$  acetyl bonds as well. These results confirm that the acetylation of GlcNAc was achieved. However, the  $^{13}\text{C}$ -NMR spectrum shows that for each carbon atom on intermediate **6** only one peak is involved, meaning that only one anomer was formed. Again, only the  $\alpha$ -anomer was produced, as the J-coupling constant of H-1 was 3.7 Hz, derived from the  $^1\text{H}$ -NMR spectrum.

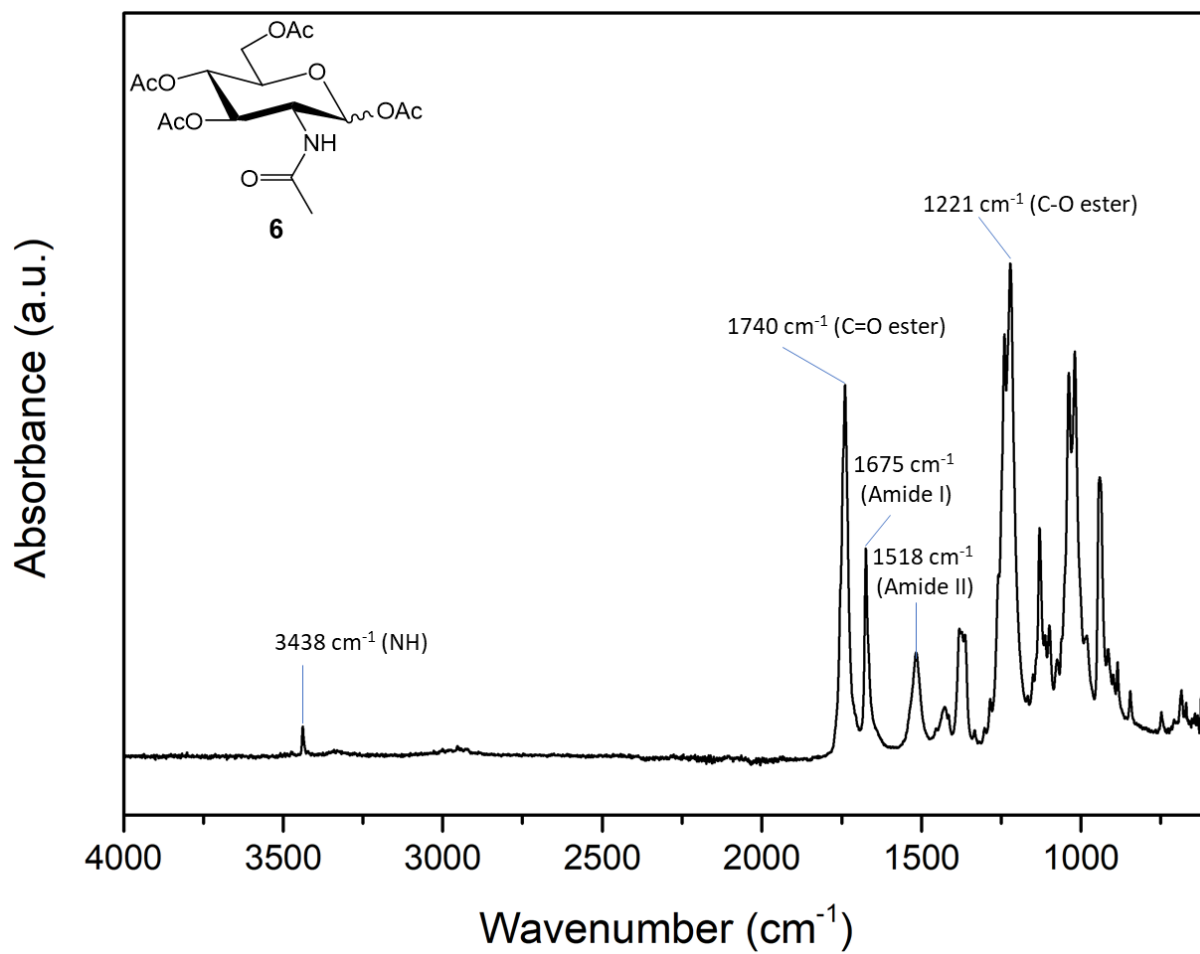


Figure 8 - Measured ATR-IR spectrum of compound 6 after acetylation of N-acetyl-D-glucosamine.

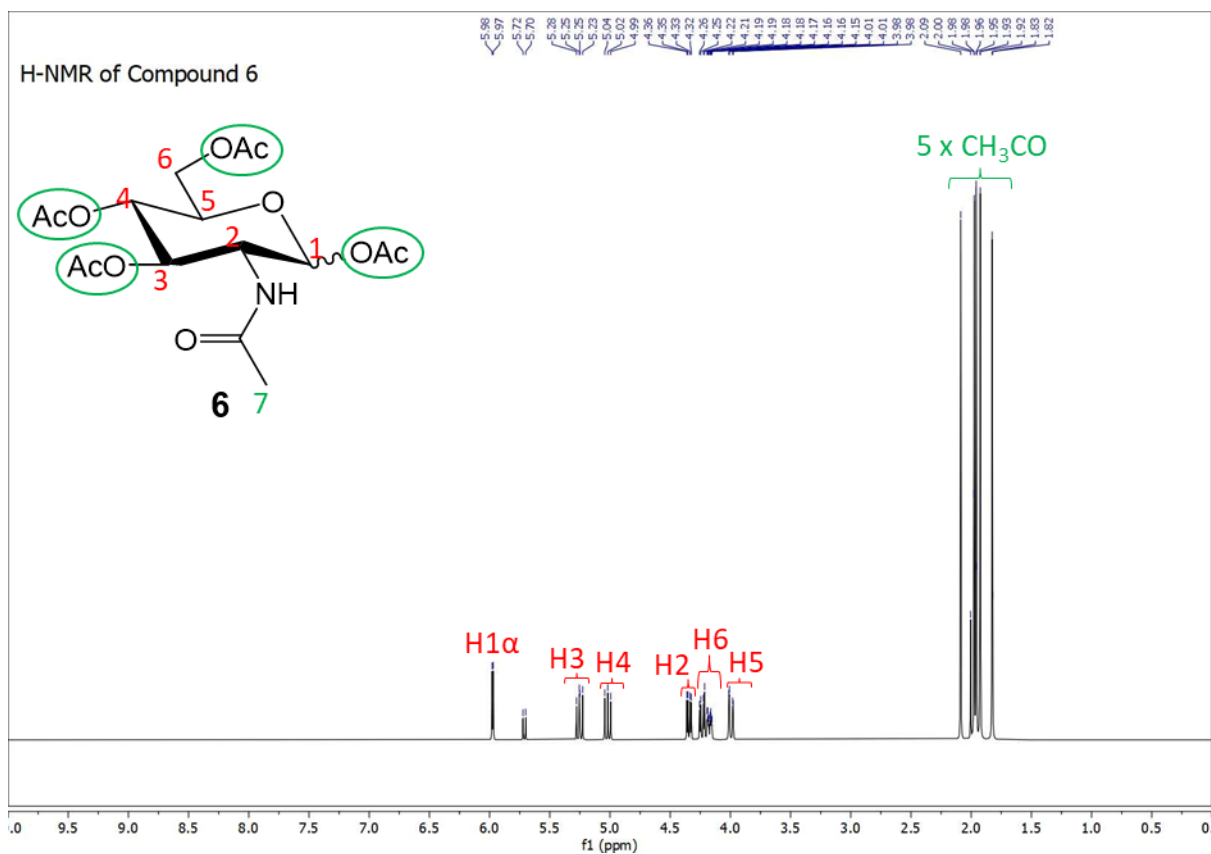


Figure 9 - Measured <sup>1</sup>H-NMR spectrum of compound 6 after acetylation of N-acetyl-D-glucosamine.

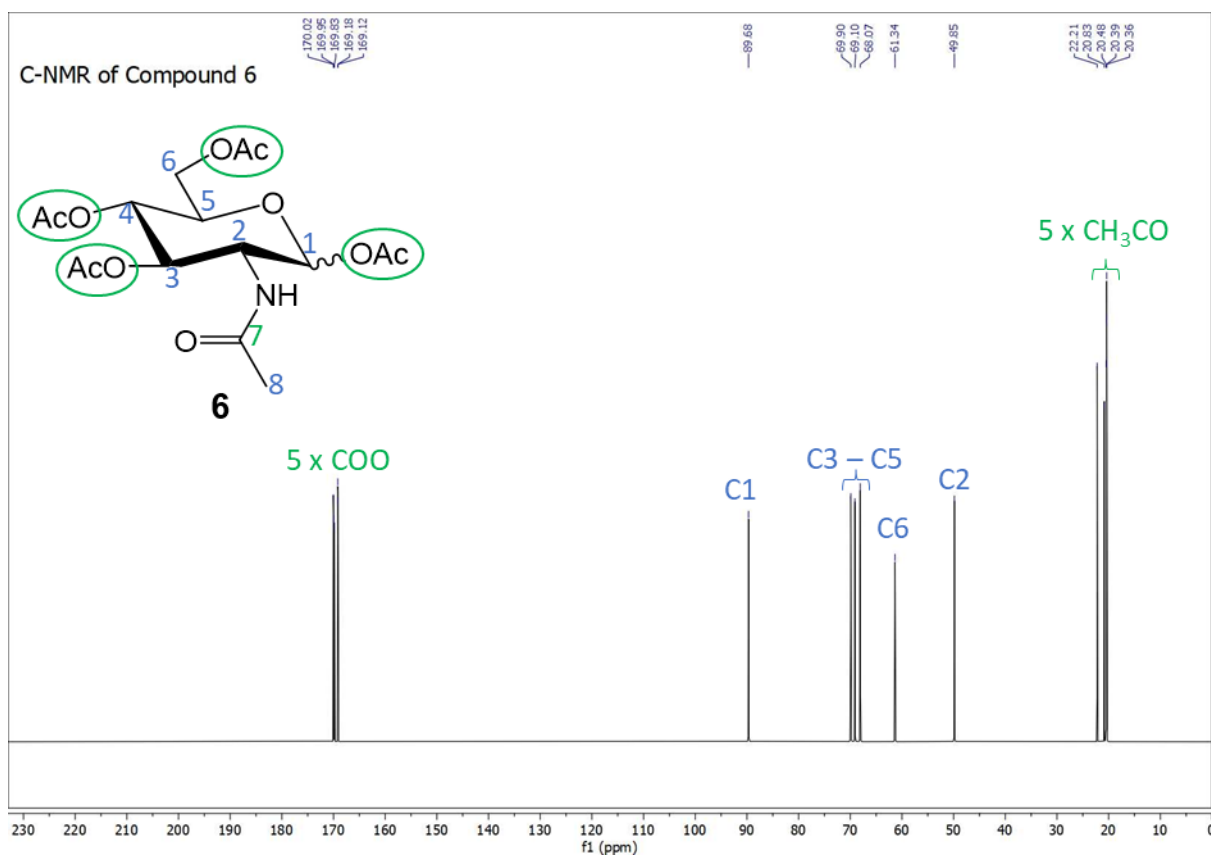


Figure 10 - Measured <sup>13</sup>C-NMR spectrum of compound 6 after acetylation of N-acetyl-D-glucosamine.

### Thio N-acetyl-D-glucosamine Donor

Next, treatment of **6** with  $\text{BF}_3\text{OEt}_2$  and thiophenol afforded the desired thioglycoside donor **C** in 38% after 7 days. The acetyl ester absorption peak  $1740\text{ cm}^{-1}$  diminished in intensity, meaning that less vibrating acetyl groups are present. Moreover, the appearance of absorption peaks around  $642 - 742\text{ cm}^{-1}$  suggests that the reaction between **6** and thiophenol has taken place on the anomeric acetyl group and a new  $-\text{SPh}$  bond had formed.

Then, the donor was measured with  $^1\text{H-NMR}$  spectroscopy, where the spectrum is shown in **Figure 12**. The disappearance of one of the acetyl peaks around 2 ppm and the appearance of a multiplet between 7.13 – 7.45 (associated with the five protons on the aromatic ring) confirms the synthesis of **donor C**.

This was further proved by the  $^{13}\text{C-NMR}$  spectrum shown in **Figure 13**. Here, the disappearance of one of the acetyl peaks between 169 – 170 ppm and the appearance of the benzene carbon peaks 127 – 134 ppm confirm the attachment of the thiobenzene group to the anomeric position of **donor C**.

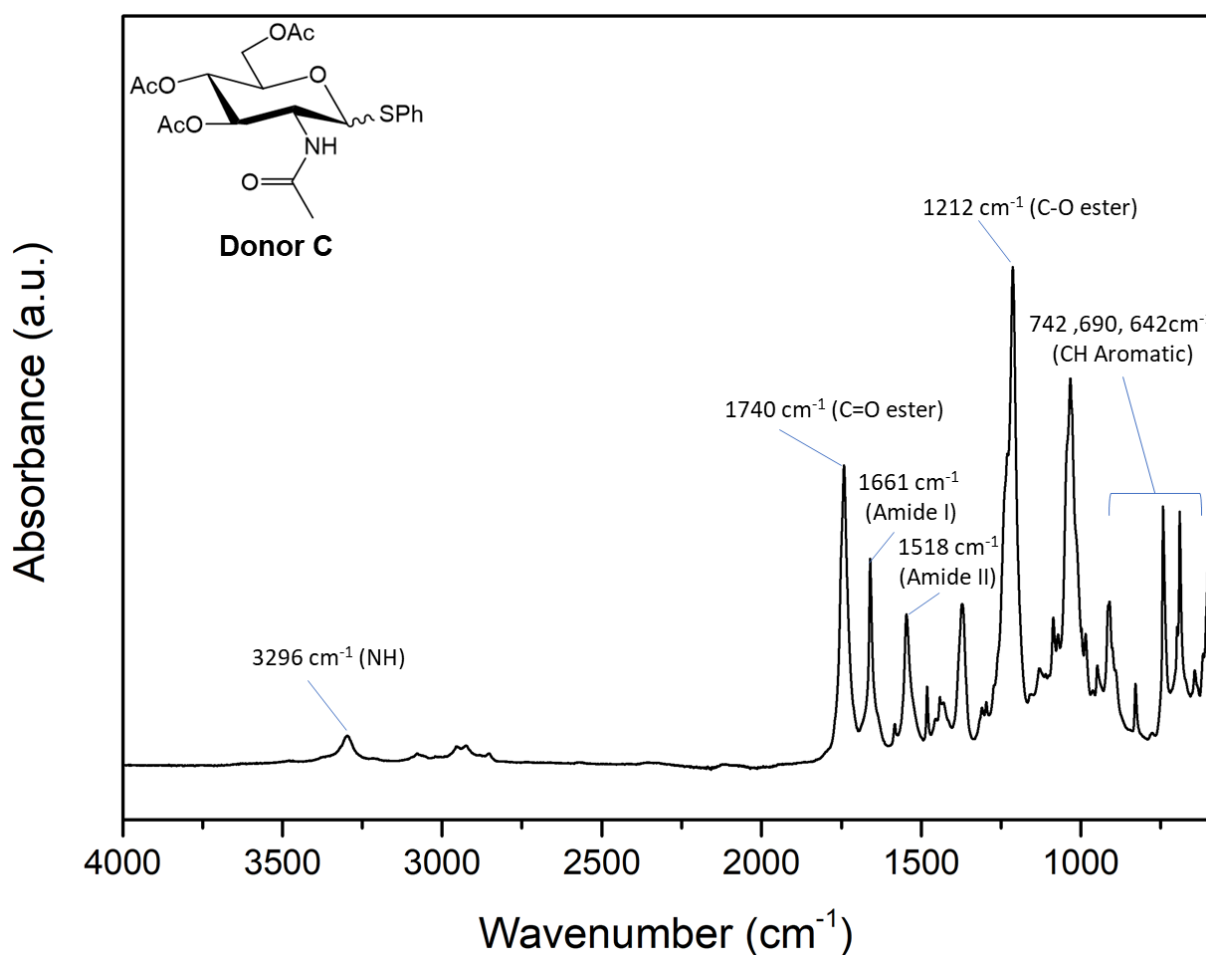


**Figure 11** - Measured ATR-IR spectrum of synthesized thioglycoside **donor C**.



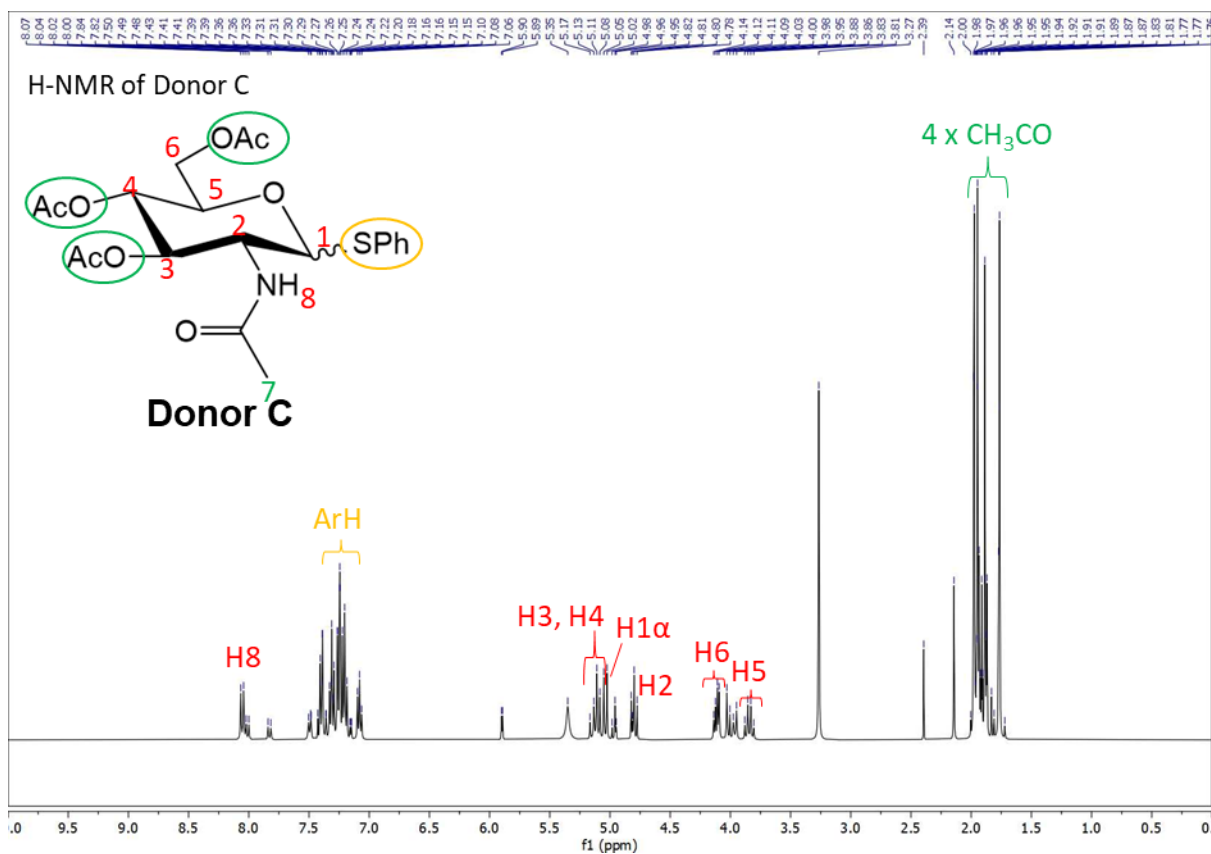


Figure 12 - Measured <sup>1</sup>H-NMR spectrum of synthesized thioglycoside *donor C*.

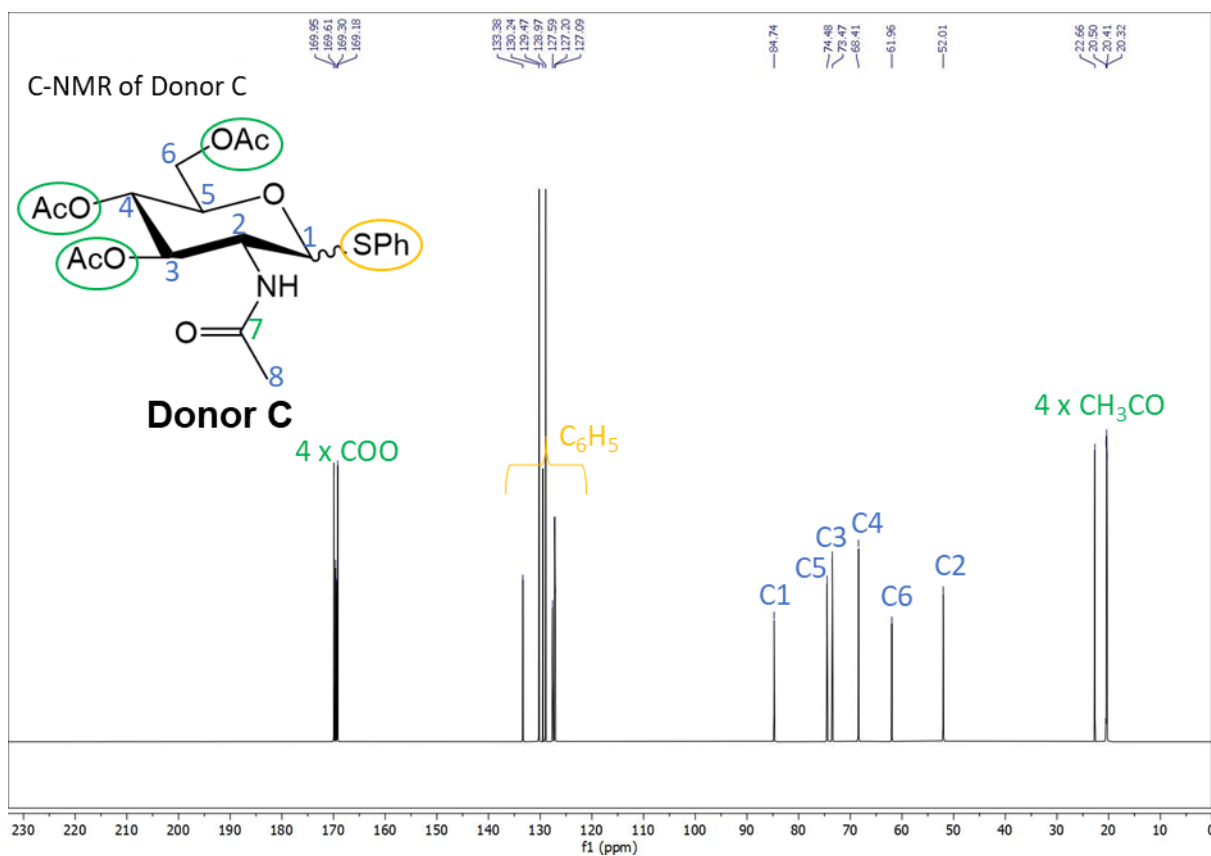


Figure 13 - Measured <sup>13</sup>C-NMR spectrum of synthesized thioglycoside *donor C*.

### 5.2.2. D-glucosamine Donor

#### *Troc Protection and Acetylation*

The preparation of the D-glucosamine **donor D** from GlcN (**Scheme 5B**) is described in the following section.

First, D-glucosamine hydrochloride was treated with trichloroethoxycarbonyl chloride (TrocCl) and NaHCO<sub>3</sub> in water. After, the product was acetylated by treatment with acetic anhydride in pyridine to isolate intermediate **9** in 15% yield after two steps. To confirm the synthesis of the amine and hydroxyl protected glucosamine monomer, the product was analyzed with ATR-IR (**Figure 14**), <sup>1</sup>H-NMR (**Figure 15**) and <sup>13</sup>C-NMR (**Figure 16**) spectroscopy.

The IR spectrum of compound **9** displays an absorption peak at 818 cm<sup>-1</sup> which corresponds to a C-Cl bond, originating from the Troc protecting group. Also, the spectrum implies that no OH bonds are present in the structure as there are no corresponding absorption peaks present around 3400 cm<sup>-1</sup>. A prominent absorption peak at 1735 cm<sup>-1</sup> derived from the acetyl ester bonds emerged as well. So, these absorption peaks imply that the amine and hydroxyl groups on GlcN are protected by the Troc and acetyl groups respectively.

To further confirm the attachment of the protecting groups, the <sup>1</sup>H-NMR spectrum displays a multiplet between 4.81 – 5.02 ppm, originating from the two protons on the -CH<sub>2</sub>CCl<sub>3</sub> part of the Troc protecting group. Additionally, the four peaks between 1.88 – 2.13 ppm are derived from the 12 protons on the four acetyl ester groups. Moreover, the J-coupling constant of H-1 was 3.5 Hz and therefore, an α-anomer was produced again.

The carbon atoms on the Troc protecting group cause the detection of the peaks at 54.76 ppm (-COON), 96.08 ppm (-CCl<sub>3</sub>) and 73.52 ppm (C-CCl<sub>3</sub>) in the <sup>13</sup>C-NMR spectrum. Moreover, the four peaks between 169 – 170 ppm and 20 – 21 ppm originate from the attachment of the acetyl protecting groups.

So, the full protection of the functional groups on GlcN was achieved, therefore the next step was to attach the thio group to finish the donor preparation.

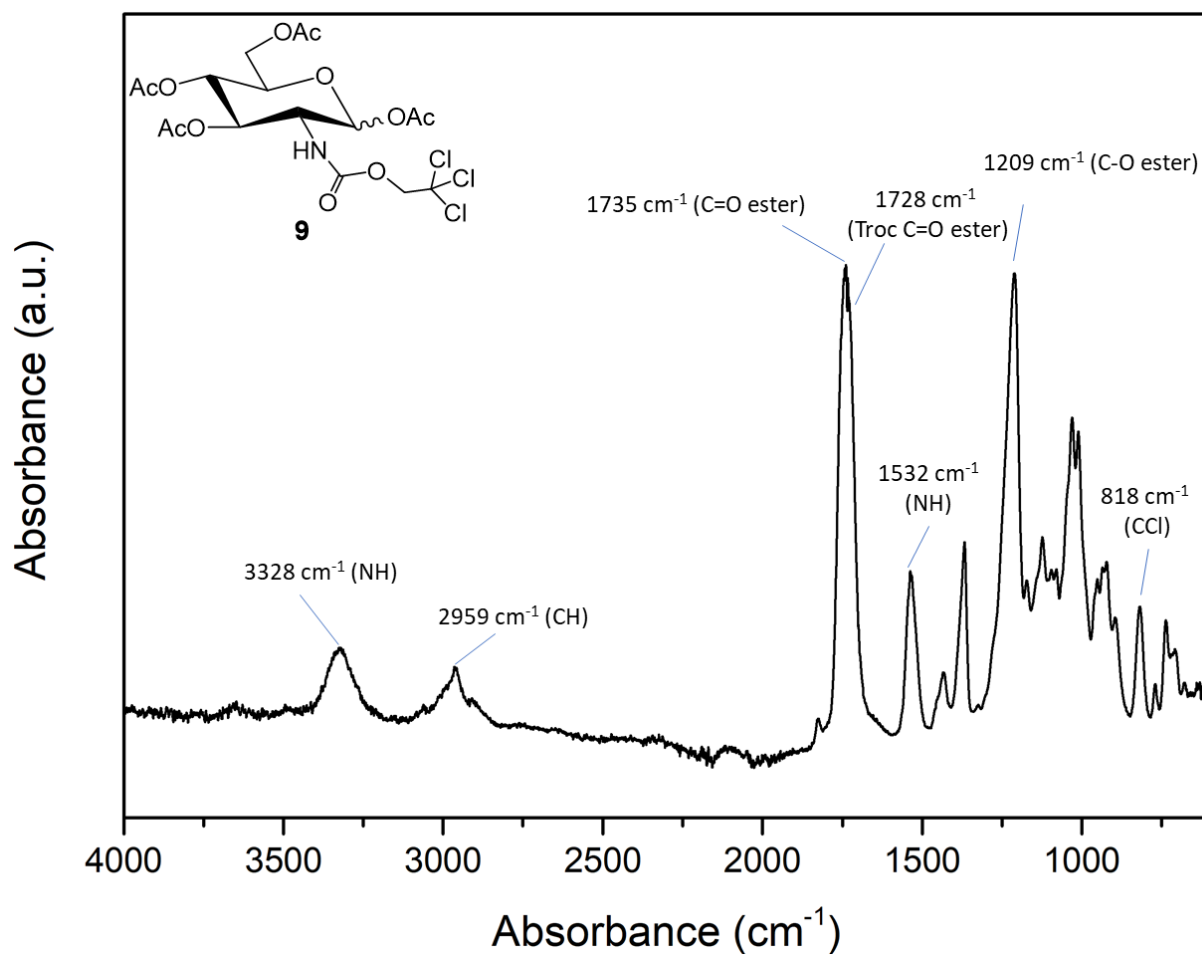
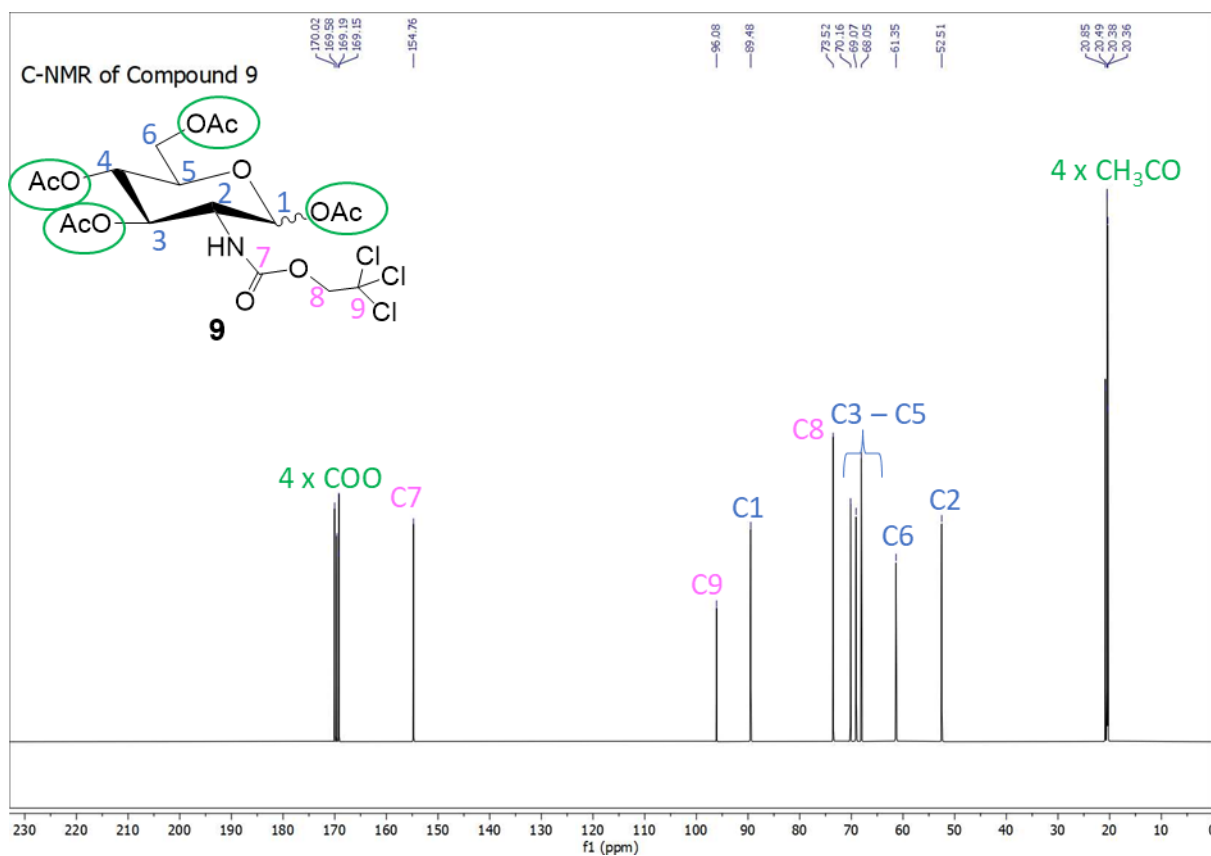
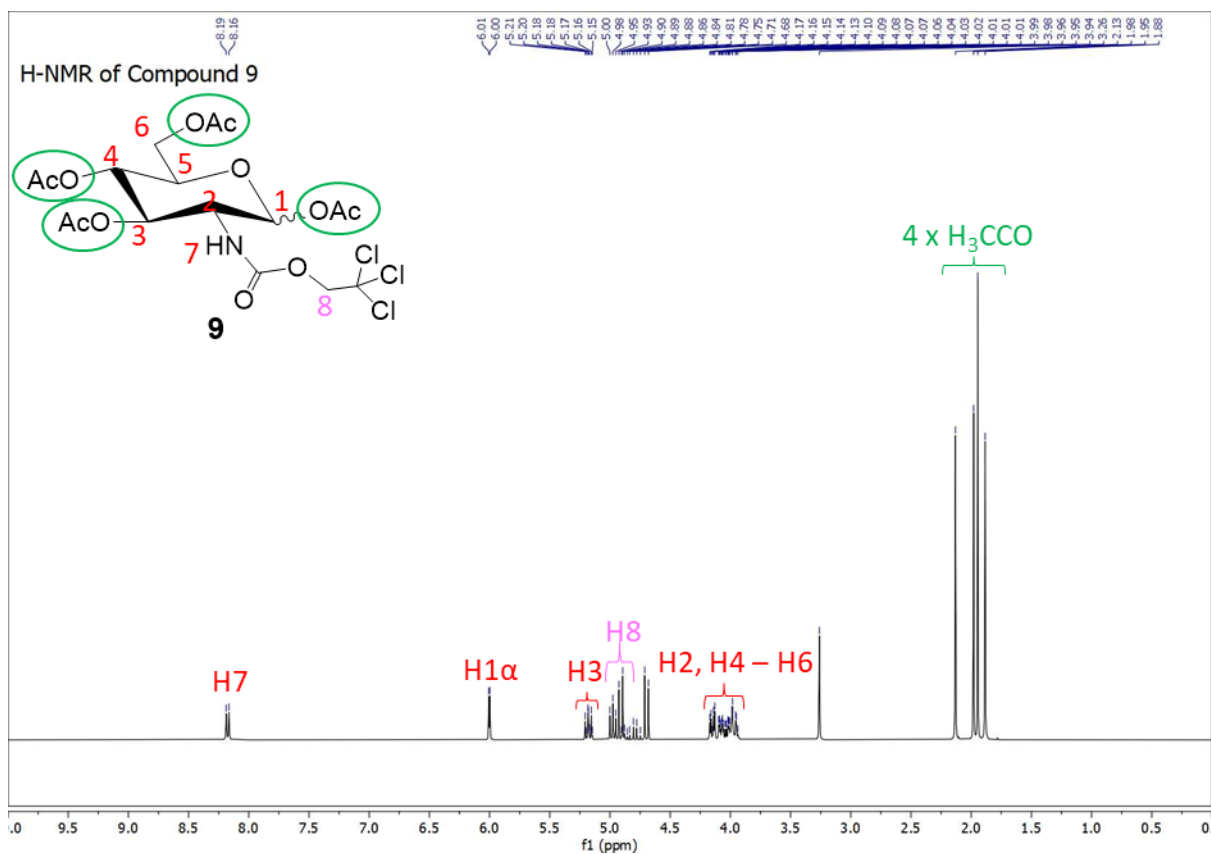


**Figure 14** - Measured ATR-IR spectrum of compound 9 after N-Troc protection and acetylation of D-glucosamine hydrochloride (GlcN•HCl).



### *N-Troc-protected Thio D-glucosamine Donor*

Subsequent treatment of compound **9** with  $\text{BF}_3\text{OEt}_2$  and thiophenol afforded the yellow thioglycoside donor **D** in 53% yield. To verify the synthesis of the thio GlcN donor, the product was analyzed by  $^1\text{H-NMR}$  and  $^{13}\text{C-NMR}$  spectroscopy, which are shown in **Figure 17** and **Figure 18** respectively.

The  $^1\text{H-NMR}$  spectrum shows a multiplet between 7.04 – 7.38 ppm, which is caused by the five protons on the aromatic thiol at the anomeric position.

Moreover, the  $^{13}\text{C-NMR}$  spectrum confirms the introduction of the aromatic thiol group due to the appearance of the four peaks between 128 – 131 ppm, corresponding to the PhS- bond. However, the spectrum also shows the disappearance of three  $-\text{COO}$  bonds between 169 – 170 ppm instead of one, suggesting that three acetyl groups disappeared. Nonetheless, both  $^1\text{H-}$  and  $^{13}\text{C-NMR}$  spectra detect peaks caused by the protons and carbon atoms on the  $\text{CH}_3\text{C=O}$  groups at 1.87 – 2.02 ppm and 20.33 – 20.50 ppm respectively. This implies that the acetyl groups are still attached to the compound and that the  $^{13}\text{C-NMR}$  measurement was at fault for not detecting the acetyl carbons.

Although both donors were synthesized, the yields obtained were disappointing. Just like the acceptor preparation described in **section 5.1.2**, the synthesis was difficult to control and the separation of the anomers was not achieved. Unfortunately, due to the failed synthesis of the acceptor, it was not possible to continue with the glycosylation reactions between the acceptor and donors. Therefore, no dimers have been prepared.

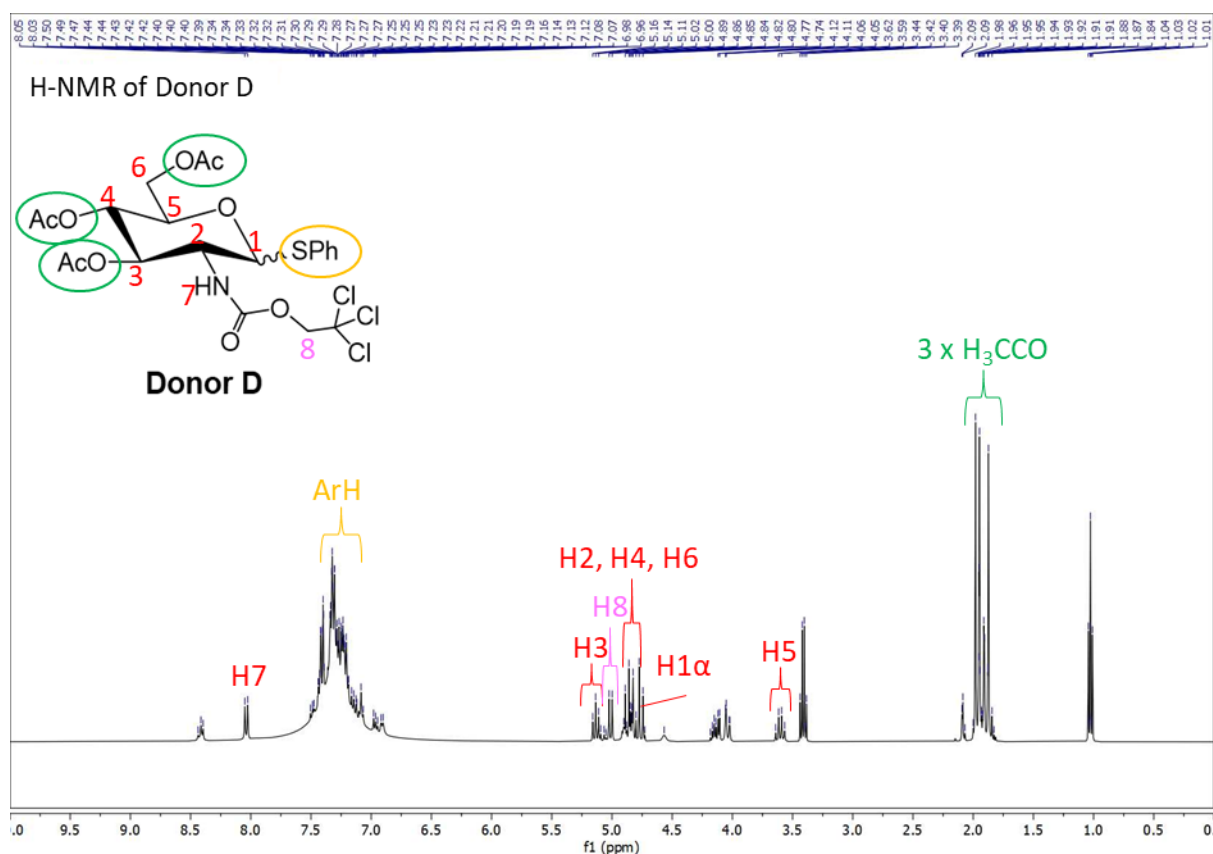


**Figure 17** - Measured  $^1\text{H-NMR}$  spectrum of synthesized thioglycoside donor **D**.

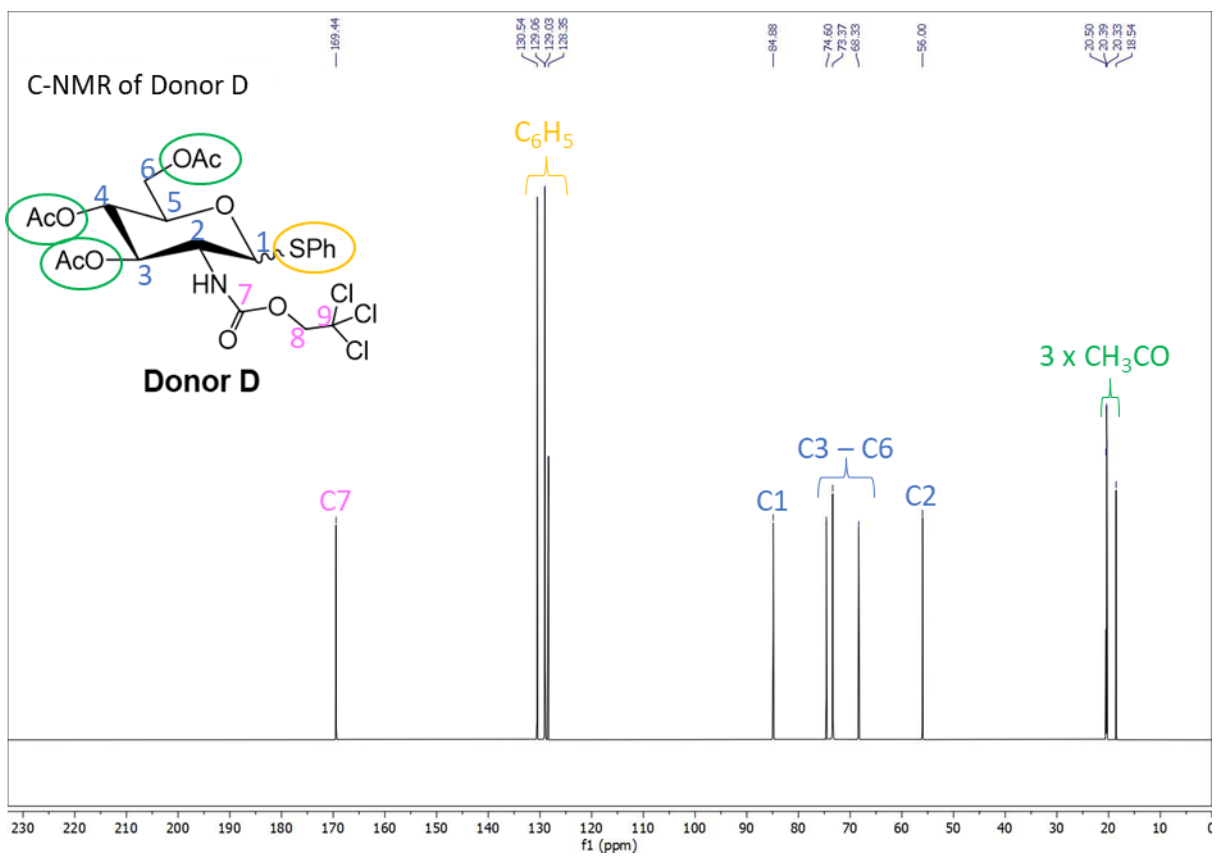
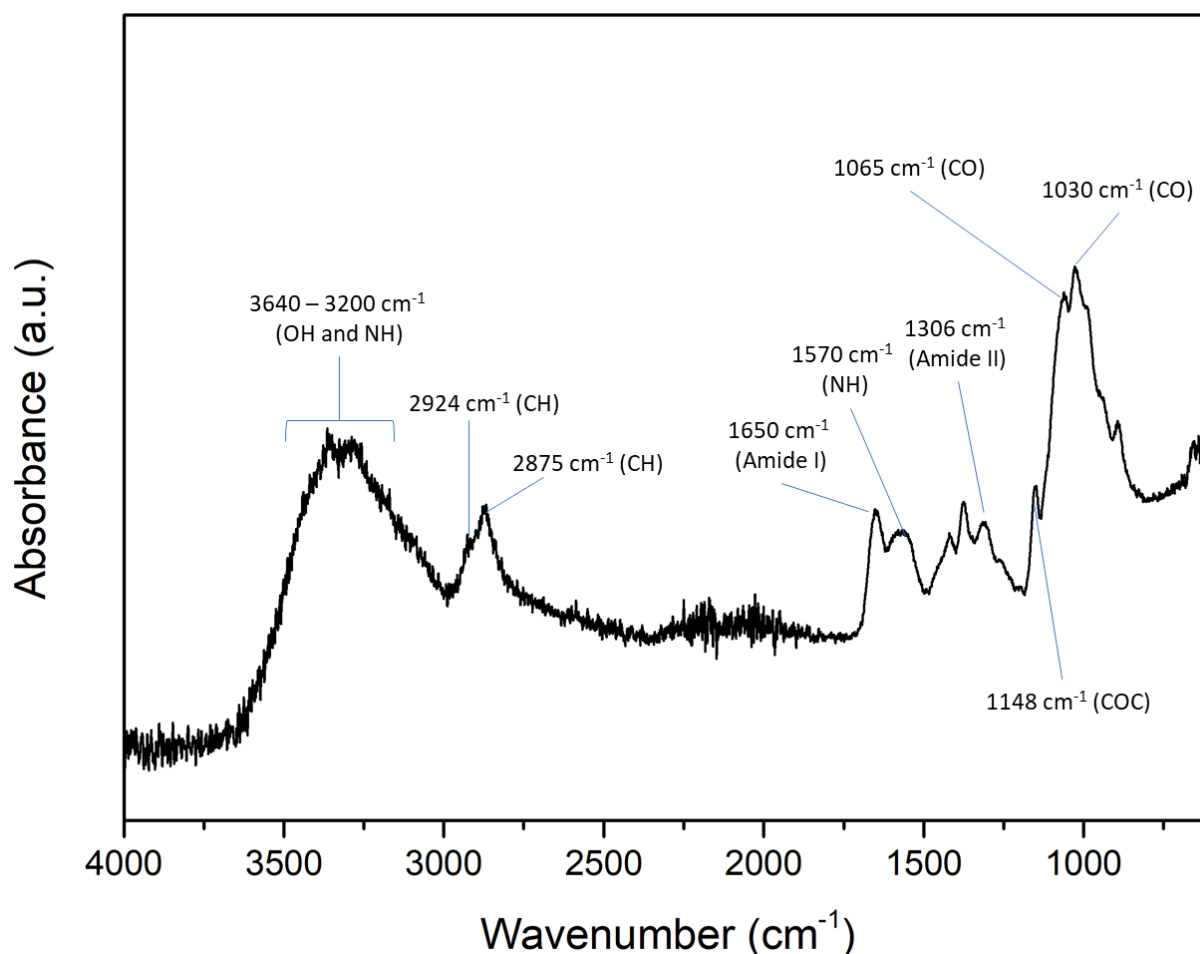


Figure 18 - Measured <sup>13</sup>C-NMR spectrum of synthesized thioglycoside donor D.

### 5.3. Crosslinking Experiments

#### 5.3.1. Chitosan Characterization

The ATR-IR spectrum of pure chitosan is shown in **Figure 19**. The broad peak around 3640 to 3200  $\text{cm}^{-1}$  is assigned to the overlapping of -NH and -OH stretching bands, while the peaks at 2924 and 2875  $\text{cm}^{-1}$  are associated with the symmetric and asymmetric stretching of C-H. The absorption bands due to the C=O of the amide group appear at 1650  $\text{cm}^{-1}$  and 1306  $\text{cm}^{-1}$  and the band due to the N-H amine appears at 1570  $\text{cm}^{-1}$ . The absorption bands at 1148  $\text{cm}^{-1}$  correspond to the anti-symmetric stretching of the C-O-C bond between the monomers, while the bands at 1065 and 1030  $\text{cm}^{-1}$  involve C-O stretching. Both absorption bands are typical aspects of a polysaccharide structure.<sup>60</sup>



**Figure 19** – ATR-IR spectrum of unmodified chitosan with assigned absorption peaks.

#### 5.3.2. Chitosan Crosslinking

##### *Crosslinking Chitosan in Acetic Acid*

ATR-IR spectroscopy was performed to determine the possible molecular interactions of the crosslinked chitosan films.

When dissolved in acetic acid, chitosan films were formed (**Figure 20**). **Figure 21** shows the ATR-IR spectra of chitosan compared to modified chitosan dissolved in 5% (w/w) acetic acid at room temperature. Comparison of the spectra of the pure chitosan powder and the chitosan crosslinked with glutaraldehyde shows that the intensity of the peak at 1570  $\text{cm}^{-1}$  increased when glutaraldehyde is added, which could indicate that an imine bond (C=N) has formed between the primary amine groups of chitosan and glutaraldehyde (**Figure 22A**). Normally, more extreme conditions are required to form an

imine bond, therefore making it unlikely that an imine bond has formed in these mild conditions.<sup>61</sup> However, some works have shown that an imine bond has formed before, when crosslinking chitosan with glutaraldehyde under similar conditions.<sup>11,62,63</sup> Khouri et al. suggest that the new bonds formed, may either be imines or a combination of imine and Michael-type adducts depending on the used method. An increase in intensity of the C-H stretching bond around 2924 and 2875  $\text{cm}^{-1}$  is observed as well, which can be explained by the increase of the contribution of the glutaraldehyde molecule in the crosslinking chain caused by the chitosan-glutaraldehyde reaction.<sup>62</sup>

After modification with maleic anhydride, the original absorption peaks of the amide groups (1650 and 1306  $\text{cm}^{-1}$ ) shifted to lower wavenumbers (1620 and 1262  $\text{cm}^{-1}$  respectively), which could be caused by the increase of hydrogen bonding between the chitosan chain and the maleic anhydride. Moreover, a new absorption peak appeared at 1705  $\text{cm}^{-1}$  corresponding to the C=O stretching vibration of the newly formed carboxylic acids and amide bonds (**Figure 22B**).<sup>52,64</sup> The crosslinking of chitosan with maleic anhydride has been shown before under slightly different conditions.<sup>64</sup> Here, maleic anhydride was dissolved in DMF beforehand and it is proposed that the DMF solvent facilitates the crosslinking reaction, but no actual proof was given. Moreover, to the best of my knowledge, no research or results were found about the isomerization of maleic anhydride after crosslinking with chitosan. Therefore, due to insufficient analytical data and reference papers, the configuration (Z or E isomer) of maleic anhydride after crosslinking cannot be concluded. The results from the ATR-IR analysis suggest that the chitosan-maleic anhydride crosslinking was successfully obtained.

The experiments with the dicarboxylic acids (oxalic acid, malonic acid and succinic acid) show a shift of the amide peaks to higher wavenumbers (1720 and 1316  $\text{cm}^{-1}$ ), due to the weakened intermolecular hydrogen bonds resulted from the decrease in  $-\text{NH}_2$  number. An increase in peak intensity of the amide bonds was also observed, due to the increase in the number of amide bonds resulting from the crosslinking reactions (**Figure 22C**). The crosslinking with suberic acid, however, did not show any signs of crosslinking reaction, as there are no peak shifts or no new peaks appeared. Moreover, a shift of the  $-\text{NH}$  band around 3370  $\text{cm}^{-1}$  to higher wavenumbers is observed for the chitosan-oxalic acid and chitosan-malonic acid crosslinking. These shifts are probably caused by the interaction between  $\text{H}^+$  from the oxalic acid, or malonic acid, and the amine group in the chitosan polymer.<sup>65,66</sup> Therefore, the crosslinking between the oxalic acid and malonic acid with chitosan resulted in the formation of salt films, formed through the electrostatic interaction between the protonated amino group in the chitosan polymer and the carboxylate ion in oxalic acid and malonic acid (**Figure 22**). The provided data for the chitosan-succinic acid is insufficient to conclude whether the interactions are ionic or covalent. Normally, amides are difficult to prepare from carboxylic acids and amines, due to the amines being bases that convert the carboxylic acid groups into unreactive carboxylate anions.<sup>56</sup> Thus, the  $-\text{OH}$  of the carboxylic acid group is usually replaced by a better leaving group. In this research, however, the added acetic acid is able to protonate the amine groups on the chitosan polymer, preventing the amine from converting the carboxylic acid into unreactive carboxylate anions. Furthermore, the formation of the amide bonds between the chitosan polymer and dicarboxylic acids have been shown before by other works under slightly different conditions, where usually the drying methods differed.<sup>14,65,67-70</sup> In all of these cases, the crosslinking was only observed with IR spectroscopy and it is implied that the crosslinking interactions were ionic.

Above results provide evidence that the crosslinking agent reacted with the amine groups of the chitosan chain. The spectra gave information that the functional groups of the crosslinkers ( $-\text{CHO}$  and  $-\text{COOH}$ ) did not react with the hydroxyl groups in chitosan, as the strong stretching vibration of C=O from the ester bond (around 1730-1750  $\text{cm}^{-1}$ ) was not found.<sup>71</sup>



The experiments were carried out at 80 °C as well and the corresponding ATR-IR spectra are shown in **Figure 21**. No distinctive differences are present between the experiments carried out at room temperature and 80 °C, except for the crosslinking with suberic acid. An increase of the absorption peak at 1704 cm<sup>-1</sup> is observed which indicates that amide bonds have formed between chitosan and suberic acid. Moreover, an increase in the intensity of the absorption peaks at 2930 and 2875 cm<sup>-1</sup> is present as well, indicating that there is an increase in the contribution of the suberic acid in the crosslinking chain during the reaction. These results suggest that the increase in temperature improves the reaction between suberic acid and chitosan.

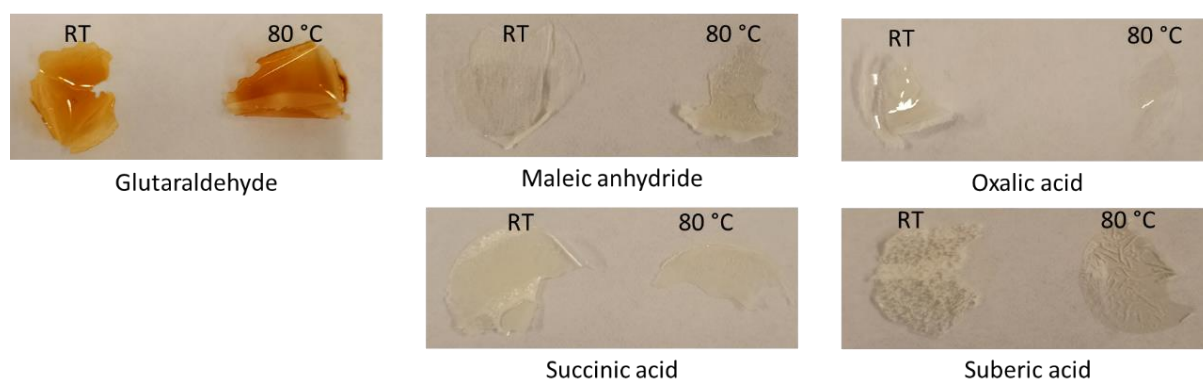


**Figure 20** - Chitosan films crosslinked with glutaraldehyde, oxalic acid, succinic acid and suberic acid when dissolved in 5 wt.% acetic acid at room temperature and 80 °C. Films with maleic anhydride are not included.

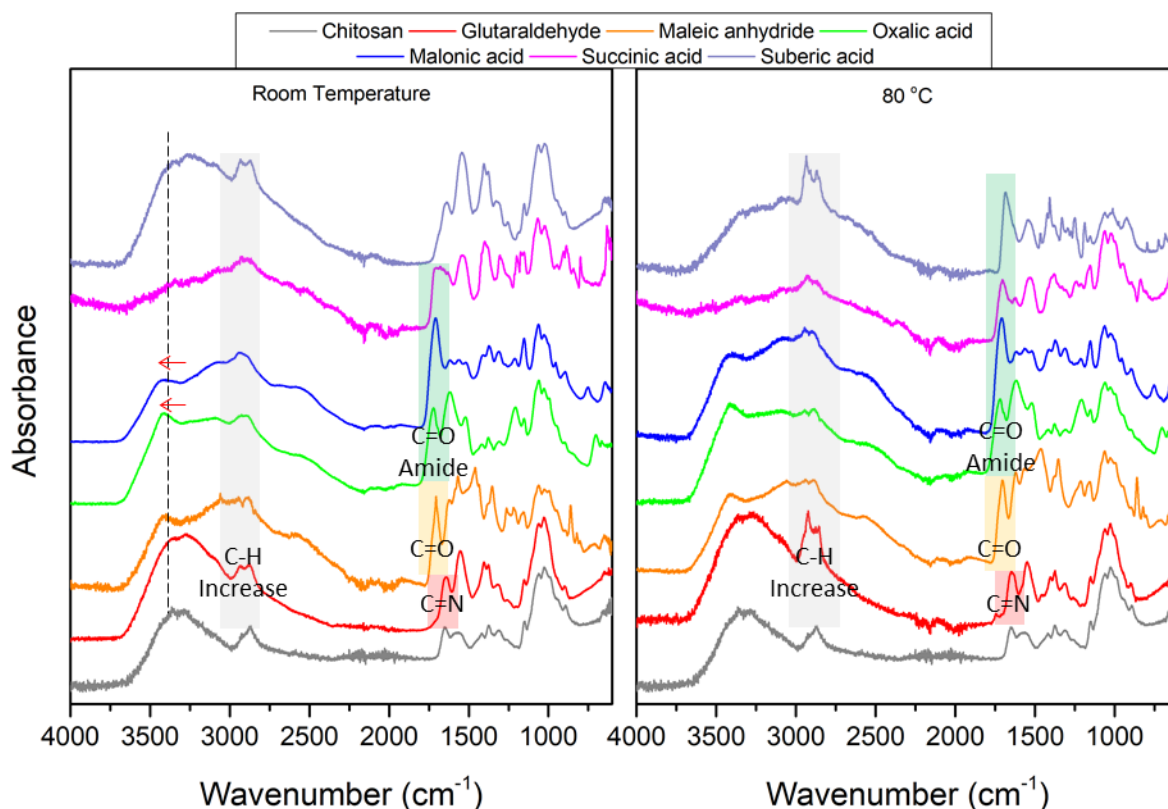


**Figure 21** - Infrared spectra of unmodified chitosan and chitosan crosslinked with glutaraldehyde, maleic anhydride, oxalic acid, malonic acid, succinic acid and suberic acid dissolved in 5% (w/w) acetic acid at room temperature (left) and 80 °C (right).

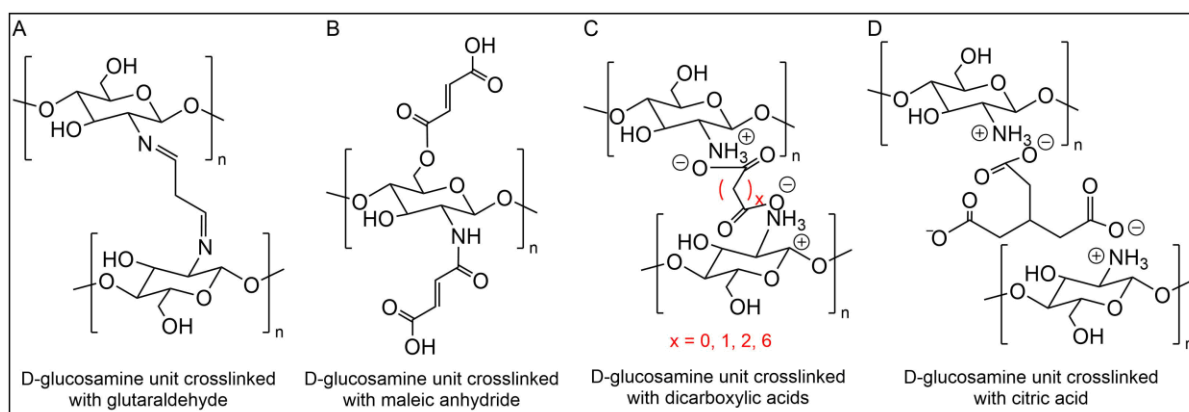


**Figure 22** – Structures of the crosslinking between the D-glucosamine monomer unit and the crosslinking agents.<sup>65,67,72,73</sup>

### Crosslinking Chitosan in Citric Acid

The same experiments were done by dissolving chitosan in 5% (w/w) citric acid at room temperature, the films are shown in **Figure 23**. The films were stickier and more brittle than the previous films, which can be caused by the citric acid. The corresponding ATR-IR spectra are shown in **Figure 24**. Here, all spectra display a distinctive absorption band at  $1703\text{ cm}^{-1}$ , which could be associated with the formation of amide bonds and carboxylic acid groups between the chitosan polymers. This suggests that citric acid is competing with the crosslinking agents, see **Figure 22D**.

Glutaraldehyde did not form bonds with the chitosan polymers since no imine peaks were observed in the spectra. So, it is implied that citric acid reacted with the polymer instead. Moreover, no proof was found for the reaction of maleic anhydride with the chitosan polymer since both maleic anhydride and citric acid form amide and carboxylic acid bonds when crosslinked with the polymer (**Figure 22B** and **22D**).<sup>11,52</sup> Citric acid has three different pKa values (2.87, 4.35 and 5.69).<sup>74</sup> Oxalic acid (1.04 and 3.82) and malonic acid (2.65 and 5.38) have lower pKa values, meaning that oxalic acid and malonic acid are more active than citric acid. While succinic acid (4.00 and 5.24) and suberic acid (4.53 and 5.50) have higher pKa values, implying that succinic acid and suberic acid are less active than citric acid.<sup>74,75</sup> This suggests that the crosslinking of oxalic acid and malonic acid with the chitosan polymer had taken place to form the amide bonds, while citric acid could have reacted with the chitosan polymer instead of succinic acid and suberic acid (**Figure 22C** and **22D**).<sup>11</sup> However, as mentioned before in the previous paragraph, preparation of amides by reaction of carboxylic acids and amines are difficult, so it is debatable whether the citric acid formed amides with the chitosan polymer. Furthermore, the broad band around  $3350\text{ cm}^{-1}$  became less intense compared to the unmodified chitosan, implying that the number of free -OH groups decreased due to the esterification between chitosan and citric acid.<sup>76</sup>

The reactions mentioned above resulted in a small shift of the NH absorption band to higher wavenumbers, suggesting that the interactions between the crosslinkers and citric acid with the amine on chitosan are ionic.<sup>11</sup> Therefore, making salt films just like the crosslinking experiments carried out in acetic acid (**Figure 22**).

**Figure 24** shows the spectra of the experiments that were carried out at  $80\text{ }^{\circ}\text{C}$ . Only the experiments with maleic anhydride and suberic acid show a new absorption peak at  $1740\text{ cm}^{-1}$ , which could originate from the unreacted crosslinker. No further reactions are observed as the spectra remain the same. So, higher temperatures did not lead to any further crosslinking between chitosan and the added crosslinkers and/or citric acid.

These results demonstrate that citric acid competes with the added crosslinking agents for forming crosslinking linkages with the polymer and the formation of ester linkages between chitosan and citric acid.

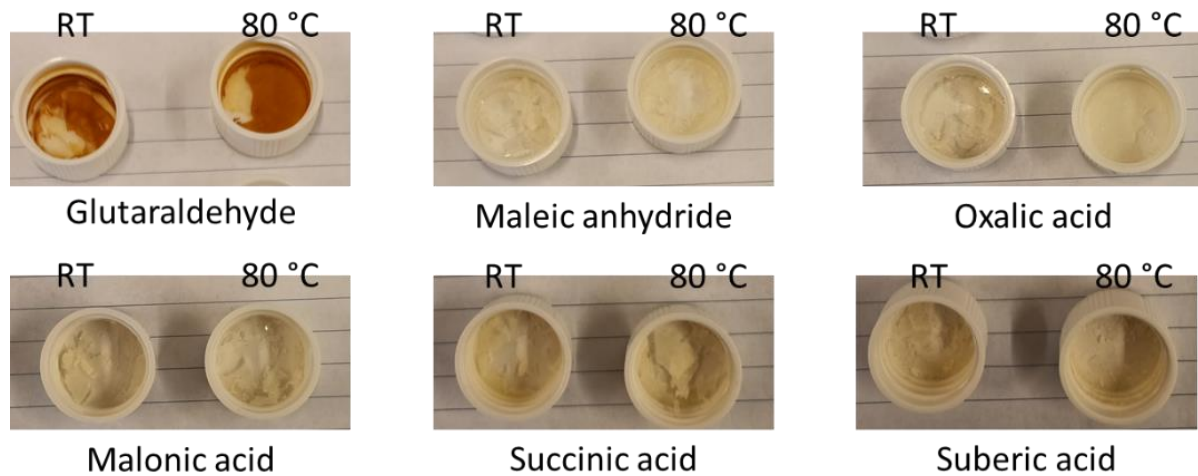


**Figure 23** – Brittle chitosan films after the crosslinking experiments with added glutaraldehyde, maleic anhydride, oxalic acid, succinic acid and suberic acid when dissolved in 5 wt.% citric acid at room temperature and 80 °C.

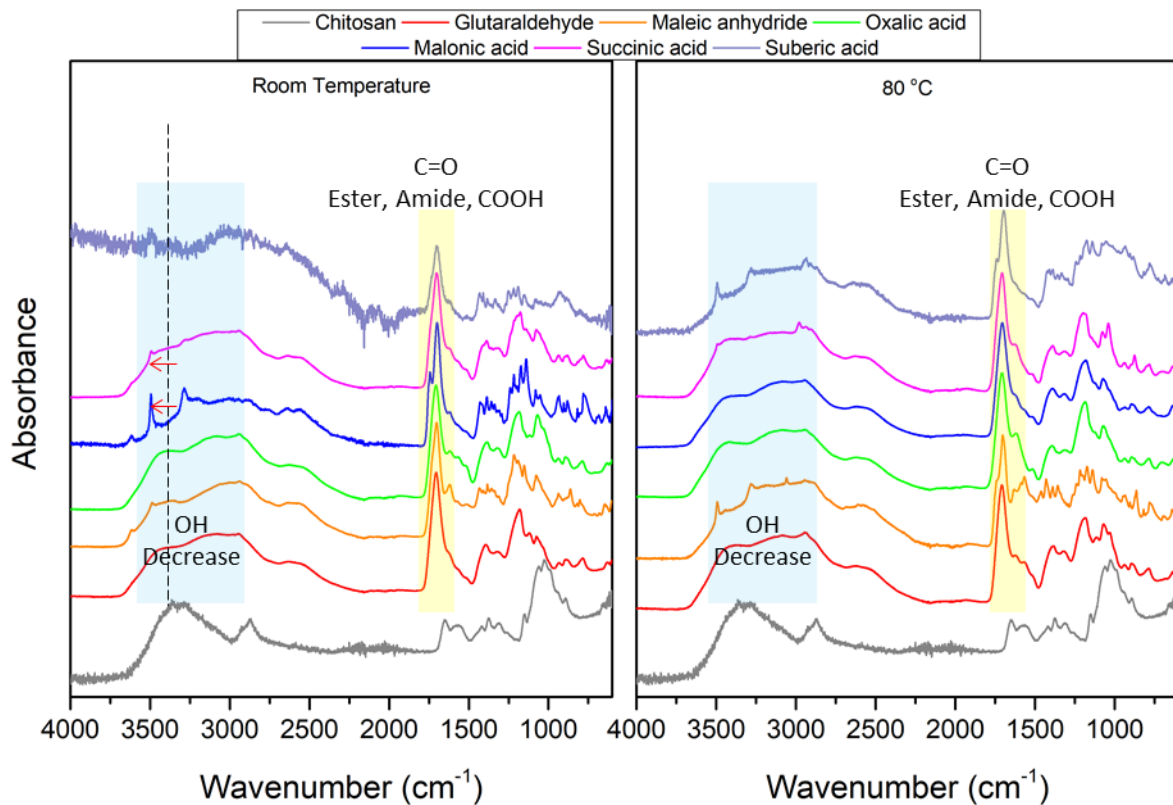


**Figure 24** - Infrared spectra of natural chitosan and modified chitosan with glutaraldehyde, maleic anhydride, oxalic acid, malonic acid, succinic acid and suberic acid dissolved in 5% (w/w) citric acid at room temperature (left) and 80 °C (right).

### 5.3.3. Crosslinking of Monomers

#### *Crosslinking GlcN and GlcNAc in Water*

As mentioned before, in contrary to chitosan, the monomers of chitosan (GlcN and GlcNAc) are already water soluble. Crosslinking reactions were carried out in water by using the same crosslinking agents that were used in the previous experiments with chitosan. Additionally, an experiment without any crosslinker was carried out to see if the monomers would bind to each other on their own. The corresponding ATR-IR spectra are shown in **Figure 26**.

In contrary to the chitosan experiments mentioned above, the experiments with the monomer mixture did not yield any films, only brittle powder was formed for both room temperature and 80 °C experiments (**Figure 25A**). The ATR-IR spectra show that the monosaccharides did not crosslink when no crosslinker was added, since the corresponding spectrum is similar to the unmodified monomers.

When glutaraldehyde was added, an increase in intensity at 1617  $\text{cm}^{-1}$  was noticed, implying that an imine bond has formed between the amine group of GlcN and the aldehyde group of glutaraldehyde. Nevertheless, it is unlikely that an imine bond has formed, since imines are usually formed in an acid-catalyzed process.<sup>56,61</sup> Since no acids were added in these experiments, the observed peak intensity increase could be associated with the aldehyde group of glutaraldehyde.

New absorption peaks at 1706, 1724, 1710, 1684 and 1690  $\text{cm}^{-1}$  appeared for the experiments where maleic anhydride, oxalic acid, malonic acid, succinic acid and suberic acid were added, respectively. Like the ATR-IR spectra of **Figure 24**, these peaks could be associated with the formation of amide bonds between the crosslinking agents and the primary amine group on the GlcN unit, since the intensity of the original free  $\text{NH}_2$  peak of the unmodified monomer mixture at 1538  $\text{cm}^{-1}$  decreased when the previously mentioned crosslinkers were added. However, amide formation between carboxylic acids and amines generally occur under more extreme conditions, making it unlikely that amide bonds were formed between the monomers and crosslinkers in just water.<sup>56</sup>

When the experiments were performed at 80 °C, no crosslinking occurred when no crosslinking agents were present. The addition of crosslinkers showed no significant changes, excluding where succinic acid and suberic acid were added. Here, a prominent increase of the peak around 1690  $\text{cm}^{-1}$  is detected. The peaks could be affiliated with the unreacted carboxylic acids of the crosslinkers, since it was implied that no amides can be formed under the current conditions.

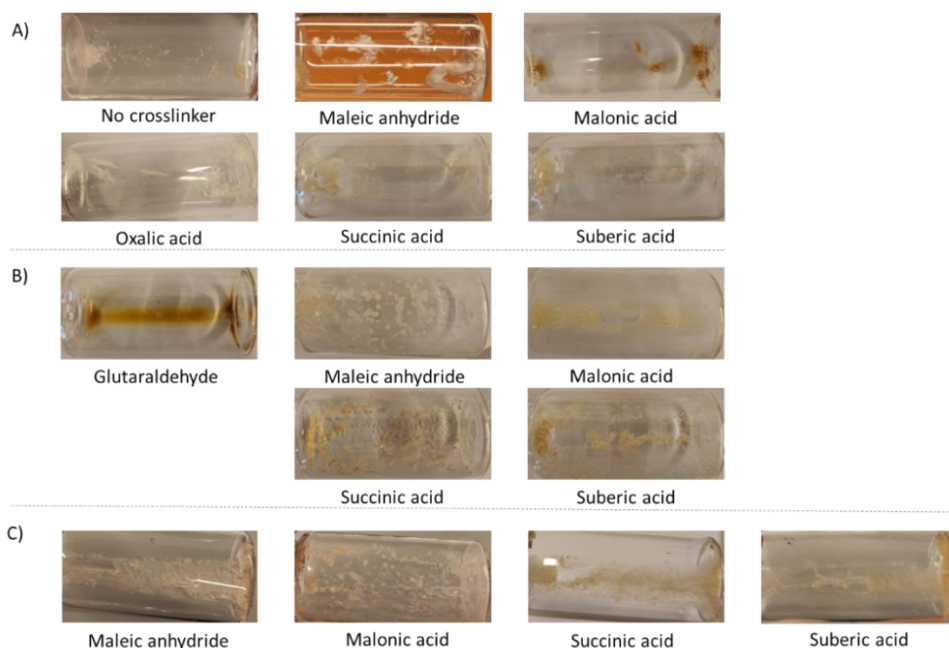


**Figure 25** – Brittle GlcN:GlcNAc (3:1, w/w) crosslinked with glutaraldehyde, maleic anhydride, oxalic acid, malonic acid, succinic acid and suberic acid when dissolved in A) water, B) 5 wt.% acetic acid and C) 5 wt. % citric acid at room temperature. Reactions with A) glutaraldehyde, B) oxalic acid and C) glutaraldehyde and oxalic acid are not included.

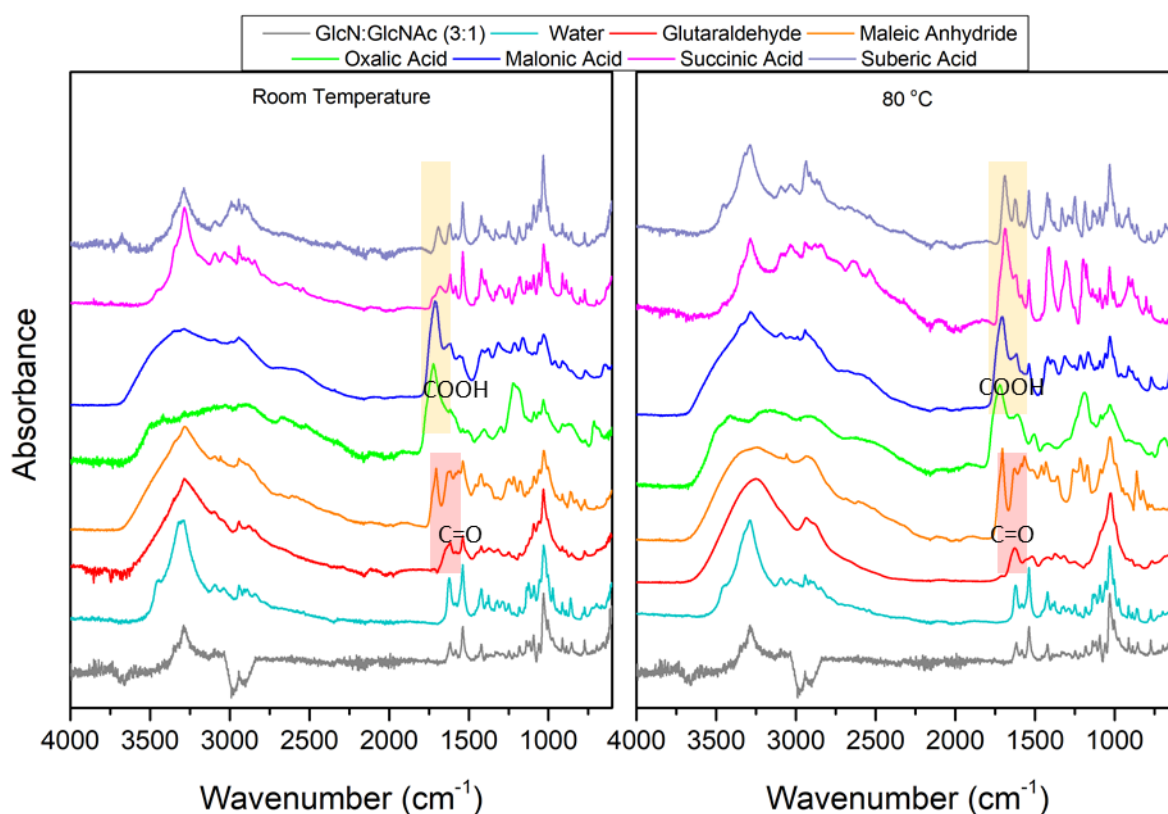


**Figure 26** - Infrared spectra of unmodified GlcN:GlcNAc (3:1, w/w) powder and modified GlcN:GlcNAc (3:1, w/w) crosslinked with no crosslinker, with glutaraldehyde, maleic anhydride, oxalic acid, malonic acid, succinic acid and suberic acid dissolved in water at room temperature (left) and at 80°C (right).

### Crosslinking GlcN and GlcNAc in Acetic Acid

Crosslinking experiments between the monomer mixture and the crosslinkers were performed in 5% (w/w) acetic acid as well. Again, no films were formed and only brittle powder was acquired (**Figure 25B**). The measured ATR-IR spectra are displayed in **Figure 27**. The experiment with glutaraldehyde leads to the appearance of a new peak at  $1710\text{ cm}^{-1}$ , which originates from the newly formed imine bond between the glutaraldehyde and the GlcN monomer. The crosslinking of the monomers with maleic anhydride, oxalic acid, malonic acid, succinic acid and suberic acid afforded a new absorption peak around  $1715\text{ cm}^{-1}$ , corresponding to the formation of new amide bonds between the crosslinkers and GlcN unit in the monomer mixture. Here, no NH peak shifts are observed, meaning that the interactions between the amine group and the dicarboxylic crosslinkers were not ionic. This implies that at room temperature, crosslinking reactions occur covalently between the free amine group of the GlcN monomer and the added crosslinking agent. Just like the chitosan experiments, the reaction between the amine groups of the GlcN monomer could have been facilitated by the acidic solvent containing acetic acid.

At higher temperature, the intensity of the free  $\text{NH}_2$  absorption peak at  $1540\text{ cm}^{-1}$  decreased, while the peak intensity at  $1710\text{ cm}^{-1}$  ( $\text{C}=\text{N}$  imine bond) heightened, suggesting that the reaction between GlcN and glutaraldehyde occur better at higher temperatures. The reactions at  $80\text{ }^\circ\text{C}$  increased the intensities of the amide peaks of the experiments with maleic anhydride and the carboxylic acids, especially for the malonic acid and succinic acid reactions, meaning that higher temperatures improved the reaction.

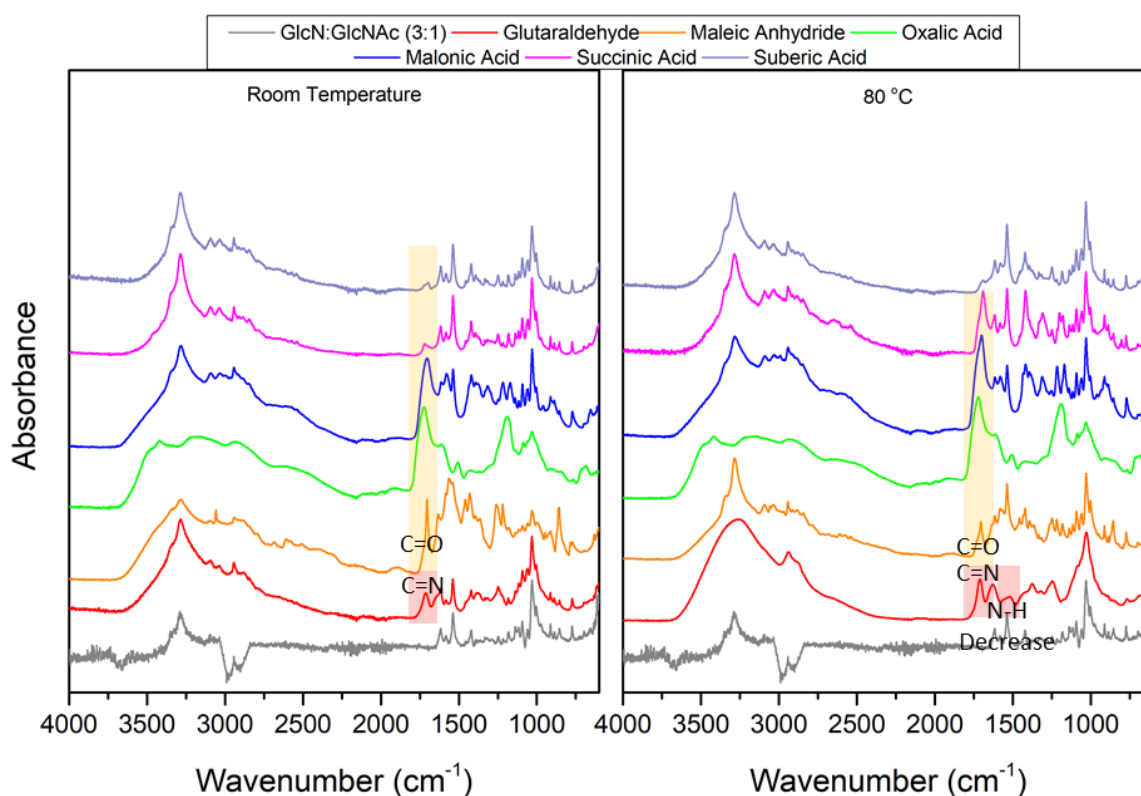


**Figure 27** - Infrared spectra of unmodified GlcN:GlcNAc (3:1, w/w) and modified GlcN:GlcNAc (3:1, w/w) crosslinked with glutaraldehyde, maleic anhydride, oxalic acid, malonic acid, succinic acid and suberic acid dissolved in 5% (w/w) acetic acid at room temperature (left) and at  $80\text{ }^\circ\text{C}$  (right).

### *Crosslinking GlcN and GlcNAc in Citric Acid*

Additionally, crosslinking experiments between the monomer mixture and the crosslinking agents were carried out in 5% (w/w) citric acid as well. Again, the experiments yielded brittle powder and no films were acquired (**Figure 25C**). The measured ATR-IR spectra are shown in **Figure 28**.

All spectra show a new distinctive absorption peak around  $1705\text{ cm}^{-1}$ , which could be associated with the formation of amide groups between the crosslinking agents and the free amine on GlcN. Just like the crosslinking experiments with chitosan (**section 5.3.2**), the monomers likely prefer to react with citric acid than glutaraldehyde, since no imine peaks are present in the spectra. However, a new peak at  $1747\text{ cm}^{-1}$  appeared, which could be affiliated with the aldehyde group of the unreacted glutaraldehyde. Moreover, no proof was found whether the GlcN monomer reacted with maleic anhydride or citric acid, since both reactions result in formation of an amide and carboxylic acid bond peak around  $1747\text{ cm}^{-1}$ . Similar to the chitosan experiments, GlcN could have reacted with oxalic acid and malonic acid than succinic acid and suberic acid due to their lower pKa values compared to citric acid, suggesting that oxalic acid and malonic acid were more active. For the latter two crosslinkers, GlcN likely prefer to react with citric acid than the crosslinkers due to the difference in activity. In these cases, amide bonds are formed between the crosslinking agents or citric acid and the free amine group of GlcN. The broad OH band around  $3400\text{ cm}^{-1}$  became less intense and the NH peak around  $3494\text{ cm}^{-1}$  became more apparent, suggesting that the citric acid reacted with the hydroxyl groups of the monomers to form ester bonds, which is in accordance with the experiments with chitosan.

Increasing the reaction temperature to  $80\text{ }^{\circ}\text{C}$  caused the aldehyde peak at  $1747\text{ cm}^{-1}$  to decrease, entailing that the glutaraldehyde reacted with the monomers. A small peak appeared around  $1620\text{ cm}^{-1}$ , which could be correlated to the formation of imine bonds. Additionally, a decrease of the peak intensities at  $1430\text{ cm}^{-1}$  and around  $1570\text{ cm}^{-1}$  at the experiment containing maleic anhydride is observed. Both peaks can be associated with OH groups and NH groups respectively, suggesting that the esterification with citric acid continued and that the monomers reacted with either maleic anhydride or citric acid to form more amide bonds. The amide absorption peak could be overlapping with the ester absorption peak mentioned above. The spectra showed no differences in the monomers crosslinked by the other crosslinking agents. These results suggest that citric acid competes with the crosslinkers in binding with the GlcN monomer. Moreover, the crosslinking reactions do not occur on the amine group on the GlcNAc monomer due to the *N*-acetyl group being less nucleophilic than the free amine group on GlcN, as mentioned in **section 5.1.2**

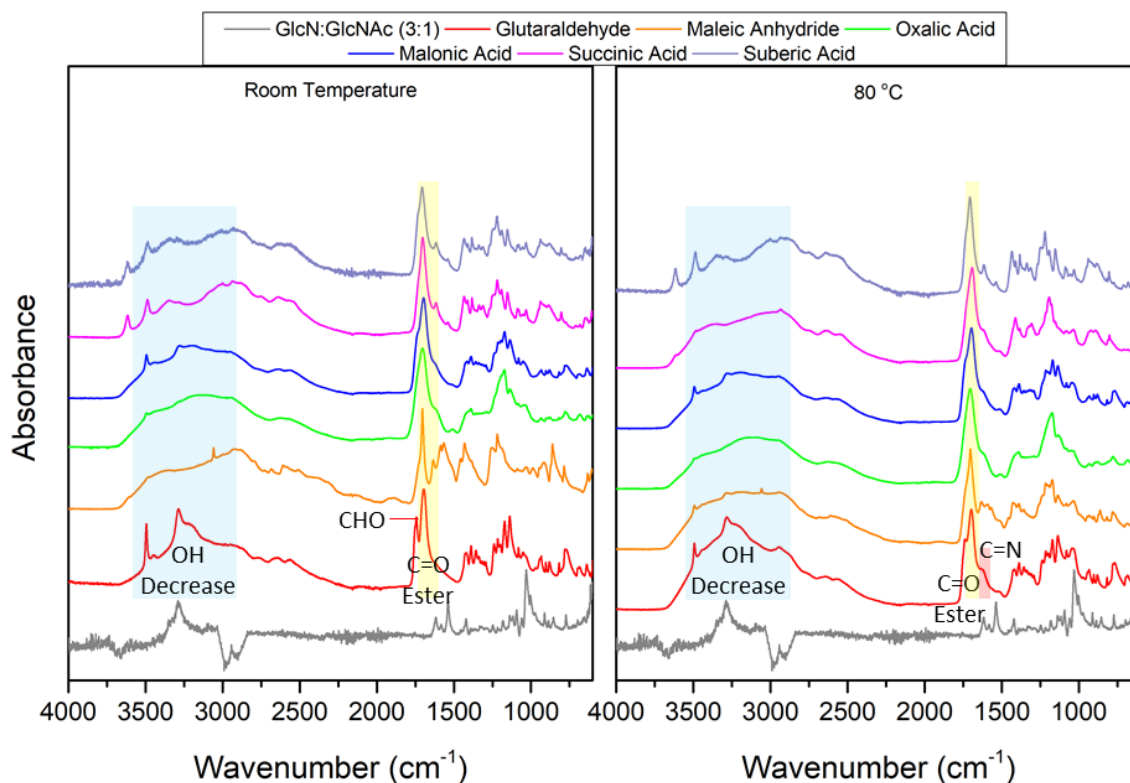


**Figure 28** - Infrared spectra of unmodified GlcN:GlcNAc (3:1, w/w) and modified GlcN:GlcNAc (3:1, w/w) with glutaraldehyde, maleic anhydride, oxalic acid, malonic acid, succinic acid and suberic acid dissolved in 5% (w/w) citric acid at room temperature (left) and at 80 °C (right).

#### Crosslinking GlcN in Water

Crosslinking reactions of pure GlcN monomer were carried out to see the difference between the fully deacetylated system and the partially deacetylated system like the experiments shown above. All experiments resulted in brittle powder and no films were formed.

The ATR-IR spectrum of the experiments conducted in water at RT and 80 °C (**Figure 29**) showed that glutaraldehyde did not react with the GlcN monomer to form an imine bond as no imine peak was present in the IR spectra. For the experiments where maleic anhydride, oxalic acid, malonic acid, succinic acid and suberic acid were added as the crosslinking agent, all showed an increase of peak intensities around 1688 – 1706  $\text{cm}^{-1}$ , corresponding to functional groups on the crosslinkers. At 80 °C, an increase of the corresponding peak intensities is observed for maleic anhydride and the dicarboxylic acid crosslinking experiments, corresponding to the increasing vibrations of the functional groups. As mentioned in the previous sections, it is unlikely that crosslinking reaction occurred between the GlcN monomers and the crosslinkers under current conditions in water, since more extreme conditions are usually required.



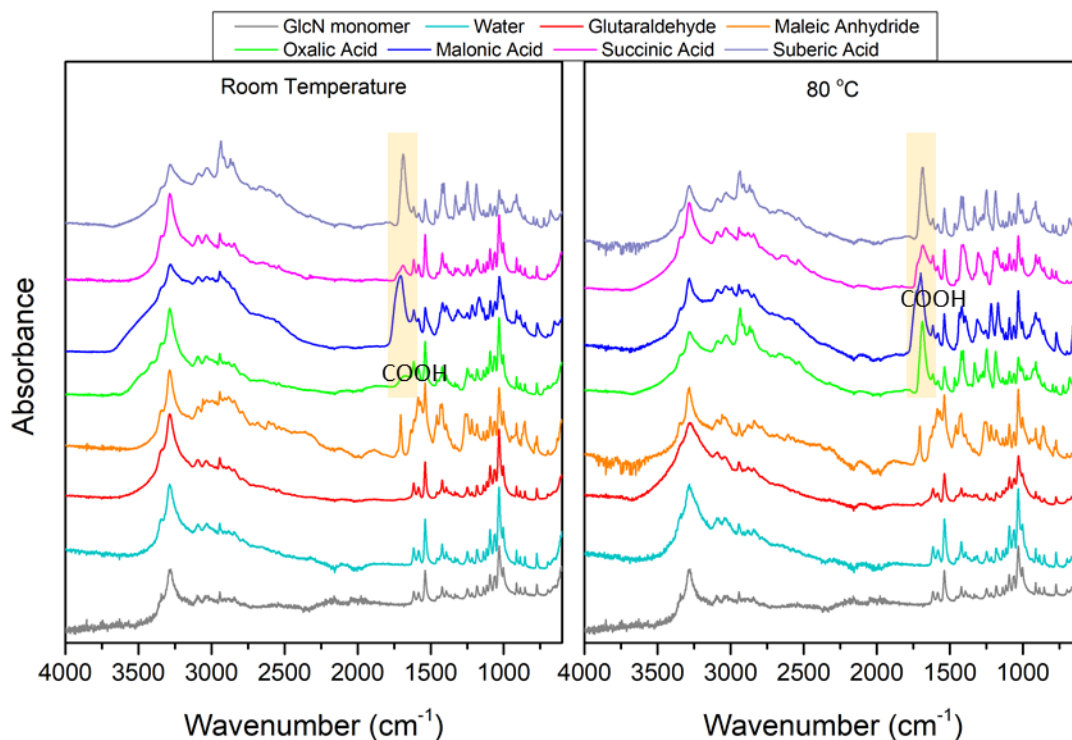


**Figure 29** - Infrared spectra of unmodified GlcN powder and modified GlcN with no crosslinker, with glutaraldehyde, maleic anhydride, oxalic acid, malonic acid, succinic acid and suberic acid dissolved in water at room temperature (left) and at 80°C (right).

#### *Crosslinking GlcN in Acetic Acid*

Analogous to the previous crosslinking experiments, when GlcN is dissolved in acetic acid, the experiment with glutaraldehyde showed an absorption peak (**Figure 3030**) at  $1710\text{ cm}^{-1}$ , corresponding to an imine bond, which had formed between the amine group of GlcN and the crosslinking agent. Additionally, new peaks have formed at  $1703$ ,  $1725$ ,  $1705$ ,  $1717$  and  $1710\text{ cm}^{-1}$  for the crosslinking with maleic anhydride, oxalic acid, malonic acid, succinic acid and suberic acid respectively, corresponding to the formation of amide bonds. The imine and amide peaks increased when the experiments were carried out at  $80\text{ }^{\circ}\text{C}$ , implying that the reactions improved at higher temperatures which cause more vibrations of these newly formed bonds. These observations matched with the assumptions mentioned previously, that acetic acid facilitates the reactions.

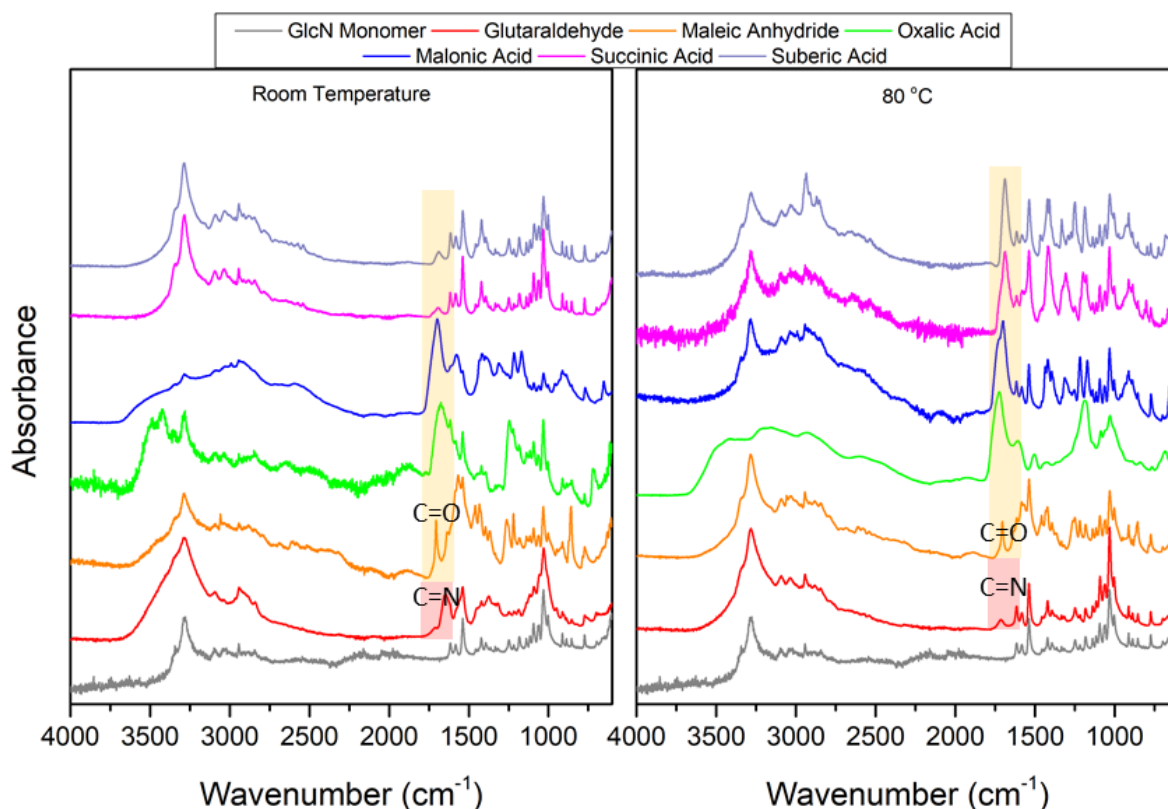


**Figure 30** - Infrared spectra of unmodified GlcN powder and modified GlcN with glutaraldehyde, maleic anhydride, oxalic acid, malonic acid, succinic acid and suberic acid dissolved in 5% (w/w) acetic acid at room temperature (left) and at 80°C (right).

#### Crosslinking GlcN in Citric Acid

In citric acid (**Figure 31**), the observations were equivalent to all the previous experiments carried out in citric acid. New peaks appeared between 1695 – 1708  $\text{cm}^{-1}$  for all procedures, which match with the formation of amide bonds between the GlcN monomers. Again, this suggests that citric acid reacted with the monomers instead of glutaraldehyde, succinic acid and suberic acid. The ATR-IR spectrum of the glutaraldehyde experiment showed a new peak appeared at 1740  $\text{cm}^{-1}$ , which matches with the aldehyde group of glutaraldehyde, implying that the reaction did not occur between the primary amine group and the aldehyde. Moreover, the presence of the peaks at 1742 and 1744  $\text{cm}^{-1}$  for the succinic acid and suberic acid experiments respectively, showed that the reactions did not occur either, as these peaks correspond to the COOH group of the dicarboxylic acids. These results are equivalent with the previous experiments, due to citric acid having lower pKa values than succinic acid and suberic acid, making citric acid more active. In contrary, the monomers prefer to bind with oxalic acid and malonic acid to form amide bonds, due to their lower pKa values than citric acid and therefore higher activity.

Subsequently, at higher temperatures, the peaks corresponding to succinic acid (1742  $\text{cm}^{-1}$ ) and suberic acid (1744  $\text{cm}^{-1}$ ) disappeared and diminished respectively. This implies that the reaction between these crosslinking agents and the GlcN monomer occurred, where either amide bonds were formed between unreacted free amine groups and the crosslinkers or new ester bonds were formed between the crosslinkers and unreacted OH groups on GlcN. Both amide or ester peaks overlap with the large peak at 1740  $\text{cm}^{-1}$  corresponding to the amide bonds between the monomer and crosslinkers. Amide formation usually require more extreme conditions, but as mentioned before, amide formation between chitosan and similar crosslinkers have been shown before under similar conditions.<sup>14,65,67–70</sup> No differences are observed for the other experiments.

Just like the previous experiments carried out in citric acid, these results suggest that citric acid competes with the added crosslinking agents during the crosslinking reactions, due to difference in activity of the functional groups.

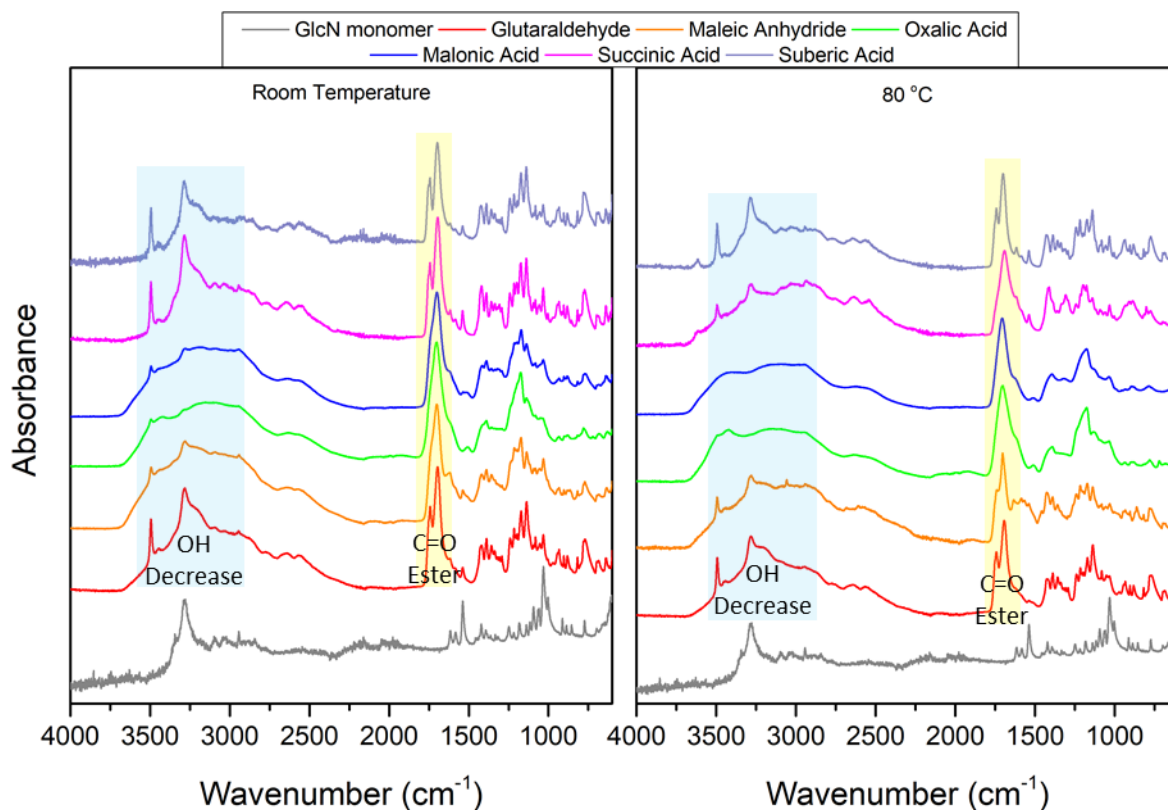


**Figure 31** - Infrared spectra of unmodified GlcN and modified GlcN crosslinked with glutaraldehyde, maleic anhydride, oxalic acid, malonic acid, succinic acid and suberic acid dissolved in 5% (w/w) citric acid at room temperature (left) and at 80°C (right).

#### 5.3.4. Comparison Chitosan and Monomers Crosslinking

All experiments carried out with the monomers, showed a reaction between the free amine group of D-glucosamine and the crosslinking agents, which were in accordance with the experiments performed with chitosan (**Figure 32**). In contrary to the chitosan protocols, no films were formed when monomers were used in the methods. From all crosslinking experiments above, it is implied that longer chains with repeating units are necessary for film formation to occur. This is probably due to the fact that the bond between the monomers is not strong enough compared to chitosan, where its strong semicrystalline structure is derived from the combination of  $\beta$ -(1 $\rightarrow$ 4) glycosidic bonds and inter- and intramolecular hydrogen bonds, making the 3D-network of crosslinked chitosan more stable.<sup>7,77</sup> Whereas, single crosslinked GlcN monomers are not stable enough, which is attributed to the more hydrophilic nature of GlcN. Because of that, the crosslinked GlcN monomers do not have the ability to form a strong and stable network.

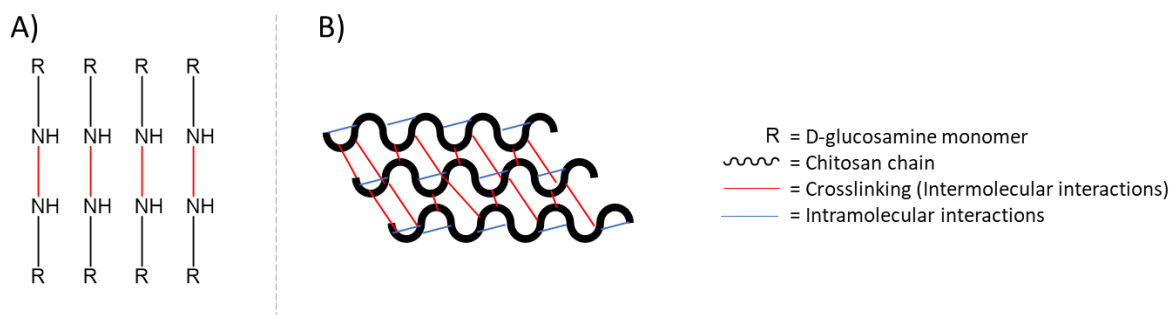


**Figure 32** - Simple representation of the interactions between the monomers and the chitosan chains. A) Crosslinked D-glucosamine monomers. B) Crosslinked chitosan chains with inter- and intramolecular interactions.

## 6. Conclusion

In summary, this work describes the preparation of a glycosyl acceptor and two glycosyl donors derived from two glucosamine derivatives which were meant for a glycosylation reaction to form a dimer. To obtain these compounds, existing procedures were adapted to acquire the desired acceptors and donors. The preparation of the protected GlcNAc and the thioglycoside donors were confirmed by ATR-IR,  $^1\text{H-NMR}$ , and  $^{13}\text{C-NMR}$ .

Throughout the process, the glycosyl acceptor was made from GlcNAc, which underwent subsequent methylation (with methanol and acetyl chloride), 4,6-*O*-benzylideneation (with benzaldehyde and ZnCl) and a benzylation (with BnBr and NaH) reaction to yield a fully protected GlcNAc compound **4** (**Scheme 4, steps a-c**). Here, an  $\alpha$ -anomer was acquired. However, the last step of the acceptor synthesis, involving the selective benzylidene acetal ring opening towards the free 4-OH acceptor **B** (**step d**), was not achieved due to the low yields of the intermediates.

Two thioglycoside donors were prepared from GlcN and GlcNAc. Both donors were prepared similarly (**Scheme 5**). The amine group of GlcN was protected by a Troc protecting group beforehand (**step g**) and the hydroxyl groups on both GlcN and GlcNAc were protected by acetyl protecting groups (**steps e and h**). Then, the anomeric acetyl groups on both compounds were subjected to the formation of thioaryl bonds to form the thioglycoside **donors C and D** (**steps f and j**). Unfortunately, in this report the glycosylation of the acceptor and the donors was not provided, as the acceptor was not fully synthesized.

Moreover, in this study an attempt was made to make films out of the D-glucosamine hydrochloride and *N*-Acetyl-D-glucosamine sugar molecules with the help of crosslinkers through a casting preparation method. Glutaraldehyde, maleic anhydride, and a group of linear dicarboxylic acids were used as the crosslinking agent. These experiments were done in three types of solvents: water, acetic acid, and citric acid. In contrary to the chitosan experiments, no films were formed during the experiments using the monomers. Instead, brittle powder was acquired. Characterization by ATR-IR shows that when the reactions were performed in water, it was implied that no crosslinking reactions occurred, as it is generally known that different conditions were required to perform these reactions.

In acetic acid, crosslinking was achieved between the free amine groups of the GlcN monomer and the functional groups of the crosslinking agents, as depicted in **Figure 32**. Glutaraldehyde formed imine bonds ( $1617 - 1710\text{ cm}^{-1}$ , **Figures 26, 27 and 30**), maleic anhydride and the dicarboxylic acids formed amide bonds with the amine group ( $1684 - 1715\text{ cm}^{-1}$ , **Figures 26 - 31**). It was implied that the acidic solvent would facilitate the crosslinking reactions.

However, when the experiments were carried out in citric acid, crosslinking between citric acid and the chitosan polymer and GlcN monomer was observed (amide bonds around  $1705\text{ cm}^{-1}$ ) instead of glutaraldehyde, succinic acid and suberic acid, as visible in **Figures 28 and 31**. In these cases, citric acid is more active than the mentioned crosslinkers, due to citric acid having lower pKa values. Alternatively, oxalic acid and malonic acid seem to bind the chitosan polymer and GlcN monomer stronger due to their lower pKa values compared to citric acid. Therefore, citric acid competes with the crosslinking agents. No films were formed, probably because the glucosamine monomers are not stable enough due to the lack of a strong 3D-network of the crosslinked monomers.

## 7. Outlook

The synthetic routes provided by this report showed some challenges. First, the conditions of some individual protecting steps were difficult to control due to the use of Schlenk lines. Also, the desired  $\beta$ -anomeric donors were not achieved, and the reaction steps resulted in low yields. In the future, more research has to be done to prevent these problems from happening, and to obtain the desired compounds at high yields.

Subsequently, glycosylation can be controlled using glycosyl acceptors and donors to provide oligomers with desired properties such as the chain length and degree of acetylation (DA). This can be achieved by making multiple acetylated and deacetylated acceptors and donors, which can be applied in a controlled multistep glycosylation reaction.

Since it is already known that oligomers are better soluble than the chitosan polymer, the limit of its solubility should be tested by finding the relationship between its structure properties (DA and chain length) and solubility. The degree of acetylation and the chain length of the obtained oligomers could be derived by analytical ultra-centrifugation (AUC) and gel permeation chromatography (GPC). The solubility can be tested by measuring the viscosity of the oligomers in the solution.<sup>7</sup>

Furthermore, the oligomers should be applied into forming films (with the aid of crosslinkers) where their solubility, strength and durability should be evaluated. The mechanical behaviors of the films can be evaluated in terms of tensile strength using a material testing machine. The solubility can be tested by testing its swelling and water vapor sorption properties.<sup>78</sup> I expect that the oligomers will be able to form films contrary to the monomers, due to the oligomers having more  $\beta$ -1,4 linkages and more intra- and intermolecular bonds. This allows the oligomers to have a more stable network and better film forming ability. Also, the oligomers are more hydrophobic than the monomers due to the presence of more acetylated monomeric units, so they will have less interactions with water. It has been proposed by other works, that linear dicarboxylic acid crosslinkers can improve the formation of chitosan films with more elasticity and better water absorptivity depending on the chain length of the crosslinking agent.<sup>79,80</sup> Therefore, the application of bi- or multifunctional crosslinking agents should be tested with the oligomers, since it could help the formation of oligomer films.

## 8. Acknowledgments

First, I want to thank Kordula Schnabl for being my daily supervisor. Also, I want to thank the Inorganic Chemistry and Catalysis (ICC) research group and the following people that have helped me during my research: dr. Razvan Cioc, Johann Jastrzebski, prof. dr. Pieter Bruijninx (Organic Chemistry and Catalysis group), dr. Eline Hutter and dr. Ina Vollmer. The mentioned people are all located at Utrecht University.

## 9. References

- (1) Yadav, M.; Goswami, P.; Paritosh, K.; Kumar, M.; Pareek, N.; Vivekanand, V. Seafood Waste: A Source for Preparation of Commercially Employable Chitin/Chitosan Materials. *Bioresour. Bioprocess.* **2019**, *6* (1).
- (2) Kumari, S.; Kishor, R. Chitin and Chitosan: Origin, Properties, and Applications. *Handb. Chitin Chitosan* **2020**, 1–33.
- (3) Alishahi, A.; Aider, M. Applications of Chitosan in the Seafood Industry and Aquaculture: A Review. *Food Bioprocess Technol.* **2011**, *53* (3), 817–830.
- (4) Zargar, V.; Asghari, M.; Dashti, A. A Review on Chitin and Chitosan Polymers: Structure, Chemistry, Solubility, Derivatives, and Applications. *ChemBioEng Rev.* **2015**, *2* (3), 204–226.
- (5) Younes, I.; Rinaudo, M. Chitin and Chitosan Preparation from Marine Sources. Structure, Properties and Applications. *Mar. Drugs* **2015**, *13* (3), 1133–1174.
- (6) Kaczmarek, M. B.; Struszczyk-Swita, K.; Li, X.; Szczesna-Antczak, M.; Daroch, M. Enzymatic Modifications of Chitin, Chitosan, and Chitooligosaccharides. *Front. Bioeng. Biotechnol.* **2019**, *7* (SEP).
- (7) Sogias, I. A.; Khutoryanskiy, V. V.; Williams, A. C. Exploring the Factors Affecting the Solubility of Chitosan in Water. *Macromol. Chem. Phys.* **2010**, *211* (4), 426–433.
- (8) Dash, M.; Chiellini, F.; Ottenbrite, R. M.; Chiellini, E. Chitosan—A Versatile Semi-Synthetic Polymer in Biomedical Applications. *Prog. Polym. Sci.* **2011**, *36* (8), 981–1014.
- (9) Ferreira, L. M. B.; dos Santos, A. M.; Boni, F. I.; dos Santos, K. C.; Robusti, L. M. G.; de Souza, M. P. C.; Ferreira, N. N.; Carvalho, S. G.; Cardoso, V. M. O.; Chorilli, M.; et al. Design of Chitosan-Based Particle Systems: A Review of the Physicochemical Foundations for Tailored Properties. *Carbohydr. Polym.* **2020**, *250*, 116968.
- (10) Elsabee, M. Z.; Abdou, E. S. Chitosan Based Edible Films and Coatings: A Review. *Mater. Sci. Eng. C* **2013**, *33* (4), 1819–1841.
- (11) Khouri, J.; Penlidis, A.; Moresoli, C. Viscoelastic Properties of Crosslinked Chitosan Films. *Process.* **2019**, *Vol. 7*, Page 157 **2019**, *7* (3), 157.
- (12) Kumirska, J.; Weinhold, M. X.; Thöming, J.; Stepnowski, P. Biomedical Activity of Chitin/Chitosan Based Materials—Influence of Physicochemical Properties Apart from Molecular Weight and Degree of N-Acetylation. *Polym.* **2011**, *Vol. 3*, Pages 1875-1901 **2011**, *3* (4), 1875–1901.
- (13) Issam Sebti, †,§; John Delves-Broughton, # and; Véronique Coma\*, †. Physicochemical Properties and Bioactivity of Nisin-Containing Cross-Linked Hydroxypropylmethylcellulose Films. *J. Agric. Food Chem.* **2003**, *51* (22), 6468–6474.
- (14) Azeredo, H. M. C.; Waldron, K. W. Crosslinking in Polysaccharide and Protein Films and Coatings for Food Contact – A Review. *Trends Food Sci. Technol.* **2016**, *52*, 109–122.
- (15) Rinaudo, M. Chitin and Chitosan: Properties and Applications. *Prog. Polym. Sci.* **2006**, *31* (7), 603–632.
- (16) S, H.; I, Y.; O, G.-B.; R, H.; M, R.; M, N.; K, J. Structural Differences between Chitin and Chitosan Extracted from Three Different Marine Sources. *Int. J. Biol. Macromol.* **2014**, *65*, 298–306.
- (17) Aiba, S. ichi. Studies on Chitosan: 3. Evidence for the Presence of Random and Block Copolymer

- Structures in Partially N-Acetylated Chitosans. *Int. J. Biol. Macromol.* **1991**, *13* (1), 40–44.
- (18) Chitosan - Deacetylated chitin, Poly(D-glucosamine) <https://www.sigmaaldrich.com/NL/en/substance/chitosan123459012764> (accessed Aug 4, 2021).
- (19) Ravi Kumar, M. N. V. A Review of Chitin and Chitosan Applications. *React. Funct. Polym.* **2000**, *46* (1), 1–27.
- (20) Schatz, C.; Viton, C.; Delair, T.; Pichot, C.; Domard, A. Typical Physicochemical Behaviors of Chitosan in Aqueous Solution. *Biomacromolecules* **2003**, *4* (3), 641–648.
- (21) Kunanusornchai, W.; Witoonpanich, B.; Pichyangkura, R.; Chatsudthipong, V.; Muanprasat, C. Chitosan Oligosaccharide Suppresses Synovial Inflammation via AMPK Activation: An in Vitro and in Vivo Study. *Pharmacol. Res.* **2016**, *113*, 458–467.
- (22) Naveed, M.; Phil, L.; Sohail, M.; Hasnat, M.; Baig, M. M. F. A.; Ihsan, A. U.; Shumzaid, M.; Kakar, M. U.; Mehmood Khan, T.; Akabar, M. D.; et al. Chitosan Oligosaccharide (COS): An Overview. *Int. J. Biol. Macromol.* **2019**, *129*, 827–843.
- (23) Roy, J. C.; Salaün, F.; Giraud, S.; Ferri, A. Solubility of Chitin: Solvents, Solution Behaviors and Their Related Mechanisms. *Solubility of Polysaccharides* **2017**.
- (24) Aranaz, I.; Mengibar, M.; Harris, R.; Panos, I.; Miralles, B.; Acosta, N.; Galed, G.; Heras, A. Functional Characterization of Chitin and Chitosan. *Curr. Chem. Biol.* **2012**, *3* (2), 203–230.
- (25) H, Z.; SH, N. In Vitro Degradation of Chitosan by a Commercial Enzyme Preparation: Effect of Molecular Weight and Degree of Deacetylation. *Biomaterials* **2001**, *22* (12), 1653–1658.
- (26) S, H.; H, T.; N, N. N-Acetylation in Chitosan and the Rate of Its Enzymic Hydrolysis. *Biomaterials* **1989**, *10* (8), 574–576.
- (27) M, H.; E, K.; LY, L. Uptake and Cytotoxicity of Chitosan Molecules and Nanoparticles: Effects of Molecular Weight and Degree of Deacetylation. *Pharm. Res.* **2004**, *21* (2), 344–353.
- (28) Kofuji, K.; Qian, C. J.; Nishimura, M.; Sugiyama, I.; Murata, Y.; Kawashima, S. Relationship between Physicochemical Characteristics and Functional Properties of Chitosan. *Eur. Polym. J.* **2005**, *41* (11), 2784–2791.
- (29) NG, S.; KM, V.; P, A. Chitosans as Absorption Enhancers for Poorly Absorbable Drugs. 1: Influence of Molecular Weight and Degree of Acetylation on Drug Transport across Human Intestinal Epithelial (Caco-2) Cells. *Pharm. Res.* **1996**, *13* (11), 1686–1692.
- (30) Philibert, T.; Lee, B. H.; Fabien, N. Current Status and New Perspectives on Chitin and Chitosan as Functional Biopolymers. *Appl. Biochem. Biotechnol.* **2016**, *181* (4), 1314–1337.
- (31) Cancogni, D.; Lay, L. Exploring Glycosylation Reactions under Continuous-Flow Conditions. *Synlett* **2014**, *25* (20), 2873–2878.
- (32) MA, F.-H.; S, M.; H, L.-M.; JM, H.-V.; E, P.-C.; ML, E.-S.; L, S.-S.; I, R.; BM, P.; J, S.-R. Synthesis of the Steroidal Glycoside (25R)-3 $\beta$ ,16 $\beta$ -Diacetoxy-12,22-Dioxo-5 $\alpha$ -Cholestan-26-Yl  $\beta$ -D-Glucopyranoside and Its Anti-Cancer Properties on Cervicouterine HeLa, CaSki, and ViBo Cells. *Eur. J. Med. Chem.* **2010**, *45* (11), 4827–4837.
- (33) Martín-Lomas, M.; Flores-Mosquera, M.; Chiara, J. Attempted Synthesis of Type-A Inositolphosphoglycan Mediators – Synthesis of a Pseudo-hexasaccharide Precursor. *European J. Org. Chem.* **2000**, *2000* (8), 1547–1562.

- (34) Rana, S. S.; Barlow, J. J.; Matta, K. L. Synthesis of P-Nitrophenyl 2-Acetamido-2-Deoxy-4-O- $\beta$ -d-Galactopyranosyl-  $\beta$ -d-Glucopyranoside, and p-Nitrophenyl 6-O-(2-Acetamido-2-Deoxy-3-O- and -4-O- $\beta$ -d-Galactopyranosyl-  $\beta$ -d-Glucopyranosyl)- $\alpha$ -d-Mannopyranoside. *Carbohydr. Res.* **1983**, *113* (2), 257–271.
- (35) Flowers, H. M.; Jeanloz, R. W. The Synthesis of a Glucosaminyl-Muramic Acid Disaccharide: Methyl 6-O-(2-Acetamido-3,4,6-Tri-O-Acetyl-2-Deoxy- $\beta$ -d-Glucopyranosyl)-2-Acetamido-4-O-Acetyl-2-Deoxy-3-O-[d-1-(Methyl Carboxylate)Ethyl]- $\alpha$ -d-Glucopyranoside. *J. Org. Chem.* **1963**, *28* (6), 1564–1567.
- (36) Dullenkopf, W.; Castro-Palomino, J. C.; Manzoni, L.; Schmidt, R. R. N-Trichloroethoxycarbonyl-Glucosamine Derivatives as Glycosyl Donors. *Carbohydr. Res.* **1996**, *296* (1–4), 135–147.
- (37) Boltje, T. J.; Li, C.; Boons, G.-J. A Versatile Set of Orthogonal Protecting Groups for the Preparation of Highly Branched Oligosaccharides. *Org. Lett.* **2010**, *12* (20), 4636.
- (38) Takashi Higashino; Satoshi Sakaguchi, and; Ishii\*, Y. Rearrangement of Allyl Homoallyl Ethers to  $\gamma,\delta$ -Unsaturated Carbonyl Compounds Catalyzed by Iridium Complexes. *Org. Lett.* **2000**, *2* (26), 4193–4195.
- (39) Scott G. Nelson, \*; Christopher J. Bungard, and; Wang, K. Catalyzed Olefin Isomerization Leading to Highly Stereoselective Claisen Rearrangements of Aliphatic Allyl Vinyl Ethers. *J. Am. Chem. Soc.* **2003**, *125* (43), 13000–13001.
- (40) Boullanger, P.; Chatelard, P.; Descotes, G.; Kloosterman, M.; Boom, J. H. Van. Use of the Allyloxycarbonyl Protective Group in Carbohydrate Chemistry. <https://doi.org/10.1080/07328308608062974> **2006**, *5* (4), 541–559.
- (41) Cancogni, D.; Lay, L. Exploring Glycosylation Reactions under Continuous-Flow Conditions. *Synlett* **2014**, *25* (20), 2873–2878.
- (42) Sakonsinsiri, C.; Turnbull, W. B. Protecting Groups at the Anomeric Position of Carbohydrates. *Prot. Groups* **2019**, 145–168.
- (43) Rana, S. S.; Barlow, J. J.; Matta, K. L. Synthesis of P-Nitrophenyl 2-Acetamido-2-Deoxy-4-O- $\beta$ -d-Galactopyranosyl-  $\beta$ -d-Glucopyranoside, and p-Nitrophenyl 6-O-(2-Acetamido-2-Deoxy-3-O- and -4-O- $\beta$ -d-Galactopyranosyl-  $\beta$ -d-Glucopyranosyl)- $\alpha$ -d-Mannopyranoside. *Carbohydr. Res.* **1983**, *113* (2), 257–271.
- (44) Wuts, P. G. M.; Greene, T. W. Greene's Protective Groups in Organic Synthesis. *Greene's Prot. Groups Org. Synth.* **2006**.
- (45) Ali, S. P.; Jalsa, N. K. Order of Reactivity of OH/NH Groups of Glucosamine Hydrochloride and N-Acetyl Glucosamine Toward Benzoylation Using NaH/BnBr in DMF. <http://dx.doi.org/10.1080/07328303.2014.907907> **2014**, *33* (4), 185–196.
- (46) Zhiyuan Zhang; Ian R. Ollmann; Xin-Shan Ye; Ralf Wischnat; Timor Baasov, † and; Wong\*, C.-H. Programmable One-Pot Oligosaccharide Synthesis. *J. Am. Chem. Soc.* **1999**, *121* (4), 734–753.
- (47) Enugala, R.; Carvalho, L. C. R.; Dias Pires, M. J.; Marques, M. M. B. Stereoselective Glycosylation of Glucosamine: The Role of the N-Protecting Group. *Chem. – An Asian J.* **2012**, *7* (11), 2482–2501.
- (48) and, D. C.; Jayalath, P. Stereocontrolled Formation of  $\beta$ -Glucosides and Related Linkages in the Absence of Neighboring Group Participation: Influence of a Trans-Fused 2,3-O-Carbonate Group. *J. Org. Chem.* **2005**, *70* (18), 7252–7259.



- (49) Codée, J. D. C.; Litjens, R. E. J. N.; Bos, L. J. van den; Overkleeft, H. S.; Marel, G. A. van der. Thioglycosides in Sequential Glycosylation Strategies. *Chem. Soc. Rev.* **2005**, *34* (9), 769–782.
- (50) Poulsen, L. T.; Heuckendorff, M.; Jensen, H. H. On the Generality of the Superarmament of Glycosyl Donors. *Org. Biomol. Chem.* **2018**, *16* (13), 2269–2276.
- (51) Vieira, M. G. A.; Da Silva, M. A.; Dos Santos, L. O.; Beppu, M. M. Natural-Based Plasticizers and Biopolymer Films: A Review. *Eur. Polym. J.* **2011**, *47* (3), 254–263.
- (52) Zhang, W.; Li, G.; Fang, Y.; Wang, X. Maleic Anhydride Surface-Modification of Crosslinked Chitosan Membrane and Its Pervaporation Performance. *J. Memb. Sci.* **2007**, *295* (1–2), 130–138.
- (53) Don, T.-M.; Chen, H.-R. Modification of Chitosan with Maleic Anhydride and Synthesis of Chitosan-g-Poly(N-Isopropylacrylamide). **2004**, 661–661.
- (54) Van Den Broek, L. A. M.; Knoop, R. J. I.; Kappen, F. H. J.; Boeriu, C. G. Chitosan Films and Blends for Packaging Material. *Carbohydr. Polym.* **2015**, *116*, 237–242.
- (55) IZUMI, M.; FUKASE, K.; KUSUMOTO, S. TMSCl as a Mild and Effective Source of Acidic Catalysis in Fischer Glycosidation and Use of Propargyl Glycoside for Anomeric Protection. *OUP* **2014**, *66* (1), 211–214.
- (56) McMurry, J. E. *Organic Chemistry*, 8th ed.; Cengage Learning, 2012.
- (57) Coxon, B. DEVELOPMENTS IN THE KARPLUS EQUATION AS THEY RELATE TO THE NMR COUPLING CONSTANTS OF CARBOHYDRATES. *Adv. Carbohydr. Chem. Biochem.* **2009**, *62*, 17.
- (58) Emmerson, D. P. G.; Hems, W. P.; Davis, B. G. Carbohydrate-Derived Aminoalcohol Ligands for Asymmetric Reformatsky Reactions. *Tetrahedron: Asymmetry* **2005**, *16* (1), 213–221.
- (59) Cavender, C. J.; Shiner, V. J. Trifluoromethanesulfonyl Azide. Its Reaction with Alkyl Amines to Form Alkyl Azides. *J. Org. Chem.* **1972**, *37* (22), 3567–3569.
- (60) Gómez-Ordóñez, E.; Rupérez, P. FTIR-ATR Spectroscopy as a Tool for Polysaccharide Identification in Edible Brown and Red Seaweeds. *Food Hydrocoll.* **2011**, *25* (6), 1514–1520.
- (61) Ciaccia, M.; Di Stefano, S. Mechanisms of Imine Exchange Reactions in Organic Solvents. *Org. Biomol. Chem.* **2014**, *13* (3), 646–654.
- (62) Monteiro, O. A. C.; Airoidi, C. Some Studies of Crosslinking Chitosan-Glutaraldehyde Interaction in a Homogeneous System. *Int. J. Biol. Macromol.* **1999**, *26* (2–3), 119–128.
- (63) Kildeeva, N. R.; Perminov, P. A.; Vladimirov, L. V.; Novikov, V. V.; Mikhailov, S. N. About Mechanism of Chitosan Cross-Linking with Glutaraldehyde. *Russ. J. Bioorganic Chem.* **2009**, *35* (3), 360–369.
- (64) Septiawan, M. R.; Permana, D.; Sabarwati, S. H.; Ahmad, L. O.; Ramadhan, L. O. A. N. Functionalization of Chitosan with Maleic Anhydride for Proton Exchange Membrane. *Indones. J. Chem.* **2018**, *18* (2), 313–320.
- (65) Fadzallah, I. A.; Majid, S. R.; Careem, M. A.; Arof, A. K. A Study on Ionic Interactions in Chitosan-Oxalic Acid Polymer Electrolyte Membranes. *J. Memb. Sci.* **2014**, *463*, 65–72.
- (66) Gabriele, F.; Donnadio, A.; Casciola, M.; Germani, R.; Spreti, N. Ionic and Covalent Crosslinking in Chitosan-Succinic Acid Membranes: Effect on Physicochemical Properties. *Carbohydr. Polym.* **2021**, *251*, 117106.
- (67) Ritonga, H.; Nurdin, M.; Ramadhan, L. O. A. N.; Salsabila, W. S.; Si, S.; Rembon, F. S. Preparation

- of Chitosan Hydrogel with Malonic Acid Crosslinker as Soil Conditioner for Soybean Plant (Glycine Max L. Merrill). *Macromol. Symp.* **2020**, *391* (1), 1–7.
- (68) Ritthidej, G. C.; Phaechamud, T.; Koizumi, T. Moist Heat Treatment on Physicochemical Change of Chitosan Salt Films. *Int. J. Pharm.* **2002**, *232*, 11–22.
- (69) Cai, M.; Gong, J.; Cao, J.; Chen, Y.; Luo, X. In Situ Chemically Crosslinked Chitosan Membrane by Adipic Acid. *J. Appl. Polym. Sci.* **2013**, *128* (5), 3308–3314.
- (70) Sailakshmi, G.; Mitra, T.; Sinha, S.; Chatterjee, S.; Gnanamani, A.; Mandal, A. B. Suberic Acid Acts as a Dissolving Agent as Well as a Crosslinker for Natural Polymers (Carbohydrate and Protein): A Detailed Discussion on the Chemistry behind the Interaction. *J. Macromol. Sci. Part A Pure Appl. Chem.* **2012**, *49* (8), 619–629.
- (71) Cai, M.; Zhang, J.; Chen, Y.; Cao, J.; Leng, M.; Hu, S.; Luo, X. Preparation and Characterization of Chitosan Composite Membranes Crosslinked by Carboxyl-Capped Poly(Ethylene Glycol). *Chinese J. Polym. Sci.* **2014**, *32* (2), 236–244.
- (72) Filipkowska, U.; Józwiak, T. Application of Chemically-Cross-Linked Chitosan for the Removal of Reactive Black 5 and Reactive Yellow 84 Dyes from Aqueous Solutions. *J. Polym. Eng.* **2013**, *33* (8), 735–747.
- (73) Timotius, D.; Kusumastuti, Y.; Putri, N. R. E.; Rochmadi. Proposed Reaction Mechanism of Chitosan-Graft-Maleic from Chitosan and Maleic Anhydride. *IOP Conf. Ser. Mater. Sci. Eng.* **2020**, *722* (1).
- (74) Appendix 1: Dissociation Constants (PKa) of Organic Acids (at 20°C). *Appl. Ion Chromatogr. Pharm. Biol. Prod.* **2012**, 449–453.
- (75) Clemente Bretti; Francesco Crea; Claudia Foti, and; Sammartano\*, S. Solubility and Activity Coefficients of Acidic and Basic Nonelectrolytes in Aqueous Salt Solutions. 2. Solubility and Activity Coefficients of Suberic, Azelaic, and Sebacic Acids in NaCl(Aq), (CH<sub>3</sub>)<sub>4</sub>NI(Aq), and (C<sub>2</sub>H<sub>5</sub>)<sub>4</sub>NI(Aq) at Different Ionic Strengths and at t = 25 °C. *J. Chem. Eng. Data* **2006**, *51* (5), 1660–1667.
- (76) Wu, H.; Lei, Y.; Lu, J.; Zhu, R.; Xiao, D.; Jiao, C.; Xia, R.; Zhang, Z.; Shen, G.; Liu, Y.; et al. Effect of Citric Acid Induced Crosslinking on the Structure and Properties of Potato Starch/Chitosan Composite Films. *Food Hydrocoll.* **2019**, *97*, 105208.
- (77) Burchard, W.; Schulz, L. Functionality of the β(1,4) Glycosidic Linkage in Polysaccharides. *Macromol. Symp.* **1995**, *99* (1), 57–69.
- (78) Kildeeva, N.; Chalykh, A.; Belokon, M.; Petrova, T.; Matveev, V.; Svidchenko, E.; Surin, N.; Sazhnev, N. Influence of Genipin Crosslinking on the Properties of Chitosan-Based Films. *Polym.* **2020**, *Vol. 12, Page 1086* **2020**, *12* (5), 1086.
- (79) Valderruten, N. E.; Valverde, J. D.; Zuluaga, F.; Ruiz-Durántez, E. Synthesis and Characterization of Chitosan Hydrogels Cross-Linked with Dicarboxylic Acids. *React. Funct. Polym.* **2014**, *84*, 21–28.
- (80) Medimagh, R.; Aloui, H.; Jemli, M.; Chaabane, H.; Belkahla, F.; Khwaldia, K. Enhanced Functional Properties of Chitosan Films Cross-Linked by Biosourced Dicarboxylic Acids. *Polym. Sci. - Ser. A* **2016**, *58* (3), 409–418.
- (81) Bragiswar, P.; Bernaki, R. J.; Korytnyk, W. . *Carbohydr. Res.* **1980**, *80*, 99–116.
- (82) α-D-Glucosamine Pentaacetate | CAS 7784-54-5 | SCBT - Santa Cruz Biotechnology <https://www.scbt.com/p/alpha-d-glucosamine-pentaacetate-7784-54-5> (accessed Aug 10,

2021).

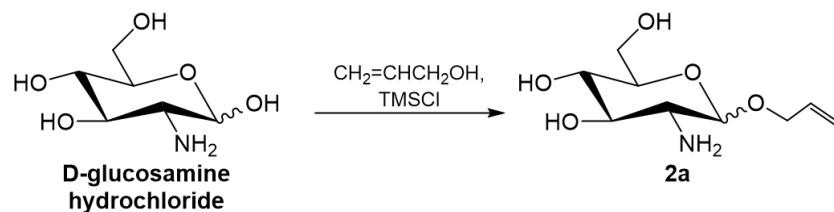
- (83) 2-Acetamido-2-deoxy- $\beta$ -D-glucopyranose 1,3,4,6-tetraacetate 98% | 7772-79-4  
<https://www.sigmaaldrich.com/NL/en/product/aldrich/859990?context=product> (accessed Aug 10, 2021).
- (84) CAS RN: 278784-83-1 | Product Number: P1642 Phenyl 3,4,6-Tri-O-acetyl-2-deoxy-1-thio-2-(2,2,2-trichloroethoxyformamido)- $\beta$ -D-galactopyranoside  
<https://www.tcichemicals.com/BE/en/p/P1642> (accessed Aug 10, 2021).

## Support Information

### Unsuccessful Experiments

#### SI1. Anomeric Alkylation of GlcN

##### Allyl 2-amino-2-deoxy- $\alpha,\beta$ -D-glucopyranoside (**2a**)<sup>31</sup>



To a solution of D-glucosamine hydrochloride (1.5 g, 6.77 mmol) in allyl alcohol (56.9 mL), chlorotrimethylsilane (TMSCl) (11.5 mL, 90.2 mmol) was added. After 12 h the allyl alcohol was removed in vacuo. The crude residue was diluted with toluene and concentrated in vacuo two times, and dried under high vacuum to get **2a**.

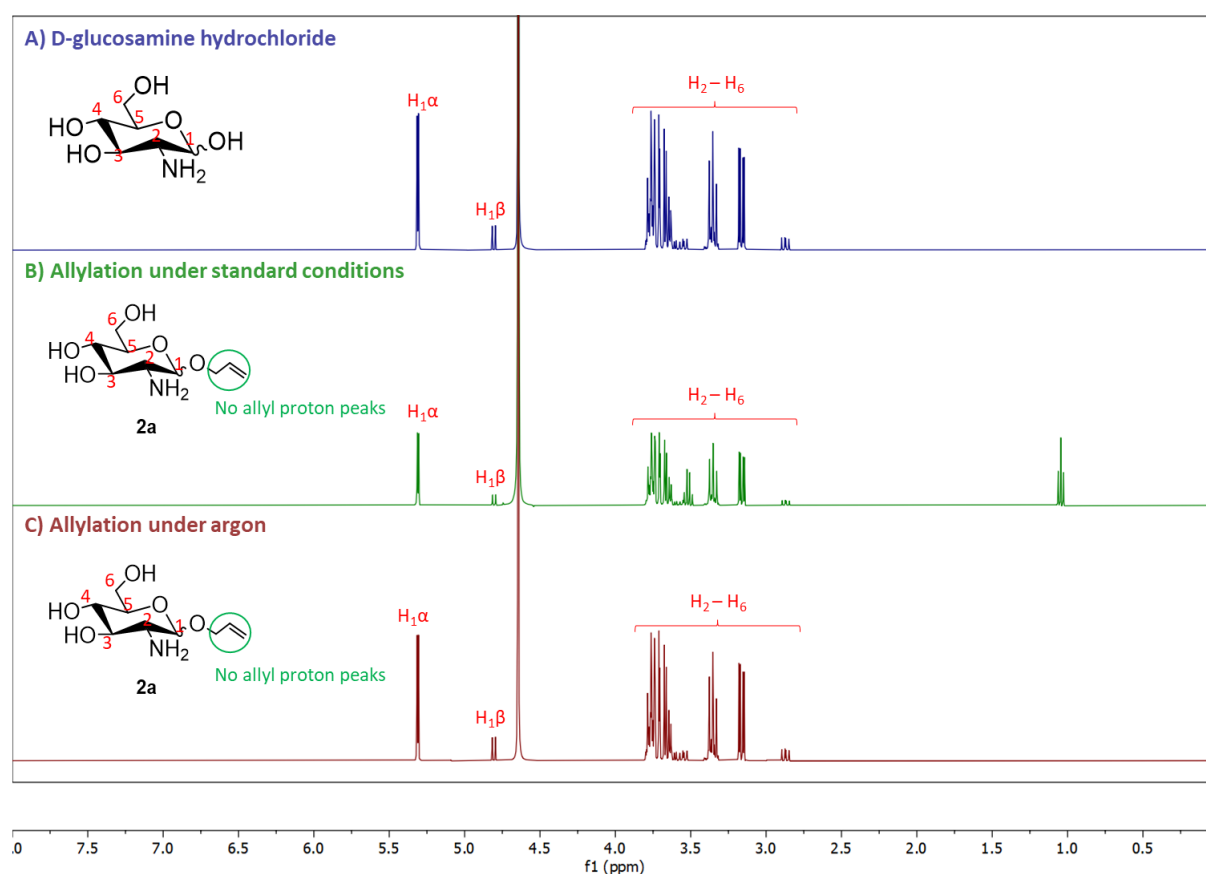
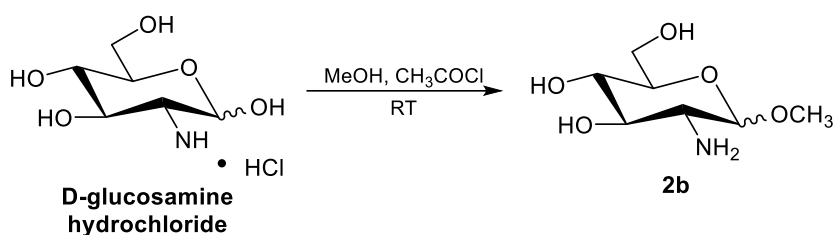


**Figure 33** - <sup>1</sup>H-NMR spectra of the anomeric allylation of D-glucosamine hydrochloride into compound **2a**. A) Unmodified D-glucosamine hydrochloride monomer. B) Reaction under standard air pressure. C) Reaction under argon flow.

#### SI2. Anomeric Methylation of GlcN

##### Methyl 2-amino-2-deoxy- $\alpha,\beta$ -D-glucopyranoside (**2b**)<sup>32</sup>



D-Glucosamine hydrochloride (1.5 g, 6.96 mmol) was suspended in MeOH (50 mL) and acetyl chloride (1.78 mL, 25 mmol) was added dropwise. The solution was stirred continuously for 2 h. The reaction was quenched by the addition of triethylamine (3.48 mL, 25 mmol). The solvent was removed under reduced pressure and dried to get a slightly yellow **2b**.

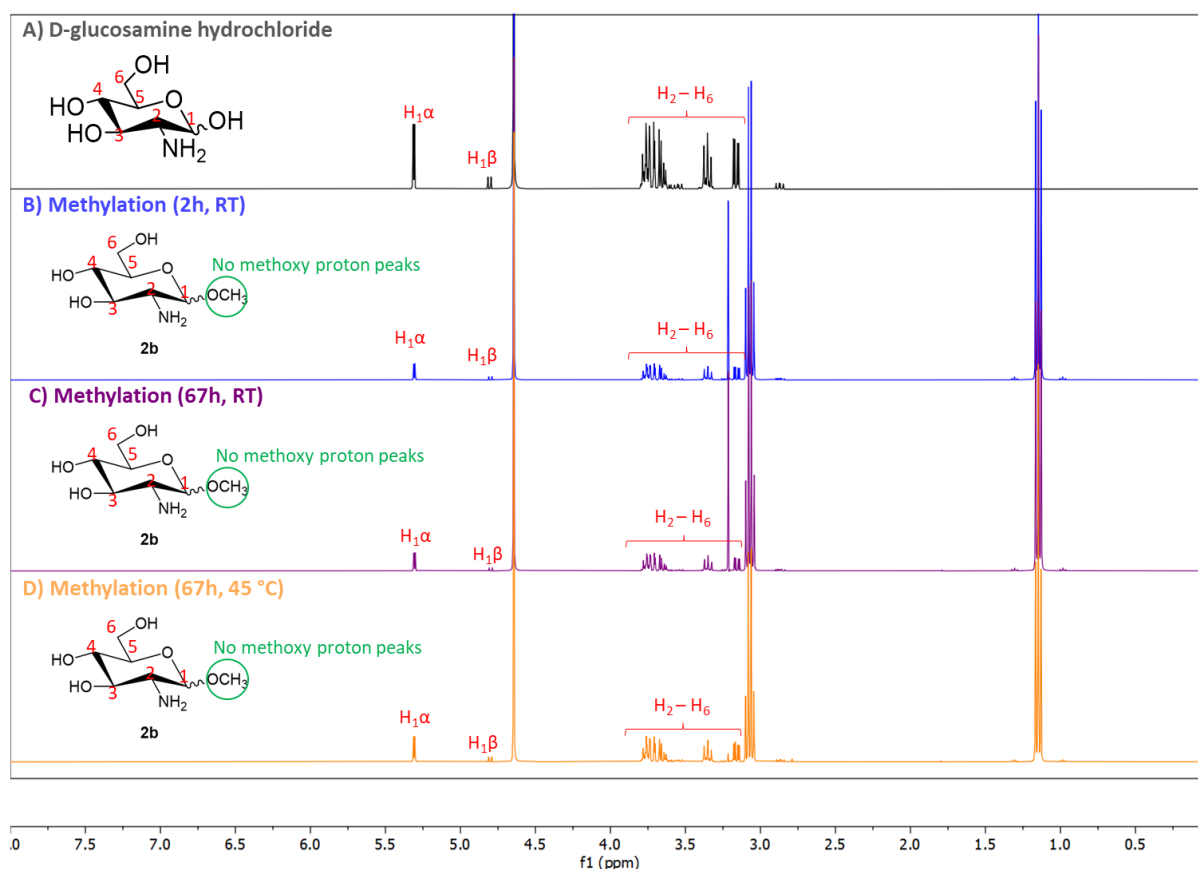
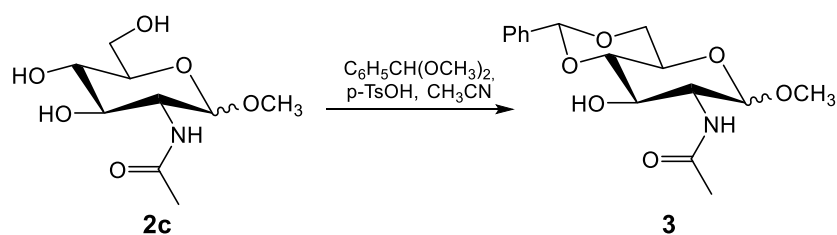


**Figure 34** – Measured  $^1\text{H-NMR}$  spectra of the anomeric methylation of D-glucosamine hydrochloride into compound **2b** under different reaction conditions. A) Unmodified D-glucosamine hydrochloride. B) Reaction after 2 h at RT. C) Reaction after 67 h at RT. D) Reaction after 67 h at 45 °C.

### SI3. Benzylidenation of methyl GlcNAc

#### Methyl 2-acetamido-4,6-O-benzylidene-2-deoxy- $\alpha$ -D-glucopyranoside (**3**)<sup>33</sup>



Under inert gas, in a 50 mL two-necked flask, the crude mixture **2c** (199.8 mg) was dissolved in CH<sub>3</sub>CN (5 mL). Benzaldehyde dimethyl acetal (0.6 mL, 3.99 mmol) and p-toluenesulfonic acid (8.58 mg, 0.045 mmol) were added and the reaction mixture was stirred for 2 h at RT. The reaction was quenched with Et<sub>3</sub>N and the solution was evaporated. The solid was purified with silica gel column chromatography (hexane/EtOAc, 6:1) to get **3**.

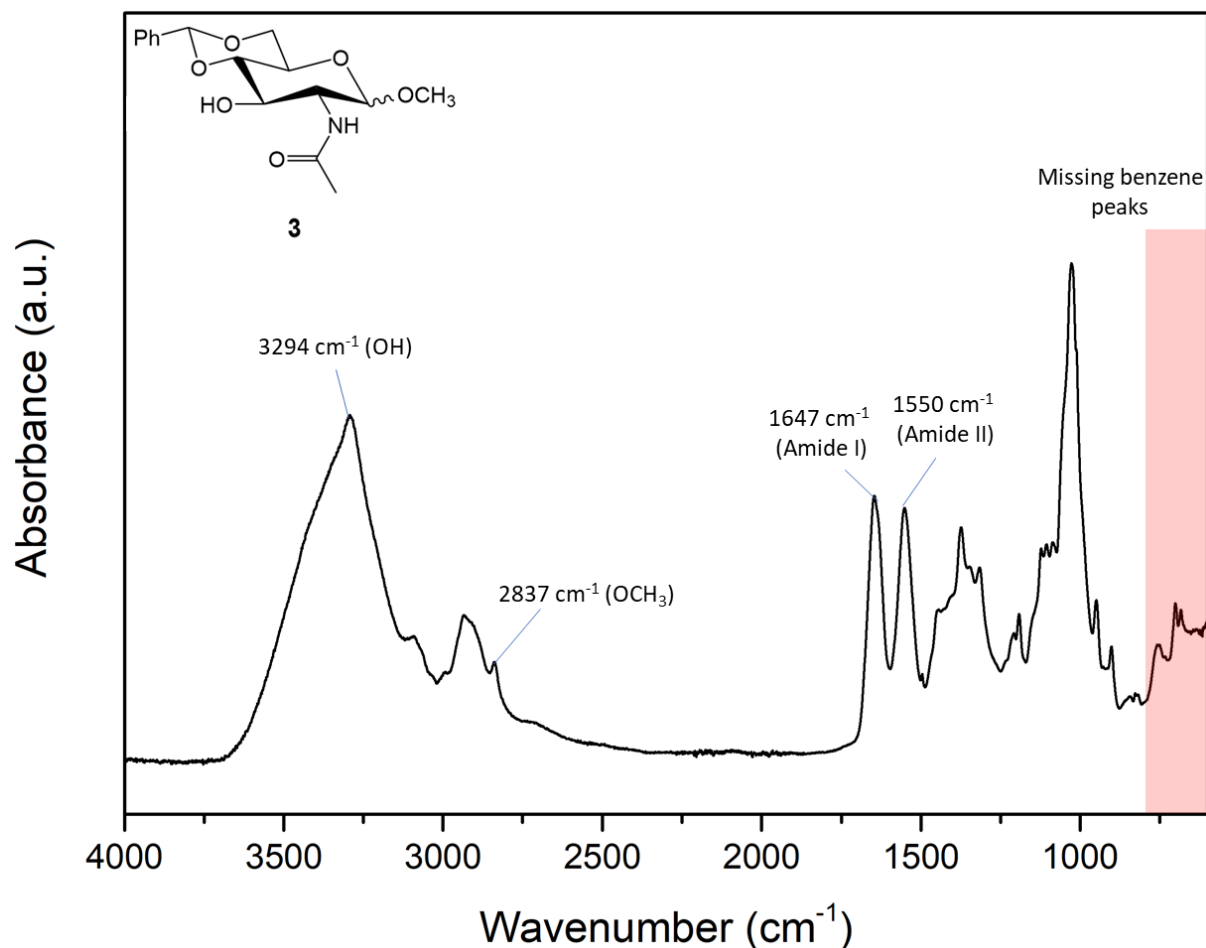
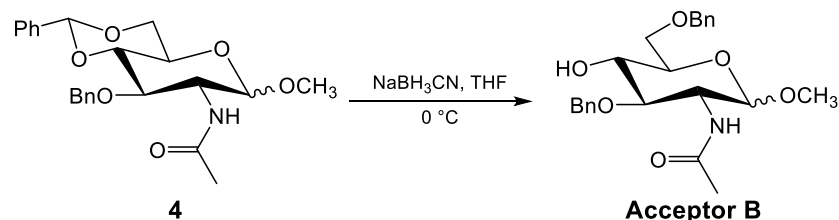


**Figure 35** - Measured ATR-IR spectrum of the attempted 4,6-*O*-benzylideneation of compound **2c** into compound **3** under benzaldehyde dimethylacetal and *p*-TsOH in acetonitrile.

#### SI4. Selective Benzylidene Acetal Ring Opening

##### Methyl 2-acetamido-3,6-di-*O*-benzyl-2-deoxy- $\alpha,\beta$ -D-glucopyranoside (**5**)<sup>43</sup>



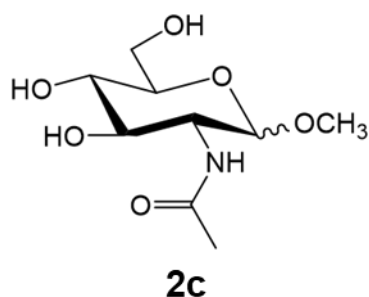
A solution of **4** (0.858 g, 2 mmol) and sodium cyanoborohydride (1.131 g, 18 mmol) in THF (30 mL) containing 3Å molecular sieves (5 g, dried) was cooled to 0° under inert gas. Saturated hydrogen chloride in diethyl ether (acetyl chloride in diethyl ether) was added until the solution was acidic (pH paper, < 7) and stirred at 0°.

After 3h at 0°, the reaction mixture was analyzed with TLC until it indicated that the reaction was completed, then the mixture was poured into ice-water. The product was extracted with dichloromethane. The extract was successively washed with saturated, aqueous sodium bicarbonate and water, dried with magnesium sulfate, and evaporated *in vacuo*, affording a solid. The solid was purified by silica gel column chromatography with 5:1 (v:v) chloroform acetone, to give **acceptor B**.

### Successful Experiments: Data of Glycosyl Acceptor

#### SI5. Anomeric Methylation of GlcNAc

#### Methyl 2-acetamido-2-deoxy- $\alpha,\beta$ -D-glucopyranoside (**2c**)<sup>35</sup>



Brown crystals **2** (1.83 g, 69%) as a mixture of the  $\alpha$  and  $\beta$  anomer.

Melting point 158 – 160 °C (lit. mp<sup>35</sup> 195 °C, lit. mp<sup>58</sup> 181 °C, lit. mp<sup>81</sup> 166 °C).

IR (LiTAO<sub>3</sub>): 3293 (OH), 2840 (OCH<sub>3</sub>), 1647 (Amide I), 1548 (Amide II).

<sup>1</sup>H NMR (400 MHz, d<sub>2</sub>O)  $\delta$  4.62 (1H, d,  $J$  = 3.6 Hz, H-1 $\alpha$ ), 4.31 (1H, d,  $J$  = 8.5 Hz, H-1 $\beta$ ), 3.80 - 3.50 (7H, m, H-2, H-3, H-4, H-5, H-6), 3.37 (3H, s, OCH<sub>3</sub>), 3.25 (3H, s, OCH<sub>3</sub>), 1.90 (3H, s, CH<sub>3</sub>CO).

<sup>13</sup>C NMR (101 MHz, dmsO)  $\delta$  173.10, 169.50 (2 x COCH<sub>3</sub>), 102.29, 98.36 (2 x C-1), 77.44, 74.83, 73.14, 71.27, 71.12, 61.28 (2 x C-3 – C-6), 56.02, 55.58 (2 x CH<sub>3</sub>O), 54.67, 54.19 (2 x C-2), 23.55, 22.42 (2 x CH<sub>3</sub>C=O).

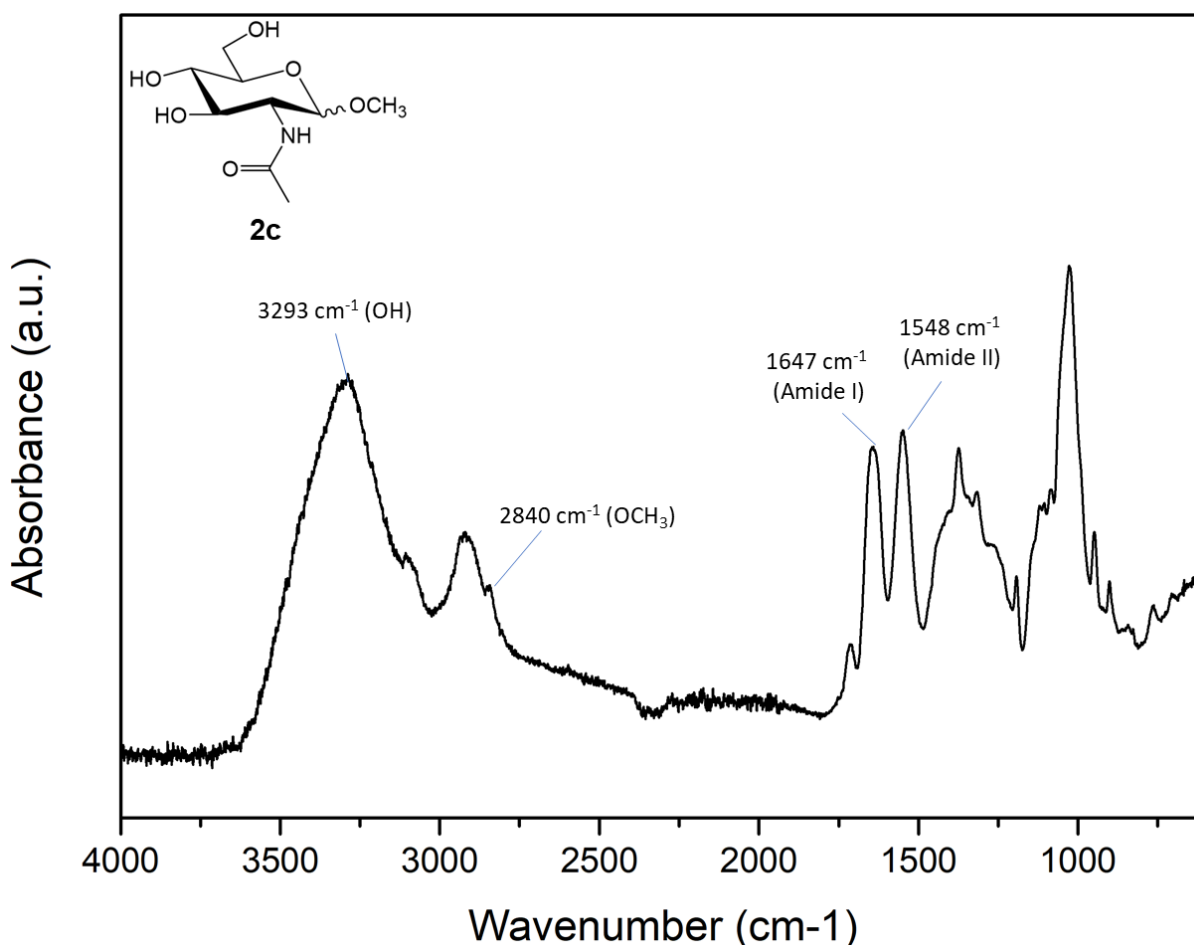


Figure 36 – Measured ATR-IR spectrum of the methylation of *N*-acetyl-*D*-glucosamine, yielding compound **2c**.

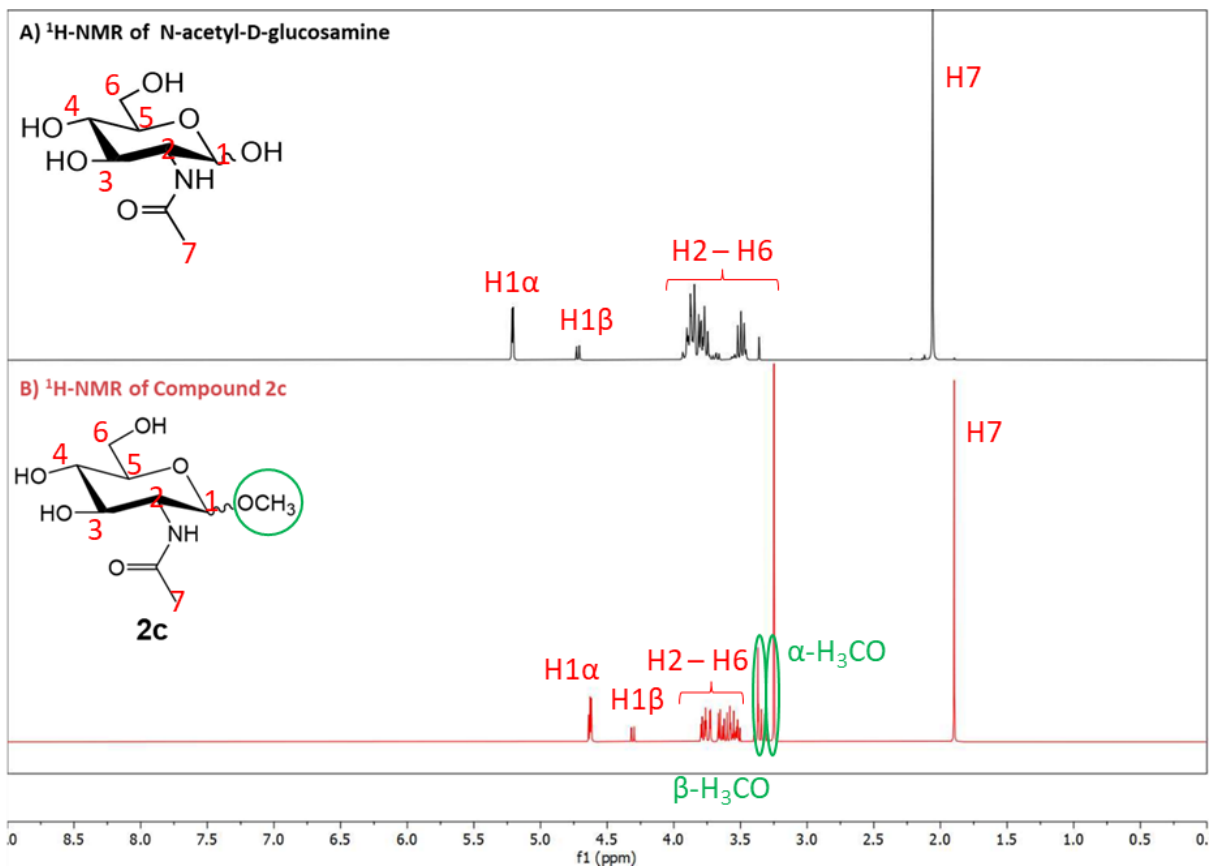


Figure 37 – Measured  $^1\text{H-NMR}$  spectra of A) unmodified N-acetyl-D-glucosamine (GlcNAc) and B) compound 2c.

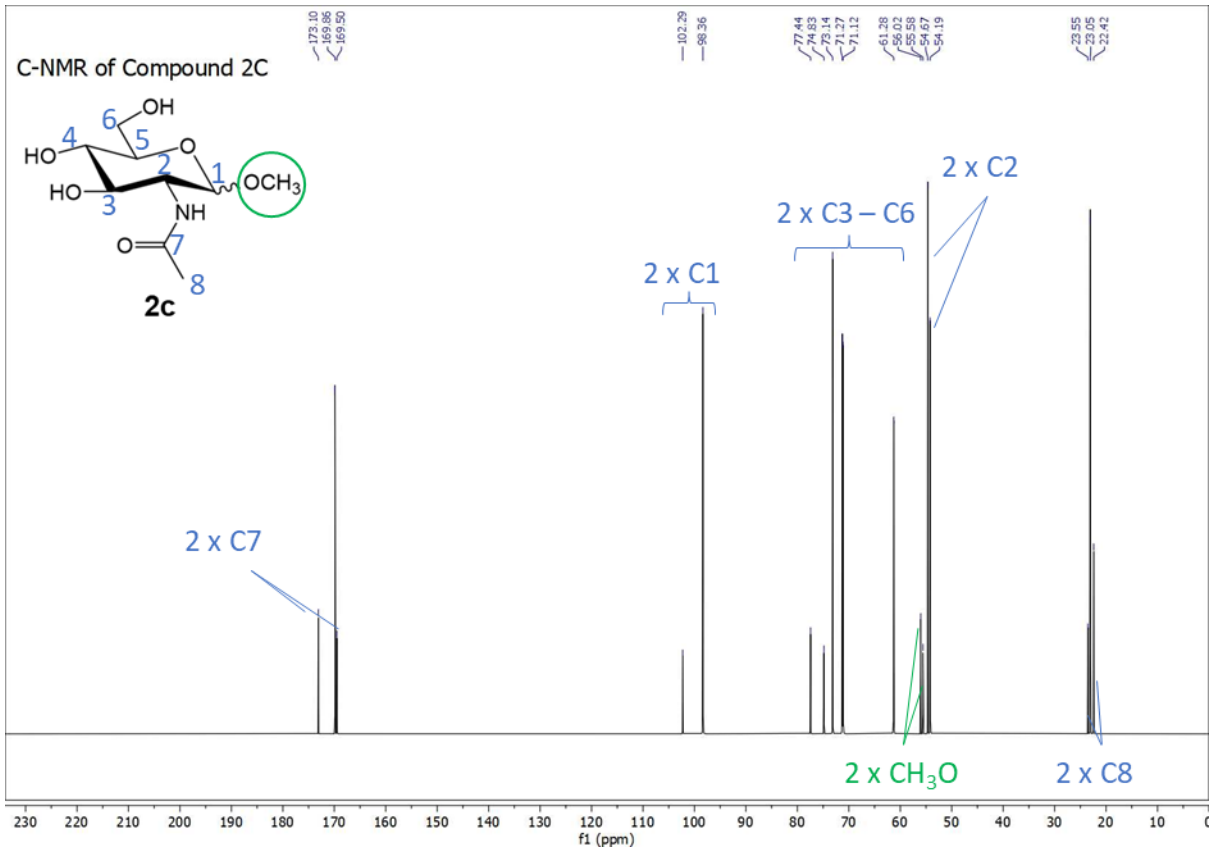
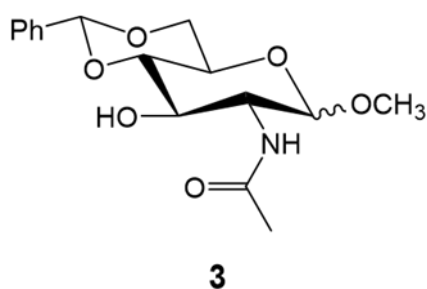


Figure 38 – Measured  $^{13}\text{C-NMR}$  spectrum of compound 2c.



SI6. 4,6-O-Benzylideneation

**Methyl 2-acetamido-4,6-O-benzylidene-2-deoxy- $\alpha$ -D-glucopyranoside (3)<sup>35</sup>**



Off-white powder **3** (188.63 mg, 34%) as a mixture of the  $\alpha$  and  $\beta$  anomer.

Melting point 243 - 246 °C (lit. mp<sup>35</sup> 260-262 °C, lit. mp<sup>58</sup> 292 - 298 °C).

IR (LiTAO<sub>3</sub>): 3297 (OH), 3290 (NH), 1647 (Amide I), 1550 (Amide II), 747, 697, 657 (Aromatic CH).

<sup>1</sup>H NMR (400 MHz, dmsO)  $\delta$  7.87 (1H, d, NH), 7.42 - 7.30 (5H, m, ArH), 5.58 (CHPh, s, 1H), 5.12 (1H, d,  $J$  = 3.6 Hz, H-1 $\alpha$ ), 4.14 (1H, m, H-3), 3.81 (1H, m, H-2), 3.71 (1H, m, H-4), 3.59 (2H, m, CH<sub>2</sub>-6), 3.45 (1H, m, H-5), 3.31 (3H, s, OCH<sub>3</sub>), 1.81 (3H, s, CH<sub>3</sub>C=O).

<sup>13</sup>C NMR (101 MHz, dmsO)  $\delta$  169.89 (COCH<sub>3</sub>), 138.20, 129.31, 128.46, 126.84, 126.79 (C<sub>6</sub>H<sub>5</sub>), 101.34 (C-1), 99.17 (CH<sub>2</sub>Ar), 82.47 (C-4), 68.48, 67.83 (C-3 and C-6), 62.89 (C-5), 55.17, 54.55 (C-2 and CH<sub>3</sub>O), 23.04 (CH<sub>3</sub>C=O).

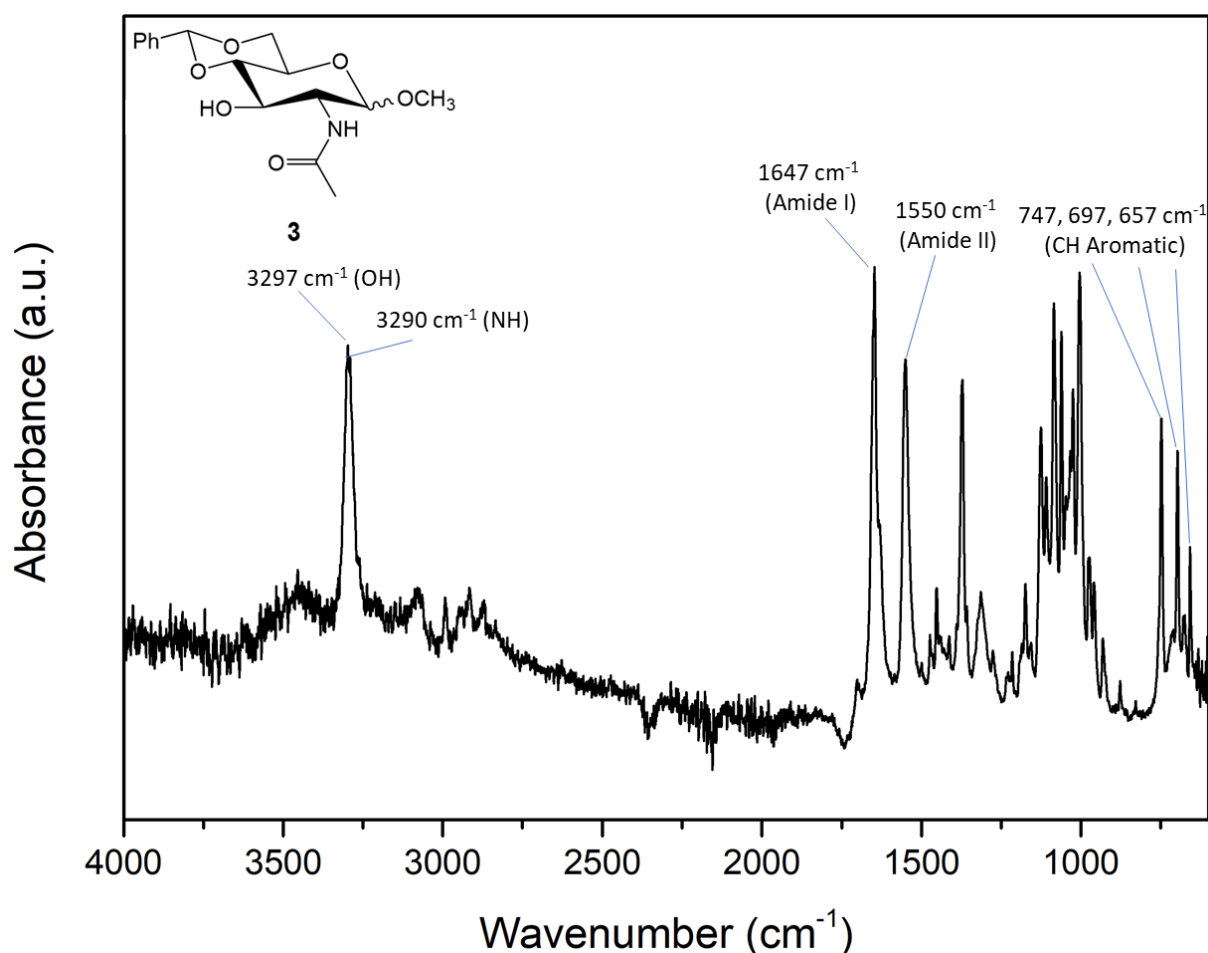


**Figure 39** - Measured ATR-IR spectrum of the 4,6-O-benzylideneation step, affording compound **3**. Conditions: benzaldehyde and ZnCl.

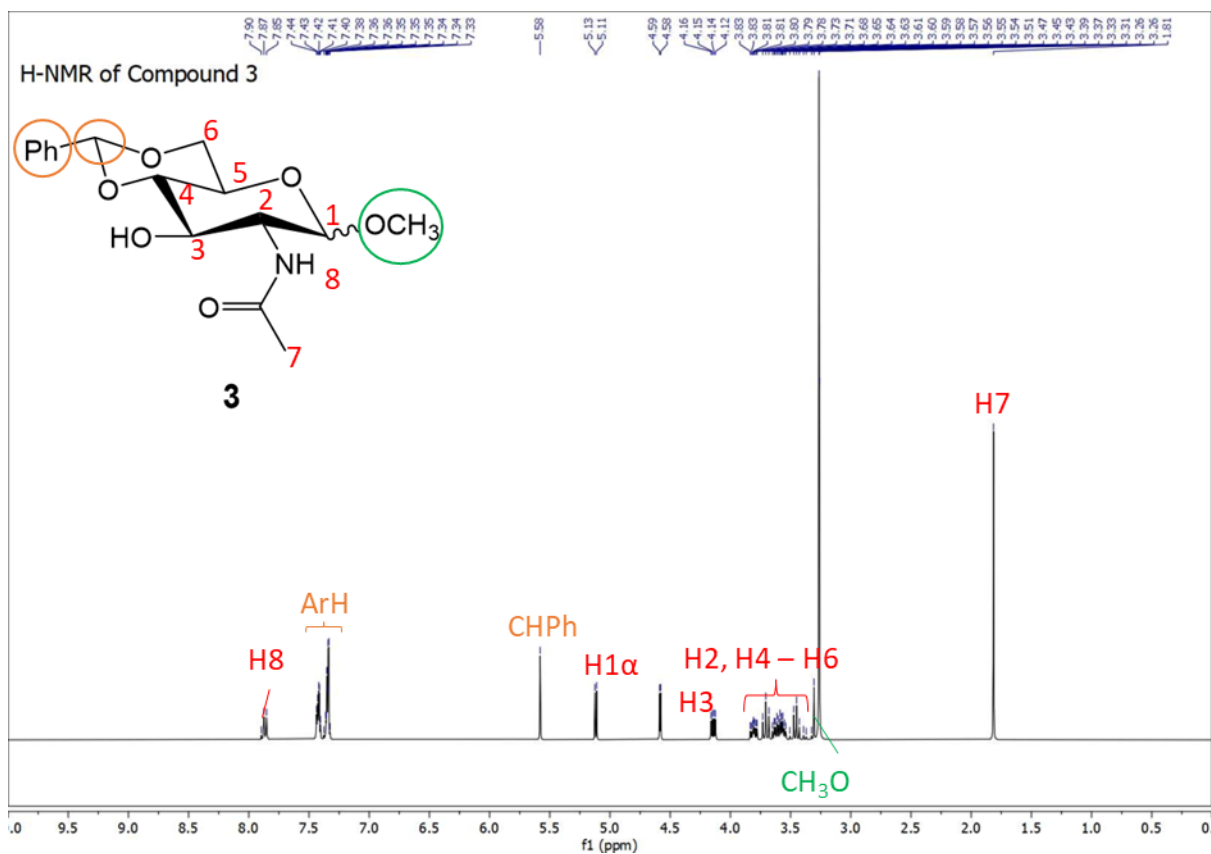


Figure 40 - Measured <sup>1</sup>H-NMR spectrum of the 4,6-O-benzylidene step, affording compound 3. Conditions: benzaldehyde and ZnCl.

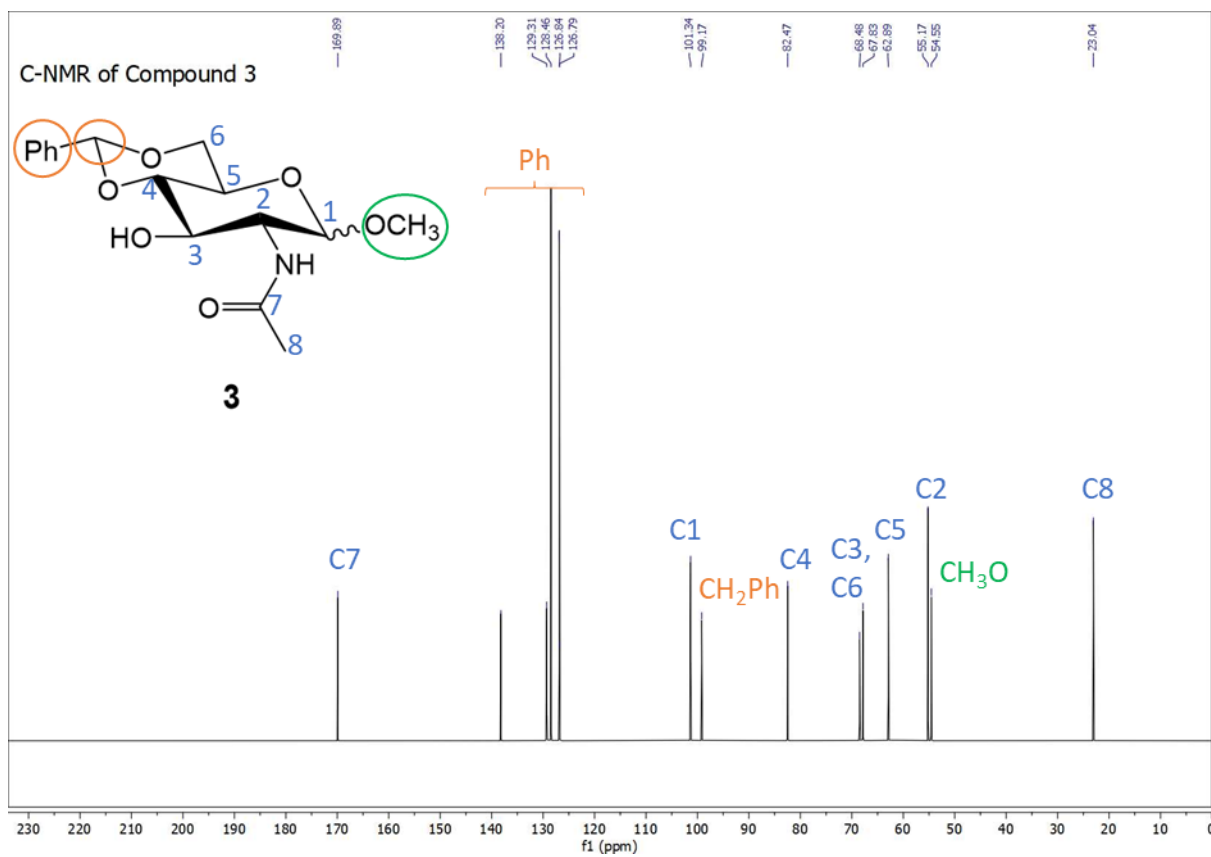
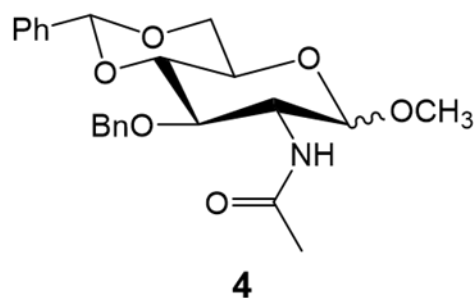


Figure 41 - Measured <sup>13</sup>C-NMR of compound 3. Conditions: benzaldehyde and ZnCl.

SI7. Benzylation

**Methyl 2-acetamido-3-O-benzyl-4,6-O-benzylidene-2-deoxy- $\alpha$ -D-glucopyranoside (4)<sup>43</sup>**



Yellow solid **4** (73.13 mg, 61%) as a mixture of the  $\alpha$  and  $\beta$  anomer.

Melting point 202 – 204 °C (lit. mp<sup>43</sup> 228-230 °C). IR (LiTAO<sub>3</sub>): 3284 (NH), 2870 (OCH<sub>3</sub>), 1646 (Amide I), 1553 (Amide II), 737, 694, 675, 656 (Aromatic CH).

<sup>1</sup>H NMR (400 MHz, dmsO)  $\delta$  8.10 (1H, d, NH), 7.40 – 7.01 (10H, m, ArH), 5.68 (1H, s, CHPh), 4.76 – 4.65 (1H, m, H-1 $\alpha$ ), 4.64 – 4.51 (2H, m, CH<sub>2</sub>Ph), 3.96 – 3.53 (4H, m, H-2, H-3, H-4, H-5), 3.29 (3H, OCH<sub>3</sub>), 1.84 (3H, s, CH<sub>3</sub>CO).

<sup>13</sup>C NMR (101 MHz, dmsO)  $\delta$  169.78 (COCH<sub>3</sub>), 139.29, 138.11, 129.20, 128.72, 128.65, 128.60, 128.58, 128.54, 128.47, 128.21, 127.94, 127.91, 127.89, 127.80, 127.71, 126.43 (2 x C<sub>6</sub>H<sub>5</sub>), 100.71 (CH-Ar), 99.36 (C-1), 81.92 (C-4), 76.78 (C-3), 73.85 (CH<sub>2</sub>Ar), 71.84 (C-6), 62.95 (C-5), 55.18 (CH<sub>3</sub>O), 53.01 (C-2), 23.00 (CH<sub>3</sub>C=O).

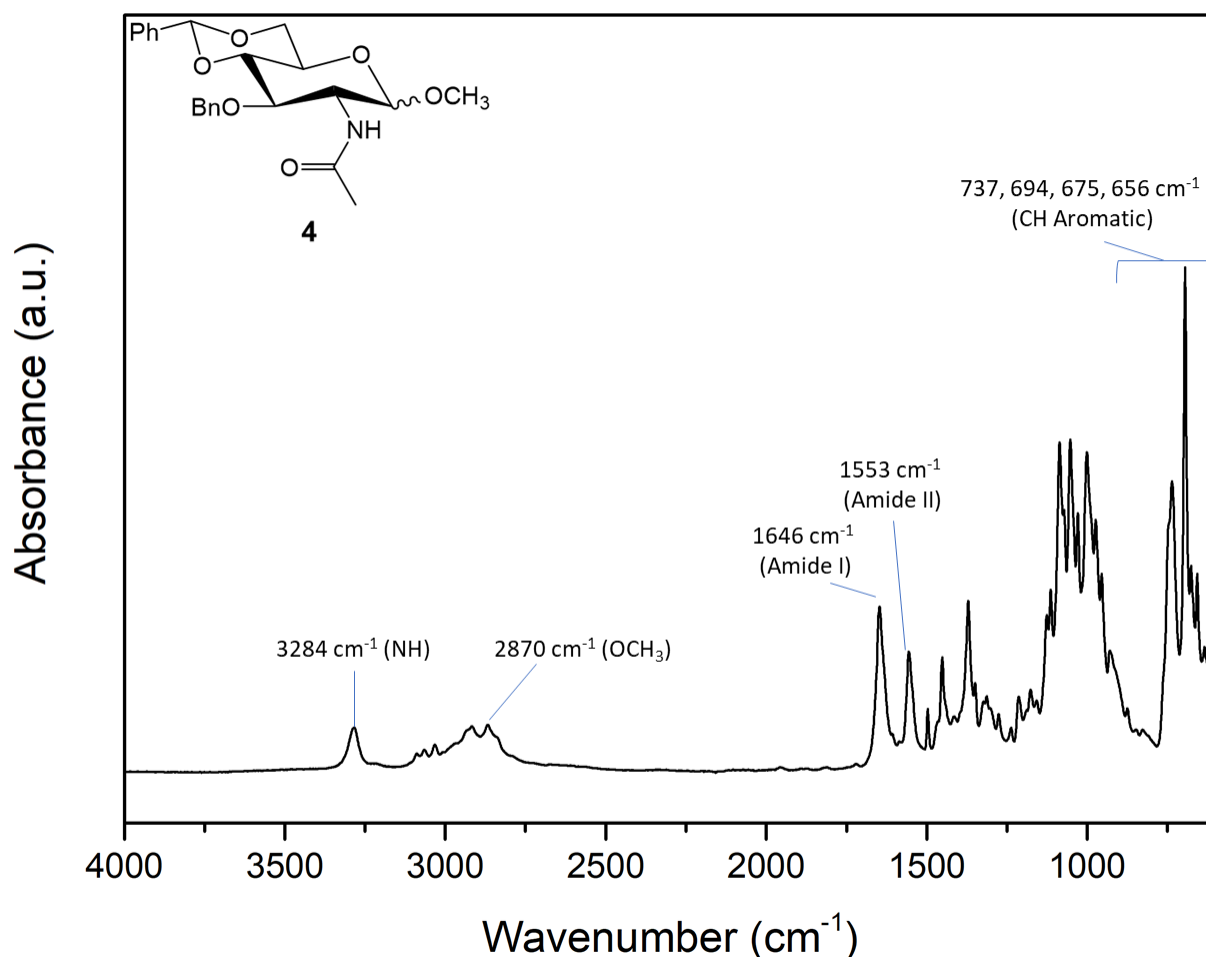


**Figure 42** - Measured ATR-IR spectrum of compound **4** after the benzylation step.

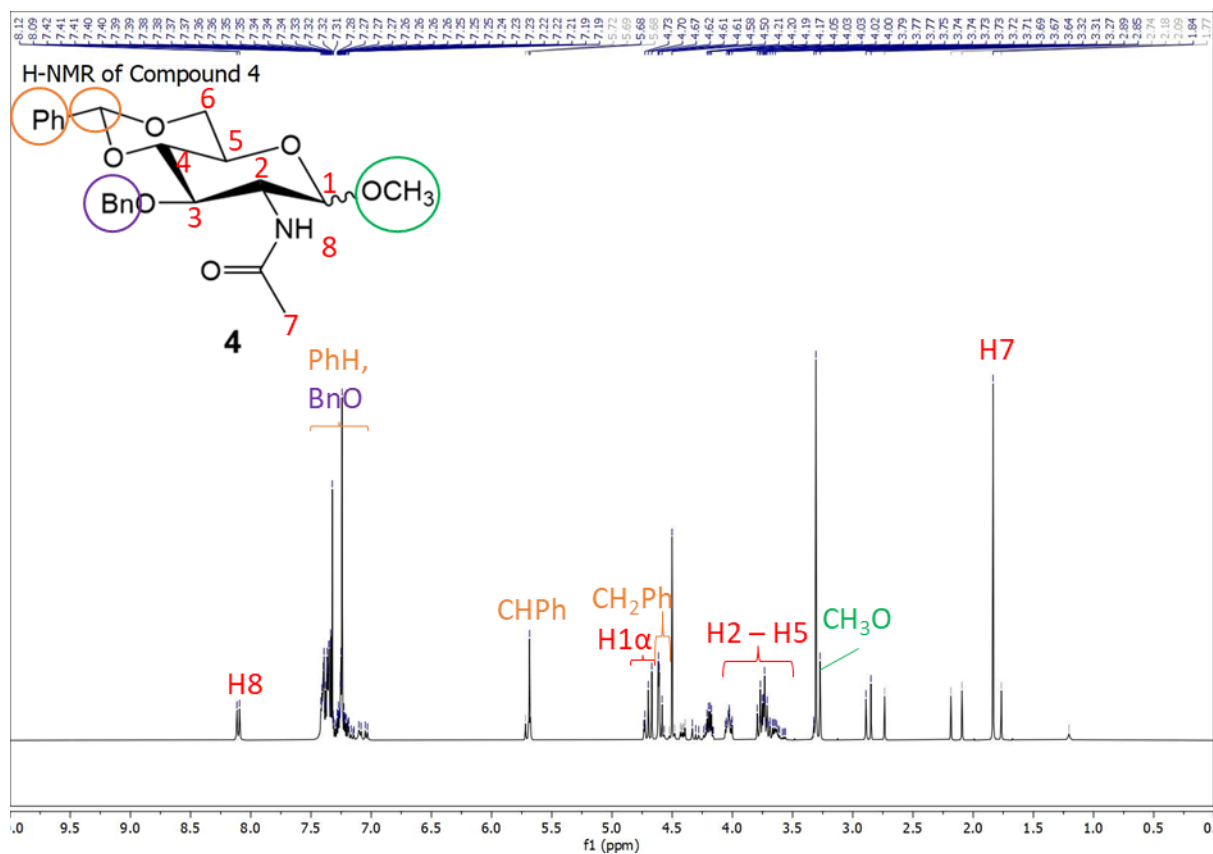


Figure 43 - Measured <sup>1</sup>H-NMR spectrum of compound 4 after the benzylation step.

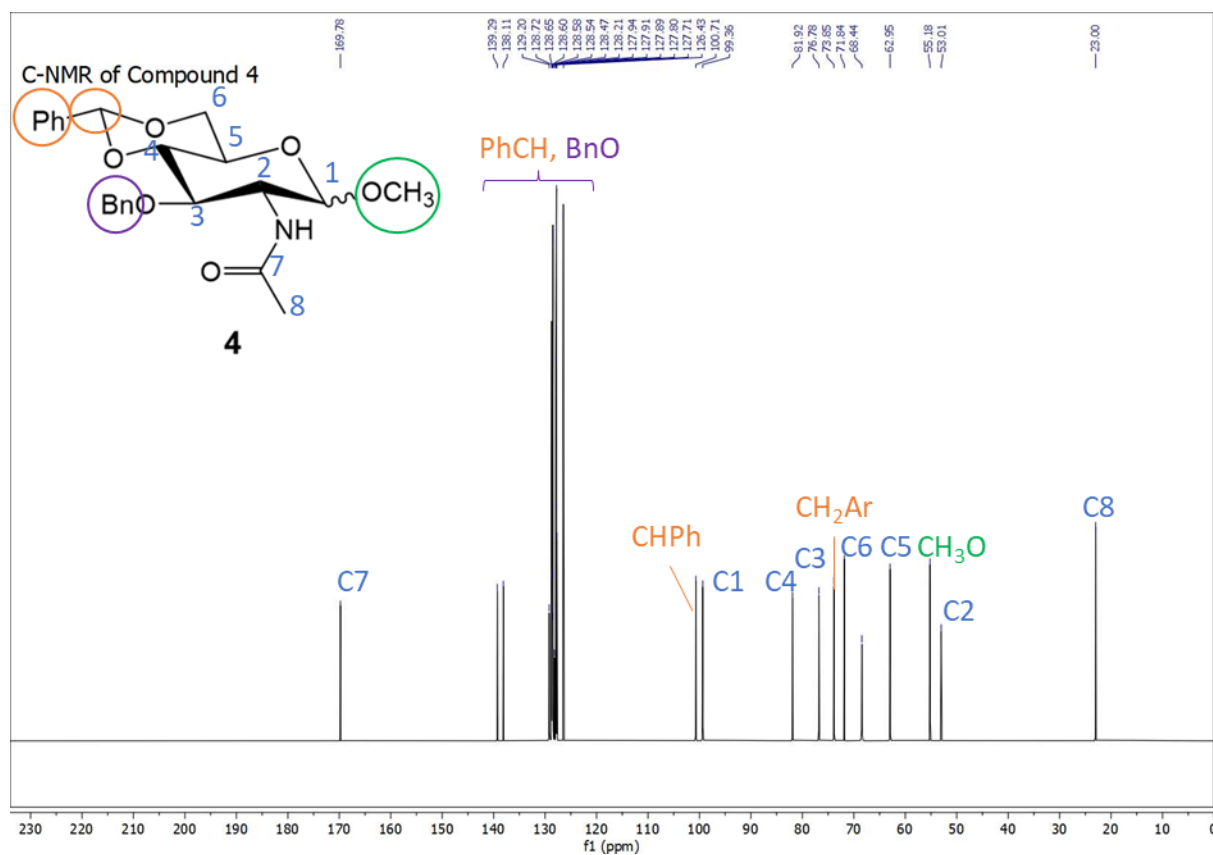
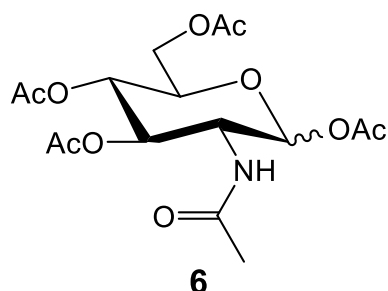


Figure 44 - Measured <sup>13</sup>C-NMR spectrum of compound 4 after the benzylation step.

## Successful Experiments: Data of Glycosyl Donors

### SI8. Acetylation of *N*-acetyl-D-glucosamine

#### 1,3,4,6-Tetra-*O*-acetyl-2-acetamido-2-deoxy- $\alpha$ -D-glucopyranoside (**6**)<sup>33</sup>



White solid **6** (2.50 g, 71%) as a mixture of the  $\alpha$  and  $\beta$  anomer.

Melting point 145 -148 °C (lit. mp $_{\alpha}$ -anomer<sup>82</sup> 127 – 130 °C, lit. mp $_{\alpha}$ -anomer<sup>83</sup> 186 – 189 °C).

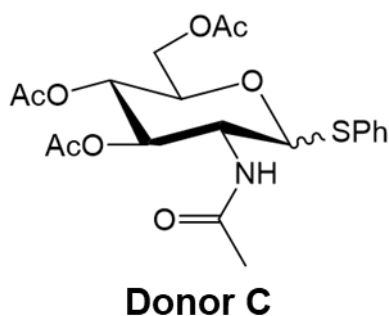
IR (LiTAO<sub>3</sub>): 3438 (NH), 1740 (Acetyl C=O), 1675 (Amide I), 1518 (Amide II), 1221 (C-O ester) .

<sup>1</sup>H NMR (400 MHz, d<sub>2</sub>O)  $\delta$  5.97 (1H, d,  $J$  = 3.7 Hz, H-1 $\alpha$ ), 5.25 (1H, m, H-3), 5.07 – 4.97 (1H, m, H-4), 4.34 (1H, m, H-2), 4.28 – 4.13 (2H, m, CH<sub>2</sub>-6), 3.99 (1H, m, H-5), 2.09 - 1.82 (15H, m, 5 x CH<sub>3</sub>CO).

<sup>13</sup>C NMR (101 MHz, dmso)  $\delta$  170.02, 169.95, 169.83, 169.18, 169.12 (5 x COO), 89.68 (C-1), 69.90, 69.10, 68.07 (C-3, C-4, C-5), 61.34 (C-6), 49.85 (C-2), 22.21, 20.83, 20.48, 20.39, 20.36 (5 x CH<sub>3</sub>C=O).

### SI9. Thio-*N*-acetyl-D-glucosamine Donor

#### Phenyl 3,4,6-Tri-*O*-acetyl-2-acetamido-2-deoxy-1-thio- $\alpha$ -D-glucopyranoside (**7**) donor<sup>33</sup>



Yellow solid **7** (129.7 mg, 38%) as a mixture of the  $\alpha$  and  $\beta$  anomer.

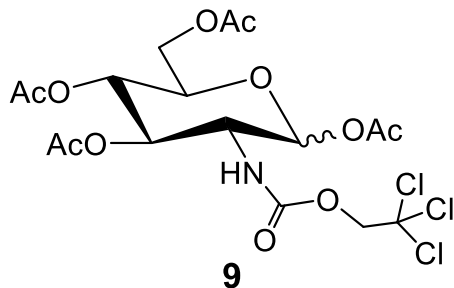
Melting point 157 – 160 °C. IR (LiTAO<sub>3</sub>): 3296 (NH), 1740 (Acetyl C=O), 1661 (Amide I), 1518 (Amide II), 1212 (C-O ester), 742,690, 642 (Aromatic CH).

<sup>1</sup>H NMR (400 MHz, dmso)  $\delta$  8.03 (1H, dd, NH), 7.45 – 7.13 (5H, m, ArH), 5.19 – 5.07 (2H, m, H-3, H-4), 5.05 (1H, m, H-1 $\alpha$ ), 4.80 (1H, t, H-2), 4.14 - 4.09 (2H, m, CH<sub>2</sub>-6), 4.05 – 3.93, 3.84 (1H, q, H-5), 1.97 - 1.76 (12H, m, 4x CH<sub>3</sub>CO).

<sup>13</sup>C NMR (101 MHz, dmso)  $\delta$  169.95, 169.61, 169.30, 169.18 (4 x COO), 133.38, 130.24, 129.47, 127.09 (C<sub>6</sub>H<sub>5</sub>), 84.74 (C-1), 74.48 (C-5), 73.47 (C-3), 68.41 (C-4), 61.96 (C-6), 52.01 (C-2), 22.66, 20.50, 20.41, 20.32 (4 x CH<sub>3</sub>C=O).

### SI10. Troc Protection and Acetylation of D-glucosamine

#### 1,3,4,6-Tetra-*O*-acetyl-2-deoxy-2-(2,2,2-trichloroethoxycarbonylamino)- $\alpha$ -D-glucopyranose (**9**)<sup>36</sup>



Colorless oil **9** (928.1 mg, 15% ) as a mixture of the  $\alpha$  and  $\beta$  anomer.

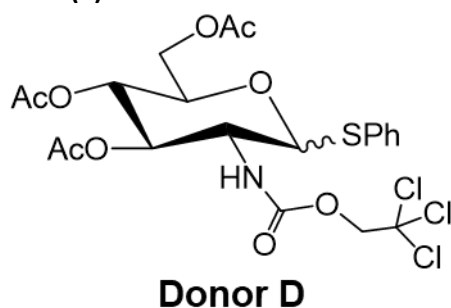
Melting point 78 – 80 °C (lit. mp $_{\beta}$ -anomer<sup>40</sup> 122-123 °C). IR (LiTAO<sub>3</sub>): 3328 (NH), 2959 (CH), 1735 (Acetyl C=O), 1728 (Troc C=O), 1532 (NH), 1209 (C-O ester), 818 (CCl).

<sup>1</sup>H NMR (400 MHz, dmso)  $\delta$  8.18 (1H, d, NH), 6.00 (1H, d,  $J$  = 3.5 Hz, H-1 $\alpha$ ), 5.21 - 5.16 (1H, m, H-3), 5.02 – 4.81 (2H, m, 2H, CH<sub>2</sub>CCl<sub>3</sub>), 4.19 – 3.92 (6H, m, H-2, H-4, H-5, H-6), 2.13 (3H, s, CH<sub>3</sub>CO), 1.98 (3H, s, CH<sub>3</sub>CO) 1.95 (3H, s, CH<sub>3</sub>CO), 1.88 (3H, s, CH<sub>3</sub>CO).

$^{13}\text{C}$  NMR (101 MHz, dmso)  $\delta$  170.02, 169.58, 169.19, 169.15 (4 x COO), 154.76 (COON), 96.08 ( $\text{CCl}_3$ ), 89.48 (C-1), 73.52 (C- $\text{CCl}_3$ ), 70.16, 69.07, 68.05 (C-3, C-4, C-5), 61.35 (C-6), 52.51 (C-2), 20.85, 20.49, 20.38, 20.36 (4 x  $\text{CH}_3\text{C}=\text{O}$ ).

SI11. N-Troc-Protected Thio-D-glucosamine Donor

**Phenyl-3,4,6-Tri-O-acetyl-2-(2,2,2-trichloroethoxycarbonylamino)-2-deoxy-1-thio- $\alpha$ -D-glucopyranose (9) donor**<sup>33</sup>



Brown solid **7** (274.35 mg, 53%) as a mixture of the  $\alpha$  and  $\beta$  anomer.

Lit. mp $_{\beta\text{-anomer}}$  117 °C<sup>84</sup>

$^1\text{H}$  NMR (400 MHz, dmso)  $\delta$  8.04 (1H, d, NH), 7.38 – 7.04 (5H, m, ArH), 5.18 – 5.08 (1H, m, H-3), 5.08 – 4.98 (2H, m,  $\text{CH}_2\text{CCl}_3$ ), 4.94 – 4.78 (6H, m, H-2, H-4, H-6), 4.76 (1H, m, H-1 $\alpha$ ), 3.60 (1H, q, H-5), 2.02 – 1.87 (9H, m, 3 x  $\text{CH}_3\text{CO}$ ).

$^{13}\text{C}$  NMR (101 MHz, dmso)  $\delta$  169.44 (COO), 130.54, 129.06, 129.03, 128.35 ( $\text{C}_6\text{H}_5$ ), 84.88 (C-1), 74.60, 73.37, 68.33 (C-3, C-4, C-5), 56.00 (C-2), 20.50, 20.39, 20.33 (3 x  $\text{CH}_3\text{C}=\text{O}$ ).